NASA Contractor Report 170402

NASA-CR-170402
19830016242

Application of Calspan Pitch Rate Control System to the Space Shuttle for Approach and Landing

Norman C. Weingarten and Charles R. Chalk

Contract NAS4-2995
May 1983

National Aeronautics and
Space Administration

NASA Contractor Report 170402

Application of Calspan Pitch Rate Control System to the Space Shuttle for Approach and Landing

Norman C. Weingarten and Charles R. Chalk, Calspan Advanced Technology Center, Buffalo, New York 14225

Prepared for
Ames Research Center
Dryden Flight Research Facility
Edwards, California
under Contract NAS4-2995

1983

National Aeronautics and
Space Administration
Ames Research Center
Dryden Flight Research Facility
Edwards, California 93523

This Page Intentionally Left Blank

SUMMARY

An analytical study was performed on a new pitch rate control system designed by the Calspan Corporation for use in the shuttle during approach and landing. Comparisons were made with a revised control system developed by NASA and the existing OFT control system. The Calspan design concept is discussed. The control system uses filtered pitch rate feedback with proportional plus integral paths in the forward loop. Control system parameters were designed as a function of flight configuration. Analysis included time and frequency domain techniques. Results indicate that both the Calspan and NASA systems significantly improve the flying qualities of the shuttle over the OFT. Better attitude and flight path control and less time delay are the primary reasons. The Calspan system is preferred by the authors over the revised NASA system because of reduced time delay and simpler mechanization. Further testing of the improved flight control systems in an in-flight simulator is recommended before a decision is made on which control system should be used in the actual shuttle.

TABLE OF CONTENTS

LIST OF FIGURES

LIST OF FIGURES (CONT'D)

LIST OF FIGURES (CONT'D)

LIST OF TABLES

LIST OF SYMBOLS

BW	=	bandwidth
$\bar{c}$	=	mean aerodynamic chord, ft
C_D	=	$D/\bar{q}S$
C_{D_o}	=	C_D at α, $\delta_e = 0$
C_{D_α}	=	$\partial C_D/\partial\alpha$
$C_{D_{\delta_e}}$	=	$\partial C_D/\partial\delta_e$
C_L	=	$L/\bar{q}S$
C_{L_o}	=	C_L at α, $\delta_e = 0$
C_{L_α}	=	$\partial C_L/\partial\alpha$
$C_{L_{\delta_e}}$	=	$\partial C_L/\partial\delta_e$
C_m	=	$M/\bar{q}S\bar{c}$
C_{m_o}	=	C_m at α, $\delta_e = 0$
C_{m_α}	=	$\partial C_m/\partial\alpha$
$C_{m_{\delta_e}}$	=	$\partial C_m/\partial\delta_e$
C_{m_q}	=	$\partial C_m/\partial\frac{q\bar{c}}{2V}$
CG	=	center of gravity
D	=	drag force, lb
D	=	denominator of transfer functions
dB	=	decibels
GDQ	=	forward loop gain in OFT system
g	=	gravitational constant, 32.17 ft/sec^2
h	=	altitude, ft
h_c	=	reference altitude, ft
h_{CG}	=	altitude at CG, ft
h_ϵ	=	altitude error, h_c-h, ft
h_p	=	altitude at pilot station, ft

I_{yy} = moment of inertia about pitch axis, slug - ft^2

$KEAS$ = knots equivalent air speed

K_{p_θ} = pilot gain in attitude loop, rad/sec/rad

K_{p_h} = pilot gain in altitude loop, rad/ft

K_q = proportional gain in Calspan system, rad/rad/sec

L = lift force, lb

L_b = reference body length, ft

M = pitching moment, lb-ft

$N^i_{q_{CMD}}$ = numerator of $\frac{i}{q_{CMD}}$ transfer function, $i = \theta, \alpha, h, N_z$

N_z = normal acceleration, g

N_{zp} = normal acceleration at pilot, g

$N_{z_{CG}}$ = normal acceleration at CG, g

m = mass, slug

OFT = orbital flight test

P_F = feedback pole in Calspan system, sec^{-1}

ph = phugoid mode

PIO = pilot induced oscillation

q = pitch rate, rad/sec

q_c, q_{CMD} = pitch rate command, rad/sec

q_{ss} = steady state pitch rate, rad/sec

$\bar{q}$ = $\frac{1}{2}\rho V^2$, dynamic pressure, lb/ft^2

s = Laplace variable

S = wing area, ft^2

SP = short period mode

t_1 = time at maximum slope intercept of time axis, sec

t_2 = time at maximum slope intercept of steady state, sec

Δt = $t_2 - t_1$ rise time, sec

$T_{\theta_{1,2}}$ = lead time constants in pitch attitude transfer function, sec

V	=	velocity, ft/sec
V_T	=	true airspeed, ft/sec
Y_{c_θ}	=	aircraft model in attitude loop
Y_{p_h}	=	pilot model in altitude loop
Y_{p_θ}	=	pilot model in attitude loop
Z_F	=	feedback zero in Calspan system, sec^{-1}
Z_I	=	integrator gain in Calspan system, sec^{-1}
α	=	angle of attack, rad
γ	=	flight path angle, rad
δ_e	=	elevon deflection, rad
δ_{SB}	=	speed brake deflection, %
ζ	=	damping ratio
ζ_{SP}	=	short period damping ratio
θ	=	pitch attitude, rad
θ	=	reference pitch attitude, rad
θ_ε	=	pitch attitude error, $\theta_c - \theta$, rad
λ	=	real root, sec^{-1}
ρ	=	air density, $slug/ft^3$
τ	=	time constant, sec
τ_{Lead}	=	lead time constant in pilot model, sec
τ_p	=	phase delay, sec
ϕ	=	phase angle, deg
ϕ_{pc}	=	phase of pilot compensation, deg
ω	=	frequency, rad/sec
ω_n	=	natural frequency, rad/sec
ω_{BW}	=	bandwidth frequency, rad/sec
ω_{SP}	=	short period frequency, rad/sec
$(\dot{})$	=	rate of change of ( ) with time

Section 1
INTRODUCTION

The use of a pitch rate gyro together with proportional plus integral branches in the forward path has been recognized as a simple control system that is effective in stabilizing aircraft that are unstable as a result of aft c.g. location. Variations of this basic design have been used in the Concorde, Space Shuttle, F-16 and AFTI/F-16 airplanes. The Space Shuttle and NT-33A simulations of the AFTI/F-16 aircraft have exhibited undesirable flying qualities during flare and touchdown consisting of a tendency to balloon and land long and, on occasion, a tendency for the occurrence of a PIO in the pitch and flight path responses. Calspan has developed a rational explanation for these piloting difficulties which identifies the criteria used to design the pitch rate command system as a primary contributor to the landing difficulties experienced in flight tests and in-flight simulation of these aircraft.

The design criteria specified by NASA/JSC for the Space Shuttle is illustrated in Figure 1. This requirement was taken from JSC-07151, Revision 1, dated 15 December 1973. The requirement applies to pitch rate for subsonic flight. There are two aspects of the design criteria that tend to cause flying qualities problems during flare and touchdown. The first is the limit on the overshoot of the transient pitch rate relative to the steady state pitch rate in response to a step command and the second is the large time delay that is permitted.

Limiting the transient pitch rate relative to the steady state requires high damping of the oscillatory short period mode, which is desirable, but it also requires the designer to configure the control system such that the differentiating effect of the numerator parameter $1/T_{\theta_2}$ is suppressed. This can be accomplished in two ways, both of which are commonly applied. One technique is to use a first-order low-pass filter on the pilot's command and the second is to cause a closed-loop pole to cancel $1/T_{\theta_2}$ in the transfer

function of q/q_c. The introduction of low frequency roots for the purpose of preventing pitch rate overshoot will cause limited bandwidth of the angle of attack response that can be commanded and this interferes with the pilot's capability to control the lift force and the flight path.

Experience has shown that effective time delay in response to pilot commands is a primary cause of pilot induced oscillations, PIO. When the flight control system includes sources of effective time delay such as digital sampling, digital processing time, smoothing filters, structural filters and actuator dynamics, it is necessary to give specific design attention to the problem of minimizing the effective time delay in the command path. Low frequency pre-filters and the closed-loop pitch control law can contribute to effective time delay even when there are no explicit sources of delay such as digital sampling and processing delay.

This report describes the results of an analysis, performed by Calspan, to compare the characteristics of two proposed control system designs with the characteristics of the OFT control system. One of the proposed control systems was designed by engineers at Calspan and the other was designed by engineers at NASA/Dryden Flight Research Facility. The objectives of both designs were to improve pilot control of flight path and to reduce the effective time delay of the response of the shuttle to pilot commands. Both designs use filtered pitch rate as the primary feedback and include integration in the forward path. The design concept developed by Calspan is unique and significantly different from that used by NASA/DFRF. The Calspan design concept is described in the following section.

Section 2
CALSPAN DESIGN CONCEPT

The Calspan design is guided by the following objectives.

1. Reduce lag and delay in the command path.

2. Stabilize and augment the short period mode in a way that does not increase the order of the net dynamic system and preserves the $1/T_{\theta_2}$ numerator of the pitch transfer function.

The first objective is pursued by the following changes from the OFT design.

- The structural bending filter is removed from the forward path and placed in the pitch rate feedback path.

- The low-pass smoothing filter is replaced by a notch filter which is tuned to the D/A output frequency.

- The flight control law is revised in a way that reduces effective time delay.

The second objective is realized through choice of design parameters in the control system defined by the block diagram in Figure 2. This loop structure came to the attention of Calspan engineers during a program to perform in-flight simulations of the AFTI/F-16 IBU control system. Company funded studies of this control loop structure resulted in the formulation of design rules which permit achieving the second design objective stated above. The parameters available to the designer are:

K_q	Loop gain control
Z_I	Integration path gain
Z_F	Feedback filter zero
P_F	Feedback filter pole
K_C	Command path gain control.

These parameters are chosen and scheduled as required to achieve the desired short period pole locations, to cause pole-zero cancellations and to establish the desired sensitivity and static gain. The following characteristics of linear closed-loop control systems are used in the design rules.

- Zeros in the forward path are factors of the closed-loop transfer function numerator.
- Zeros in the feedback path do not appear as factors of either the numerator or denominator of the closed-loop transfer function.
- Poles in the feedback appear as factors of the closed-loop transfer function numerator.

$$\frac{q}{q_c} = \frac{K_q M_{\delta_e} s \left(s+\frac{1}{T_{\theta_1}}\right)\left(s+\frac{1}{T_{\theta_2}}\right)\left(s+Z_I\right)\left(\frac{1}{P_F}s+1\right)}{s\left[\underbrace{(s-\lambda_1)(s+\lambda_2)}_{[\zeta,\omega_n]_{SP}}[\zeta,\omega_n]_{ph}(s+\lambda_s)\left(\frac{1}{P_F}s+1\right)+K_q M_{\delta_e}\left(s+\frac{1}{T_{\theta_1}}\right)\left(s+\frac{1}{T_{\theta_2}}\right)\left(s+Z_I\right)\left(\frac{1}{Z_F}s+1\right)\right]}$$

Design such that

$$P_F = 1/T_{\theta_2}$$

$$Z_I = \lambda_2 \quad when \quad \left|\lambda_2\right| > \left|1/T_{\theta_2}\right|$$

$$= 1/T_{\theta_2} \quad when \quad \left|\lambda_2\right| < \left|1/T_{\theta_2}\right|$$

$$= 1/T_{\theta_2} \quad when\ short\ period\ is\ complex.$$

Choose Z_F to influence root locus as K_q is increased. Select Z_F and K_q to establish desired short period poles. The $\left|Z_F\right|$ should be larger than $\left|\lambda_2\right|$ or $\left|1/T_{\theta_2}\right|$ for robust design.

Closed loop system when $\left|\lambda_2\right| > \left|1/T_{\theta_2}\right|$

$$\frac{q}{q_c} = \frac{K_q M_{\delta_e} \not{s} \left(s + 1/T_{\theta_1}\right)\left(s + 1/T_{\theta_2}\right)}{\not{s}\,(s + \lambda'_1)\left[\zeta'_{SP},\ \omega'_{n_{SP}}\right](s + \lambda'_s)} \doteq \frac{K_q M_{\delta_e} \left(s + 1/T_{\theta_2}\right)}{\left[\zeta'_{SP},\ \omega'_{n_{SP}}\right](s + \lambda'_s)}$$

This transfer function is of conventional order and exhibits the desired short period poles, an overdamped "phugoid" with one pole at the origin, an augmented servo root and the conventional airplane numerator factors. Assuming that the augmented short period frequency is greater than $1/T_{\theta_2}$, the closed loop transfer function will have unity gain in the frequency range $1/T_{\theta_1} < \omega < 1/T_{\theta_2}$.

Closed loop system when $\left|\lambda_2\right| < \left|1/T_{\theta_2}\right|$

$$\frac{q}{q_c} = \frac{K_q M_{\delta_e} s\left(s + 1/T_{\theta_1}\right)\left(s + 1/T_{\theta_2}\right)(s + Z_I)}{s(s + \lambda_1')(s + \lambda_2')\left[\zeta_{SP}', \omega_{n_{SP}}'\right](s + \lambda_s')} \doteq \frac{K_q M_{\delta_e}\left(s + 1/T_{\theta_2}\right)}{\left[\zeta_{SP}', \omega_{n_{SP}}'\right](s + \lambda_s')}$$

where $\left|\lambda_1'\right| < \left|1/T_{\theta_1}\right|$; $\left|\lambda_2'\right| < \left|Z_I\right|$

The closed loop transfer function gain is unity in the frequency range $1/T_{\theta_1} < \omega < \lambda_2'$. The closed loop system is of the same form when the unaugmented short period is complex but in that case

$$\left|\lambda_1'\right| > \left|1/T_{\theta_1}\right| \; ; \; \left|\lambda_2'\right| < \left|Z_I\right|$$

and the closed loop transfer function gain is unity in the frequency range $\lambda_1' < \omega < \lambda_2'$.

The sketches in Figure 3 illustrate the root locus for the three situations described above and indicates the closed loop poles and zeros for the q/q_c and α/q_c transfer functions.

When $\left|\lambda_2\right| < \left|1/T_{\theta_2}\right|$ and when the short period is complex, there will be a dipole at

$$\frac{S + Z_I}{S + \lambda_2'}$$

which will not exactly cancel unless the loop gain is very high. For practical values of loop gain, the residue of the closed loop pole at λ_2' will be low

in all the responses to commands because the zero at Z_I is control system related and appears in all the transfer functions.

The parameters in the control system must be scheduled with configuration, loading and flight condition in order to achieve the indicated pole-zero cancellation and desired short period frequency and damping ratio. The purpose of the study is to establish the values of the control system parameters required to improve the shuttle flying qualities during the terminal portion of the descent and for landing. Variations in gross weight, C.G. location, speed, altitude and flight path angle are considered. The effect on the closed loop dynamics for several conditions of fixing the feedback filter parameters at the optimum for one case is also investigated in the study.

The transfer function of elevator to pitch rate for this control system has the following form.

$$\frac{\delta e}{q} = \frac{K_q P_F}{Z_F} \quad \frac{S + Z_F}{S + P_F} \quad \frac{S + Z_I}{S}$$

The frequency response of $\delta e/q$ is shown on Figure 4 for the two situations that can occur, i.e., for

$$Z_I = \lambda_2 \quad when \quad \left|\lambda_2\right| > \left|1/T_{\theta_2}\right| \quad and$$

$$Z_I = 1/T_{\theta_2} \quad when \left|\lambda_2\right| < \left|1/T_{\theta_2}\right| \quad or \ short \ period \ is \ complex.$$

Figure 4 indicates that the control system effectively feeds back pitch attitude at low frequency and pitch rate at high frequency. The value of the feedback zero, Z_F, determines at what frequency the feedback changes from attitude to rate. The combination of values selected for K_q and Z_F give control of the augmented short period frequency and damping ratio.

The transfer function for elevator deflection in response to the pitch rate command is derived as follows:

$$\frac{\delta e}{q_c} = \frac{q/q_c}{q/\delta e} .$$

This transfer function is as follows for the case where $|\lambda_2| > |1/T_{\theta_2}|$

$$\frac{\delta_e}{q_c} = \frac{\left[\zeta_{ph}, \omega_{n_{ph}}\right]}{s(s+\lambda_1')} \frac{K_q(s-\lambda_1)(s+\lambda_2)}{\left[\zeta'_{SP}, \omega'_{n_{SP}}\right]} \frac{\lambda_s'(s+\lambda_s)}{\lambda_s(s+\lambda_s')}$$

From this equation it can be seen that for a step command q_c, the initial elevator deflection is $\frac{K_q \lambda_s'}{\lambda_s} q_c$ and the static value would be infinite because of the free s in the denominator. Ignoring the low frequency terms of the transfer function, the "static" gain would be

$$\delta_e\Big|_{\text{"static"}} = \frac{K_q \lambda_1 \lambda_2}{\omega'^2_{n_{SP}}}$$

A typical time history of elevator response to a step pitch rate command for an airplane with an aft C.G. location is shown in the following sketch.

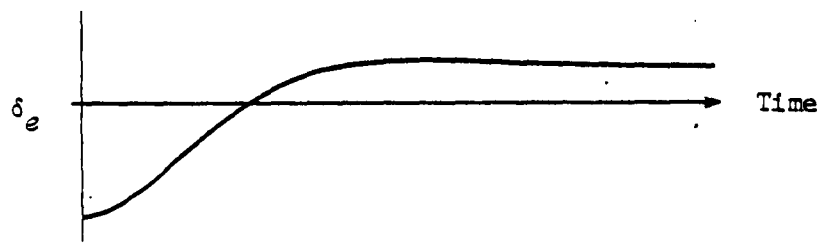

This time history does not include servo dynamics or phugoid terms. The elevator initially responds to the step command and then travels to the "steady state" value which is of opposite sign. The transient dynamics are that of the augmented short period mode. The initial response will be modified by digital time delay, smoothing filter, servo dynamics and the servo rate limit. These effects are included in the analysis and time histories calculated for the shuttle in the body of this report.

The feedback filter zero, Z_F, and the loop gain, K_q, of the Calspan control system were used to augment the short period poles so as to satisfy the $\omega_n^2/n/\alpha$ requirements of MIL-F-8785C and to exhibit a damping ratio of at least $\zeta_{SP} \geq .70$.

The control system proposed by Calspan in Figure 2 includes an active command signal limiter. The equations for the q_c command limits are as follows.

$$+q_L = \frac{g}{V_T}\left[n_z - n_L\right] + q$$

$$-q_L = \frac{g}{V_T}\left[n_z + n_L\right] + q$$

This active limiter together with the pitch rate control system is intended to provide load factor protection that is effective at all attitudes.

The control system of Figure 2 also includes an angle of attack feedback which is open below a selected bias value of angle of attack but becomes active when angle of attack exceeds this bias. The intent of this feature is to require additional control force to command angle of attack greater than the bias or limit value. As the aircraft slows down in the absence of any pilot input and reaches the angle of attack limit, the control system will essentially hold this α, maintaining speed and reducing pitch attitude. The q limit and the angle of attack limiting features were not analyzed in this study.

Calspan has investigated an alternate mechanization of the pitch rate control system which eliminates the lag-lead filter from the feedback path and adds a lead-lag prefilter which operates on the pilot's stick commands. The concept with the prefilter is documented, analyzed and compared to the feedback filter concept in Appendix 2.

Section 3
CONFIGURATIONS AND AERODYNAMIC MODELS

3.1 CONFIGURATIONS

In order to fully evaluate the control systems under investigation various shuttle configurations were chosen. In these configurations velocity, weight, and C.G. position were varied. A summary of these flight configurations is shown in Table 1.

TABLE 1
FLIGHT CONFIGURATIONS

Configuration	1	2	3	4
Velocity, KEAS	290	190	190	190
Altitude (MSL), ft.	10,000	2,500	2,500	2,500
Weight, lb.	240,000	240,000	191,000	240,000
C.G., % L_b	67.5	67.5	65.	65.
Pilot Position (fwd. of C.G.), ft.	50.8	50.8	48.1	48.1
Flight Path Angle, deg.	-20.	-3.	-3.	-3.
Dynamic pressure, lb/ft^2	285.2	122.4	122.4	122.4

Configuration 1 is typical of the shuttle in the upper portion of the approach when it is in a stabilized steep descent. It is a heavy weight configuration with most aft C.G. position. Configurations 2, 3 and 4 are in the final flare portion of the approach with a flight path angle of -3 deg. Weight and C.G. position are varied among them. Configuration 2 is a heavy weight, most aft C.G. configuration which yields the most unstable configuration evaluated. Configuration 3 is a light weight most forward C.G. case, and Configuration 4 a heavy weight, forward C.G. case.

3.2 AERODYNAMICS

The aerodynamics for the various shuttle configurations were taken from the last Total In-Flight Simulator (TIFS) evaluation program in 1979 (Reference 1). A summary of these aerodynamics and other physical characteristics for each configuration is shown in Table 2. The shuttle was trimmed with realistic speed brake deflection to yield the proper stabilized descent angle for Configuration 1 and an approximate 6 ft/sec^2 deceleration for Configurations 2-4. Ground effect was not taken into account.

The following linearized longitudinal equations of motion were used in the analysis:

$$\dot{V} = -g\sin\gamma - \frac{\bar{q}S\,C_D}{m}$$

where $C_D = C_{D_o} + C_{D_\alpha}\,\alpha + C_{D_{\delta_e}}\,\delta_e$

C_{D_o} includes speed brake and landing gear effect

$$\dot{\alpha} = q + \frac{1}{V}\left[g\cos\theta - \frac{\bar{q}S\,C_L}{m}\right]$$

where $C_L = C_{L_o} + C_{L_\alpha}\,\alpha + C_{L_{\delta_e}}\,\delta_e$

$$\dot{q} = \frac{\bar{q}\,S\,\bar{c}}{I_{yy}}\left[C_m + \frac{CG - 65}{100}\,\frac{L_b}{\bar{c}}\,C_L\right]$$

where $C_m = C_{m_o} + C_{m_\alpha}\,\alpha + C_{m_{\delta_e}}\,\delta e + C_{m_q}\,\frac{q\bar{c}}{2V}$

C_{m_o} includes landing gear effect

TABLE 2

AERODYNAMIC CHARACTERISTICS

Constant physical characteristics:

Wing area, S, ft^2 2690

Mean aerodynamic chord, $\bar{c}$, ft. 39.57

Reference body length, L_b, ft. 107.53

(All angular coefficients in units of radians)

Configuration	1	2	3	4
True airspeed, V, ft/sec	570.	333.	333.	333.
Weight	240,000	240,000	191,000	240,000
Pitch moment of inertia, I_{yy}, slug-ft^2	7,450,000	7,450,000	6,760,000	7,450,000
CG, % L_b	67.5	67.5	65.	65.
C_{D_α}	.252	.762	.607	.785
$C_{D_{\delta_e}}$	.149	.309	.229	.281
C_{L_α}	2.73	2.73	2.73	2.73
$C_{L_{\delta_e}}$	.98	.98	.98	.98
C_{m_α}	.029	.109	-.029	-.029
C_{m_q}	-2.69	-1.01	-1.15	-.85
$C_{m_{\delta_e}}$	-.48	-.45	-.50	-.50
Trim - α, deg.	5.0	13.3	12.1	15.3
θ, deg.	-15.0	10.3	9.1	12.3
γ, deg.	-20	-3	-3	-3
δ_e, deg.	5.4	7.7	2.3	2.0
δ_{SB}, %	100.	50.	50.	50.
Landing gear	up	down	down	down
$C_{L_{Trim}}$	.294	.728	.579	.728
$C_{D_{Trim}}$	.107	.180	.140	.177

3.3 UNAUGMENTED CHARACTERISTICS

The longitudinal characteristics were calculated for the unaugmented configurations. The full transfer functions are presented in the Appendix. The significant characteristics are shown in Table 3.

TABLE 3

UNAUGMENTED CHARACTERISTICS

Configuration	1 (290 KEAS, Heavy Wt., Aft C.G.)	2 (190 KEAS, Light Wt., Aft C.G.)	3 (190 KEAS, Light Wt., Fwd C.G.)	4 (190 KEAS Heavy Wt., Fwd C.G.)
Characteristic Eq. Roots:				
ζ_{SP} or (λ_1)	(.066)	(.268)	.87	.82
ω_{SP} (λ_2)	(-.793)	(-.700)	.364	.314
ζ_{ph} or ζ_3	.80	.32	.023	-.049
ω_{ph} ω_3	.127	.139	.089	.099
Pitch Rate Numerator:				
$1/T_{\theta_2}$	.52	.41	.45	.36
$n_z/\alpha = \frac{V}{g}\frac{1}{T_{\theta_2}}$	9.21	4.20	4.67	3.75

It can be seen that aft C.G. Configurations 1 and 2 are statically unstable. Configuration 2 is the most unstable with a time to double amplitude of 2.6 sec ($ln2/\lambda_1$) for the unstable pole. The forward C.G. Configurations 3 and 4 are stable but have very low short period frequencies. These configurations are spotted on the MIL-8785C short-period frequency requirement plot in Figure 5. It is apparent that all unaugmented configurations are worse than level 3 on this requirement, with Configurations 1 and 2 being statically unstable and Configurations 3 and 4 clearly lower than the Level 3 boundary.

Section 4
CONTROL SYSTEMS

4.1 INTRODUCTION

This section describes the pitch rate control systems which were investigated in this study. Three control systems were defined to augment each of the four flight configurations under study. These control systems are the Calspan-designed, NASA/Revised, and Orbital Flight Test (OFT) flight control systems.

The Calspan-designed control system is the one of primary interest in this study. The philosophy behind its design is described in Section 2. The NASA/Revised control system is one which the NASA/Dryden Flight Research Facility has developed to improve the flying qualities of the shuttle in landing approach. The OFT control system is the one which is presently in the shuttle. The latter two control systems were analyzed in the same manner as the Calspan system in order to provide a comparison for its characteristics.

Block diagrams for each of these control systems are shown in Figures 6, 7, and 8.

4.2 COMMON CHARACTERISTICS

There are a few common characteristics in each of the control systems. First of all, the input to each of the systems is the pitch rate command (q_{cMD}) and not the pilot force input or rotational hand controller deflection. This avoids complicating the analyses with the nonlinear feel characteristics, the pilot-induced-oscillation suppressor dynamics, and nonlinear command gearing.

The actuator is the same for each control system. It is modelled as a cascade of a first and second order filter:

$$\text{Actuator} = \frac{(27.65)(36^2)}{(s + 27.65)[s^2 + (.707)(36.)s + 36^2]}$$

A body bending filter (BBF) is included in each control system, but at different locations, to remove structural dynamics from the closed loop system. It is defined as:

$$\text{BBF} = \frac{s^2 + 2(.04)(32.75)s + 32.75^2}{s^2 + 2(.4)(20)s + 20^2} \cdot \left(\frac{20}{32.75}\right)^2$$

A pure time delay of .040 sec is included in the forward loop of each control system to account for .015 sec computational delay and .025 sec actuator delay. In addition, there is an average sampling delay of .020 sec on the input.

4.3 CALSPAN CONTROL SYSTEM

The Calspan-designed control system is shown in Figure 6. The primary feedback is filtered pitch rate. The control system uses proportional plus integral gains in the forward path.

The following methodology is used to choose the various gains and filter roots:

Z_I - Integrator gain is set equal to the most stable real pole of the unaugmented shuttle (but not less than $1/T_{\theta_2}$, or set equal to $1/T_{\theta_2}$ if the aircraft has a complex pair for the short period mode.

P_F - Pitch rate feedback filter pole set equal to $1/T_{\theta_2}$

Z_F - Pitch rate feedback filter zero chosen to yield good augmented ζ_{SP} and ω_{SP} (The system is robust if Z_F is not less than any unaugmented real pole or zero).

K_q - Loop gain chosen to yield good augmented ζ_{SP} and ω_{SP}.

A root locus technique is used to choose Z_F and K_q. All of the four parameters change with flight condition, weight, and C.G. postition. Table 4 shows the values of the parameters chosen for the Calspan system. The Z_F and K_q were chosen to yield a Level 1 short period mode according to MIL-8785C requirements (Reference 2). The desired damping ratio was .71. The desired short period frequency was that which yielded a $\frac{\omega}{N_z/\alpha}$ or Control Anticipation Parameter (CAP) of approximately .32 (see Figure 9). This is twice the lower Level 1 boundary for CAP. Higher values of CAP could be achieved but would require higher gains and elevon rates. Values of the augmented short period mode are also shown in Table 4. Complete transfer functions are presented in Appendix 1.

Functional variations of the gains with respect to velocity, weight, and C.G. were calculated. Configuration 1 was compared to 2 to determine the effects of velocity alone (290 to 190 KEAS). It should be noted that the pitch angle also changed from -15 to +10 degrees in these configurations and the resulting gravity vector orientation also has an effect on the gains. Configuration 4 was compared to 3 to determine the effects of weight alone (240,000 to 191,000 lb). Configuration 4 was compared to 2 to determine the effects of C.G. shift alone (most forward, 65% to most aft, 67.5%). Ratios of the changes in configurational parameters and system gains were calculated and results are shown in Table 5.

A direct functional relation with velocity was not obtained due to the additional effects of pitch attitude, but it appears that P_F and Z_F are directly proportional, while K_q is inversely proportional to velocity. This would be similar to the GDQ gain in the NASA/Revised and OFT system being inversely proportional to the square root of $\bar{q}$. Velocity has only a minor effect on Z_I . The Z_I , P_F and Z_F gains are inversely proportional, while the K_q gain has only a small functional relation to weight. As the C.G. was moved aft through its maximum range of 2.5%L_b, the effect on the gains was to increase Z_I 40% per 1% C.G. travel and increase K_q 15% per 1% C.G. travel. The C.G. effects on P_F and Z_F were minor.

Other features of the Calspan control system include a notch filter in the command path and a body bending filter in the q feedback path. The notch filter at 25 Hz (157 r/s) is used to smooth the stair stepping command out of the digital computer at its update rate. It replaces the smoothing filter used in the NASA/Revised and OFT systems and accomplishes similar results with less lag.

$$\text{Notch Filter} = \frac{s^2 + 157^2}{s^2 + 2(.5)(157)s + 157^2}$$

The body bending filter (defined earlier) is in the feedback path instead of the forward path as it is in the OFT, to reduce command path delay. It still eliminates structural mode excitation in the closed loop system.

TABLE 4

CALSPAN CONTROL SYSTEM GAINS AND CHARACTERISTICS

Configuration	1 240,000 lb. 290Kt.,AFT CG	2 240,000 lb. 190Kt.,AFT CG	3 191,000 lb. 190Kt.,FWD CG	4 240,000 lb. 190Kt.,FWD CG
Z_I	.793	.700	.45	.36
P_F	.52	.41	.45	.36
Z_F	1.1	.7 (on lower limit)	.8	.7
K_q	2.2	3.9	2.6	2.8
Augmented:				
ζ_{SP}	.71	.71	.72	.71
ω_{SP}	1.74	1.28	1.22	1.07
$\omega^2 \Big/ \frac{N_z}{\alpha}$	.33	.39	.33	.32

TABLE 5

VARIATION OF GAINS WITH CONFIGURATION PARAMETERS

Parameter Variation	Velocity* $\frac{\text{Conf.1}}{\text{Conf.2}} = \frac{290}{190} = 1.53$	Weight $\frac{\text{Conf.4}}{\text{Conf.3}} = \frac{240000}{191000} = 1.26$	CG Conf. 4 → Conf. 2 most fwd → most aft = 2.5% L_b
Z_I Ratio	1.13	.80 = 1/1.25	1.94 ∿ 40% incr/1% CG
P_F Ratio	1.27	.80 = 1/1.25	1.14
Z_F Ratio	1.57	.88 = 1/1.14	1.0
K_q Ratio	.56 = 1/1.77	1.08	1.39 ∿ 15% incr/1% CG

* θ also changes $-15°/+10°$

4.4 NASA/REVISED CONTROL SYSTEM

The NASA/Revised control system is shown in Figure 7. The primary feedback is filtered pitch rate, the forward path has positive feedback of elevon position. The positive feedback puts a pole at the origin just like an integral in the forward path would.

The NASA/Revised control system includes the following features:

Pitch rate is fedback through a body bending filter (same as that in Calspan system) and proportional plus lead/lag filter. The lead/lag filter is:

$$\text{feedback lead/lag} = \frac{.6(-7.81)(s - 3.2)(s + 2)}{(s + 100)(s + .5)}$$

The steady state gain of q feedback is 1.6, so a q_{CMD} gain of 1.6 is used to yield unity closed loop gain for comparison to the other control systems.

The forward loop gain is GDQ times a lead/lag filter where:

$$GDQ = 16/\sqrt{\bar{q}} = \begin{matrix} .947 \text{ @ } 290 \text{ KEAS} \\ 1.446 \text{ @ } 190 \text{ KEAS} \end{matrix}$$

$$\text{forward loop lead/lag} = 1.5\,\frac{(s + 2)}{(s + 3)}$$

A smoothing filter is inserted in the command path to smooth the descretization steps:

$$\frac{36^2}{[s^2 + (2)(.7)(36)s + 36^2]}$$

The elevon feedback lag filter is:

$$\frac{1}{(s + 1)}$$

4.5 OFT CONTROL SYSTEM

The OFT control system is shown in Figure 8. It is similar to the NASA/Revised system, but has the following differences:

The feedback path is straight pitch rate without the additional lead/lag filter path.

The forward loop GDQ gain is the same but the lead/lag filter is:

$$1.42\ \frac{(s + .588)}{(s + .833)}$$

The body bending filter is in the command path instead of the feedback path.

The elevon feedback filter is:

$$\frac{1.5}{(s + 1.5)} \quad .$$

Section 5
AUGMENTED CHARACTERISTICS AND TIME HISTORIES

5.1 AUGMENTED CHARACTERISTICS

The augmented characteristics for the shuttle with the three control systems under study were obtained. The complete transfer functions are presented in Appendix 1. A comparison of the augmented short period mode is shown in Table 6 and plotted on the MIL-8785C short period requirement in Figure 9. It is apparent that all of the control systems yield fairly similar Level 1 short period roots. However, the complete pole-zero locations for the various control systems are vastly different. Figures 10, 11 and 12 show the pole and zero locations for Configuration 2 with the Calspan, NASA/Revised and OFT systems, respectively. Pitch rate and angle of attack transfer functions with only the dominant lower frequency roots are shown. Also shown are the approximate equivalent roots when pole/zero cancellations are made.

TABLE 6
AUGMENTED SHORT PERIOD MODE

Configuration	Control System	ζ_{SP}	ω_{SP}
1 (290 KEAS, Heavy Weight, Aft CG)	Calspan	.71	1.74
	NASA	.79	1.27
	OFT	($\lambda_1 = -2.98$)	($\lambda_2 = -1.13$)
2 (190 KEAS, Heavy Weight, Aft CG)	Calspan	.71	1.28
	NASA	.50	1.08
	OFT	.82	1.05
3 (190 KEAS, Light Weight, Fwd CG)	Calspan	.72	1.22
	NASA	.61	1.32
	OFT	.83	1.46
4 (190 KEAS, Heavy Weight, Fwd CG)	Calspan	.71	1.07
	NASA	.55	1.27
	OFT	.77	1.34

The Calspan system yields a first order zero over a well damped second order pole for pitch rate and just a well damped second order pole in angle of attack. The zero at $1/T_{\theta_2}$ that preserved in pitch rate produces a large overshoot for a step input. Angle of attack will come to a steady state until the speed starts to bleed off.

The NASA/Revised system retains the $1/T_{\theta_2}$ zero in pitch rate but the real pole is not cancelled. This results in a pitch rate overshoot plus some additional effects due to the residue of the real pole. Angle of attack also has the effects of the uncancelled real pole.

The OFT system essentially yields a pure, well damped second order system in pitch rate with the zero at $1/T_{\theta_2}$ being effectively cancelled. No pitch rate overshoot will be produced for a step input. The angle of attack transfer function then contains a pole at $1/T_{\theta_2}$ which will dominate its response, preventing it from obtaining a steady state before the speed bleeds off.

5.2 TIME HISTORIES

Time histories were calculated with each control system for two types of inputs:

- q_{CMD} step of one deg/sec (.01745 r/s)
- Discrete (one-cosine) angle of attack gust equivalent to a maximum 10 ft/sec vertical gust over a 4 second period:

$$\alpha_{gust} = \frac{10}{2V_{True}} \left(1-\cos \frac{4\pi}{2} t\right)$$

The time histories were run for 8 seconds. The complete set of time histories are presented for the q_{CMD} step input in Figures 13 through 24 for the twelve control system/configuration combinations. The discrete α gust inputs produced very similar responses for each control system used. Therefore, only the time histories for Calspan Configuration 2 are presented (Figure 25). The following traces are shown: (All are incremental from time = 0).

Q, pitch rate, r/s
TH, pitch attitude, r
V, true airspeed, ft/sec
AL, angle of attack, r
DE, elevon, r
*DE**, elevon rate, r/s
NZP and *C.G.*, normal acceleration at pilot and center of gravity, *g*
*H*P* and *C.G.*, altitude rate at pilot and center of gravity, ft/sec
HP and *C.G.*, altitude at pilot and center of gravity, ft.

Section 6
ANALYSIS

6.1 INTRODUCTION

This section describes the analysis that was performed on the various shuttle configurations and control systems. Most of the analyses were carried out for all of the configurations but some of the techniques were only applied to Configuration 2 (190 KEAS, heavy weight, aft C.G.), the most unstable configuration, when analyses of one configuration was sufficient to demonstrate a point.

Analyses techniques included time domain and frequency domain techniques. In the time domain, features of the time histories are discussed. General characteristics, time delay, rise time, elevon rate, flare response are covered. In the frequency domain the bandwidth and phase delay criteria, of the aircraft alone, closed loop Neal-Smith analysis, and multi-loop control analysis are discussed. The effects of simplifying the Calspan system by using fixed time constants in the feedback filter instead of scheduling them with flight condition is also investigated.

6.2 PITCH RATE COMMAND-STEP INPUT TIME HISTORY CHARACTERISTICS

The following discussion refers to the time histories of the various control system/configuration combinations for the one-degree/sec pitch rate command (q_{CMD}) inputs:

Figure No.	Control System/Configuration Number
13	Calspan/1
14	NASA/1
15	OFT/1
16	Calspan/2
17	NASA/2
18	OFT/2
19	Calspan/3
20	NASA/3
21	OFT/3
22	Calspan/4
23	NASA/4
24	OFT/4

The most readily apparent feature of these time histories is the shape of the pitch rate response. All of the Calspan configurations have larger overshoots (70-100% of steady state) compared to the overshoots with the NASA/Revised system (70-80%) and relatively small overshoot with the OFT system (15-35%). Along with the overshoot in pitch rate for the Calspan and NASA systems comes a fairly rapid angle of attack response which reaches a a well defined steady state. The angle of attack for the OFT system continuously ramps up without reaching any steady state. The cause of this behavior is the pole-zero locations described in the previous section. With the Calspan system the zero in the q/q_{CMD} transfer function at $1/T_{\theta_2}$ is preserved producing a large overshoot. In the α/q_{CMD} transfer function this zero is not present, resulting in a well damped second order response. With the OFT system the zero at $1/T_{\theta_2}$ is effectively cancelled out in the q/q_{CMD} transfer function resulting in a slow non-overshooting well damped pitch rate response. In addition, the α/q_{CMD} transfer function of the OFT has a pole at $1/T_{\theta_2}$ which makes its response third order and prevents it from achieving a steady state before long term velocity changes take effect. The NASA/Revised system responses are closer to the Calspan responses than the OFT. The zero

at $1/T_{\theta_2}$ is preserved but an extra pole-zero pair is introduced which reduces the overshoot tendency in q and increases the effective order of the q/q_{CMD} transfer function.

In summary, these characteristics indicate that the OFT system achieves a pitch rate response with small overshoot at the expense of slow angle of attack response, while the Calspan and NASA/Revised systems yield rapid angle of attack control and more rapid pitch rate response at the expense of pitch rate overshoot.

It is postulated that the type of response that the Calspan system provides will exhibit better flying qualities in the flare portion of the approach.

Specific numerical measurements were made from the pitch rate time histories and compared to recommended flying qualities criteria for landing approach(Reference 3). Expanded time histories of the first 1.8 seconds were run to make measurements easier. These are presented in Figures 26 through 37 for each of the control system/configuration combinations. On each of these figures a maximum slope line is drawn to intersect the time axis. This maximum slope intercept is called t_1 or effective time delay. (Included in this t_1 is the average sampling delay of .02 sec which is not shown in the figures). The time t_2 is the time at which the maximum slope reaches the steady state of one deg/sec (.01745 rad/sec). The incremental time between t_1 and t_2 is called Δt or effective rise time. The rise time, Δt, can be related to $\omega_{SP}^2/N_z/\alpha$ by the following:

$$\frac{\omega_{SP}^2}{N_z/\alpha} = \frac{\dot{q}_{Initial}}{N_{z_{ss}}} = \frac{q_{ss}/\Delta t}{q_{ss}\, V_T/g} = \frac{g}{V_T\, \Delta t}$$

The maximum and minimum limits on $g/V_T\ \Delta t$ are analogous to ω_{SP}^2/N_z limits on MIL-8785C short period frequency requirements.

Values for t_1 , Δt, and $g/V_T \Delta t$ are presented in Table 7. They are also presented in Figure 38, along with flying qualities level boundaries from Reference 3. It is apparent that the Calspan system yields middle Level 2 results, while the NASA/Revised system yields lower Level 2, and the OFT system worse than Level 3 results. The primary reason for this is the time delay difference. The Calspan and NASA system have much reduced time delay primarily due to the placement of the body bending filter in the feedback path rather than the forward path as in the OFT. In addition, the Calspan system replaces the smoothing filter with a notch filter, further reducing the time delay. The rise time parameter with the Calspan and NASA systems are significantly better than with the OFT. This is primarily due to the pitch rate overshoot which allows the maximum slope to be steeper with the Calspan and NASA systems, even though the ω_{SP} are similar for all three systems.

Another parameter measurement taken from the step-input time histories was the effective time delay in altitude rate at the pilot station - $t_{1_{\dot{h}_p}}$ (which is the same as in flight path angle as $\gamma = \dot{h}/V$). This is measured similarly to t_{1_q} on the q time history. The results are presented in Table 7 and Figure 39. No criteria has been presently formulated on $t_{1_{\dot{h}_p}}$, but it can be seen that significantly shorter flight path time delays are achieved as one goes from the OFT to NASA and then to the Calspan control system. With further examination of the complete time histories (Figures 13 through 24) one can see the relatively large lags in the normal acceleration, $\dot{h}$, and h time histories. With the pilot sitting slightly behind the instantaneous center of rotation there is no lead in the perceived N_z due to $\dot{q}$ as there is in a conventional aircraft with the pilot forward of the center of rotation. One can vividly see the non-minimum phase effect on N_z at the C.G. in these figures. A recent experiment was run in which effects of pilot position in large aircraft were investigated (Reference 4). It was shown that configurations which yielded Level 1 flying qualities ratings in the flare portion of the approach with the pilot forward of the center of rotation, deteriorated to Level 3 when the pilot was far enough aft of the center of rotation. Lack of initial N_z , $\dot{h}$, and h cues caused the pilot to overcontrol and PIO.

TABLE 7

COMPARISON OF CALSPAN, NASA/REVISED, AND OFT CONTROL SYSTEMS - TIME HISTORY CHARACTERISTICS

Configuration	① 240,000 # 290 Kt, $\gamma = -20°$ AFT C.G.			② 240,000 # 190 Kt, $\gamma = -3°$ AFT C.G.			③ 191,000 # 190 Kt, $\gamma = -3°$ FWD C.G.			④ 240,000 # 190 Kt, $\gamma = -3°$ FWD C.G.		
	CALSPAN	NASA	OFT	CALSPAN	NASA	OFT	CALSPAN	NASA	OFT	CALSPAN	NASA	OFT
1 deg/sec q_{CMD} Step Input:												
t_{1_q}, sec	.14	.17	.22	.15	.17	.22	.14	.17	.22	.15	.17	.22
Δt, sec	.235	.255	.38	.30	.40	.59	.40	.33	.48	.39	.36	.54
$g/V\ \Delta t$, sec^{-2}	.24	.22	.15	.32	.24	.16	.24	.29	.20	.24	.27	.18
$t_{1_{\dot{h}_p}}$, sec	.87	1.12	1.67	1.02	1.37	1.72	1.22	1.17	1.62	1.28	1.22	1.76
$max\ \delta_e$, deg/sec	23.	23.	7.	40.	32.	11.	26.	32.	11.	29.	32.	11.
10 ft/sec Vertical *(1-cos)* Gust:												
$max\ N_{z_p}$, g's	.11	.11	.11	.085	.085	.085	.09	.09	.09	.07	.07	.07
$\Delta\ h_{CG}$ @ 8sec, ft	18.	18.	18.	14.	15.	15.	15.	15.	15.	13.	13.	13.

Where : t_1, Δt defined from:

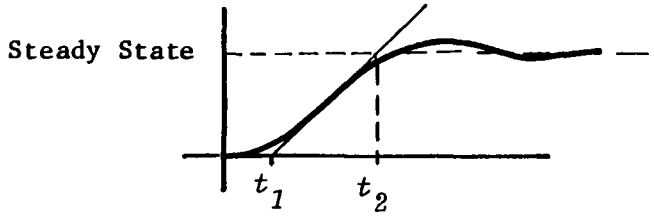

$\Delta t = t_2 - t_1$

One further characteristic of interest on these time histories is the elevon rate trace. The maximum elevon rate is tabulated in Table 7. It is apparent that significantly higher elevon rates are commanded by the step input with the Calspan and NASA/Revised systems than with the OFT system. It should be noted that large sharp step inputs used in these time histories may not be representative of actual pilot inputs. In fact, with a control system which yields better flying qualities, a pilot may use smaller and slower inputs. It cannot be determined if elevon rate limits will be saturated without running a piloted simulation. One additional benefit of the Calspan system over the NASA or OFT system is the lack of the slight oscillations or "ringing" in the elevon rate trace. The source of this oscillation is the body bending filter pole at 20 rad/sec and .4 damping ratio. In the closed-loop system this root migrates to lower damping for the OFT and NASA systems than it does for the Calspan design. The higher frequency gain in the q feedback path is also much higher in the NASA system than the Calspan system (e.g., 3.5 times higher for Configuration 2 when including the effects of K_q , GDQ , and the (lead/lag) which may result in a noisy elevon command.

6.3 DISCRETE VERTICAL GUST TIME HISTORIES

Time histories were obtained for discrete vertical gust inputs into each control system/configuration combination. The gust had the form of a $(1\text{-}cos)$ curve with a period of 4 seconds and a maximum amplitude corresponding to 10 ft/sec:

$$\alpha_{gust} = \frac{10}{2V_{True}}\left(1\text{-}cos\ \frac{4\pi}{2}\ t\right)$$

The resulting time histories were similar for each control system, with only slight variations with flight configuration. Therefore, only the resulting time histories for the Calspan Configuration 2 are presented (Figure 25). The reason for the similarity between the cases is that all the control systems provide attitude stabilization. Since there is no angle of attack fed back to the elevon and all configurations have low aerodynamic moments due to angle of

attack, the only significant response is a heaving motion with little pitching. Measurements were made of the maximum N_{z_p} and incremental altitude at 8 sec and are listed in Table 7.

6.4 FLARE TIME HISTORIES

Time histories of a typical flare profile were run for each control system on Configuration 2 (heavy weight, aft C.G.). The shuttle was assumed to be descending with a flight path angle of -3 degrees which is -17.43 ft/sec at the true airspeed of 333 ft/sec. A one deg/sec pitch rate command was used to arrest the sink rate and was held in until the sink rate was reduced to -7 ft/sec. The altitude at which the flare command was initiated was chosen such that the minimum sink rate occurred at a C.G. altitude of ten to fifteen feet. The resulting time histories are presented in Figures 40 through 42 for the Calspan, NASA/Revised, and OFT control systems, respectively. Pitch rate (Q), pitch attitude (TH), angle of attack (AL), altitude (HCG), altitude rate (H*CG), and pitch rate command (QCMD) are shown.

It can be seen from the altitude time history that for the Calspan system, the sink rate reduces to near zero, then the aircraft settles down with no ballooning tendency. With the NASA/Revised system, a slight ballooning (2-3 feet) is seen. Using the same flare technique (hold one deg/sec pitch rate command until -7 ft/sec achieved), the OFT system results in a significant overcontrol or ballooning tendency with the shuttle rising 5 to 10 feet before starting to descend again. Of course, the pilot might use a different flare technique when he knew that this floating tendency was present. He could start his flare command earlier (it already starts about ten feet higher with the OFT than with the Calspan system) with a smaller command, and perhaps reverse his command near the end. It can be seen that this would require more pilot compensation and perhaps lead to a PIO.

To see what form the pilot's pitch rate command would have to take with the NASA/Revised or OFT to exactly match the flare response of the Calspan system, the following calculations are made.

Flare attitude profile:

$$\theta \text{ (flare)} = \frac{N^{\theta}_{q_{CMD}}}{D} \cdot q_{CMD} \text{ (flare)}$$

Equate OFT and Calspan flare attitude:

$$\theta \text{ (flare)}_{OFT} = \theta \text{ (flare)}_{CALSPAN}$$

$$\left[\frac{N^{\theta}_{q_{CMD}}}{D}\right]_{OFT} \cdot q_{CMD_{OFT}} = \left[\frac{N^{\theta}_{q_{CMD}}}{D}\right]_{CALSPAN} \cdot q_{CMD_{CALSPAN}}$$

Solve for OFT flare command:

$$q_{CMD_{OFT}} = \left[\frac{D}{N^{\theta}_{q_{CMD}}}\right]_{OFT} \cdot \left[\frac{N^{\theta}_{q_{CMD}}}{D}\right]_{CALSPAN} \cdot q_{CMD_{CALSPAN}}$$

Similarly, the NASA/Revised flare command is:

$$q_{CMD_{NASA}} = \left[\frac{D}{N^{\theta}_{q_{CMD}}}\right]_{NASA} \left[\frac{N^{\theta}_{q_{CMD}}}{D}\right]_{CALSPAN} \cdot q_{CMD_{CALSPAN}}$$

Using a 3.3 second, one deg/sec pitch rate command for the Calspan flare input and simplifying the transfer functions to include only the roots with frequency less than $\omega = 10$ sec^{-1}, q_{CMD} (flare) for the NASA/Revised and OFT control systems were calculated. Figure 43 shows the results. It is readily apparent that flare inputs required to match Calspan response with the NASA/Revised and OFT systems are much more complex than the simple step in/out required for the Calspan system. The flare commands shown would be very difficult to perform, since they require pilot lead compensation (seen in the overdriven commands and reversal). Pilots are inhibited from making the control reversal required for the OFT when near the ground because the large time delay makes overcontrol likely.

There are some other characteristics seen in these flare time histories which illustrate the improvement in controllability as one goes from the OFT to NASA/Revised to Calspan systems. The time between the release of the pitch rate command and maximum incremental altitude rate (equivalent to maximum flight path angle change) reduces from 3.2 seconds with the OFT to 1.9 seconds with the NASA/Revised and 1.7 seconds with the Calspan system. With the flight path response more solid with less of a tail, the pilot should be able to predict the final sink rate much easier with the Calspan system.

The pitch rate and attitude time histories also reveal some interesting characteristics. With the OFT system, there is only a slight overshoot in pitch rate compared to the large overshoot with the Calspan and NASA/Revised systems. The attitude response, though slow, stops very close to where it is when the command is released for the OFT system instead of dropping back about 25% as with the Calspan and NASA/Revised systems. If the OFT did not have excessive time delay, this system might provide more precise attitude control which may make the aircraft more pleasant to fly in the low gain outer approach portion of the landing task. In the flare maneuver however, the attitude control characteristic is not such an advantageous feature. The non-overshooting pitch rate is accompanied by an angle of attack response with a long response time. It takes longer to change angle of attack and thereby flight path angle, and the angle of attack holds up much longer when the pitch rate command is removed. This results in a long tail or response time in altitude rate or flight path angle. Overcontrol may easily occur as flight path angle continues to change long after control is released. With the Calspan system, it can be seen that the pitch attitude drops back as the angle of attack returns to near the trim value which results in a much more precise and crisp control of the altitude rate and flight path angle. Less pilot compensation is required to predict where the final sink rate will be and the overcontrolling and ballooning tendency is greatly reduced.

6.5 OPEN-LOOP BANDWIDTH ANALYSIS

The open-loop (no pilot loop closure) shuttle configurations were analyzed according to the bandwidth criterion proposed for the flying qualities MIL Standard (Reference 5). For this method the attitude to pitch rate command transfer function (θ/q_{CMD}) is analyzed to obtain the bandwidth and phase delay. Included in the transfer function is the .04 sec delay in the augmentation loop and the .02 sec sampling delay. The bandwidth is defined as the minimum of the following two frequencies:

- Frequency for 45° phase margin (i.e., frequency at which the phase lag is -135°)
- The crossover frequency existing when the gain is adjusted for 6 dB margin at the frequency for which the phase lag is -180°.

One can easily measure these frequencies off of a Nichols chart which plots open-loop amplitude versus phase.

Another parameter in the bandwidth criteria is the phase delay, τ_p which is a measure of phase rolloff and is similar to equivalent time delay. The phase delay is measured as the time delay associated with the incremental phase lag beyond -180°.

$$\tau_p \ (sec) = \frac{-\left(\phi_{2(\omega_{-180})} + 180\right)}{(57.3)2(\omega_{-180})}$$

This parameter can also be measured off of a Nichols chart.

All of the shuttle control system/configurations were plotted on Nichols charts. Only plots for Configuration 2 are presented in Figures 44 through 46. For all cases the bandwidth was phase limited (i.e., ω_{BW} at $\phi = -135°$. The measured ω_{BW} and τ_p are shown in Table 8 and plotted in Figure 47 against the proposed MIL Standard boundaries.

It is apparent that the OFT configurations are border line Level 3 while the NASA/Revised and Calspan control systems progressively yield better Level 2 values. Generally, higher bandwidth and reduced phase delay is achieved as you go from the OFT to Calspan control system.

6.6 NEAL-SMITH ANALYSIS

The Neal-Smith closed loop flying qualities criterion was originally developed as a longitudinal flying qualities evaluation tool, or "yardstick," for highly augmented fighter aircraft performing precision tracking tasks (Reference 6). The application of the criterion was later extended to the approach and landing task (Reference 7). Complete details on the criterion are contained in Reference 6. Briefly, the criterion assumes a simple closed-loop pitch attitude tracking task as shown in Figure 48. The pilot block in the closed loop should be viewed, more properly, as a pitch attitude compensator since even though the form of the "pilot model" used is representative, the model was not experimentally confirmed. The criterion represents a "flying qualities test" and as such is not dependent on the accuracy of the "pilot model" assumed.

The criterion assumes a certain "performance standard," or degree of aggressiveness, with which the "pilot" closes the loop. This standard is defined in the frequency domain as a bandwidth frequency (ω_B). This bandwidth is task dependent; the value for a particular task is determined emperically using pilot rating and comment data to obtain the best overall correlation with the criterion parameters. For a given desired bandwidth, the "loop is closed" and the compensator, or pilot model, parameters are varied to yield the best overall closed-loop performance.

TABLE 8

COMPARISON OF CALSPAN, NASA/REVISED AND OFT CONTROL SYSTEMS - ATTITUDE BANDWIDTH CRITERIA

Configuration	① 240,000 # 290 Kt, $\gamma = -20°$ AFT C.G.			② 240,000 # 190 Kt, $\gamma = -3°$ AFT C.G.			③ 191,000 # 190 Kt, $\gamma = -3°$ FWD C.G.			④ 240,000 # 190 Kt, $\gamma = -3°$ FWD C.G.		
	CALSPAN	NASA	OFT	CALSPAN	NASA	OFT	CALSPAN	NASA	OFT	CALSPAN	NASA	OFT
Bandwidth, open-loop (θ/q_{CMD}), ω_{BW} @ 45° phase margin rad/sec	2.1	2.1	1.6	1.6	1.3	1.0	1.5	1.7	1.4	1.4	1.5	1.3
Phase Delay, τ_p, sec $= \frac{-\left(\phi_{2\omega_{-180}} + 180\right)}{57.3\ 2(\omega_{-180})}$	.13	.17	.18	.13	.15	.17	.12	.16	.18	.12	.15	.18

The criterion output parameters are the pilot compensation (workload) required and the resulting closed-loop performance as measured by the maximum value of closed-loop resonance $\left|\theta/\theta_c\right|_{max}$. Low frequency performance is constrained by limiting the "droop" up to the bandwidth frequency. These criterion parameters are illustrated in Figure 49.

Evaluation of a specific configuration using the Neal-Smith criterion consists of the following steps:

- Specify the bandwidth appropriate for the task; must be determined for each task by data correlation.

- Adjust pilot model parameters, the compensation, (using a fixed value of time delay) to meet the "performance standard" set by the bandwidth requirement.

- Measure the closed-loop compensation required (pilot workload) and the closed-loop maximum resonance $\left|\theta/\theta_c\right|_{max}$.

- Typically, pilot workload is measured by the phase angle of the compensation required at the bandwidth frequency (ϕ_{pc}).

- Plot measured values against Neal-Smith flying qualities boundaries to evaluate the flying qualities. Flying qualities boundaries are shown in Figure 50; typical pilot comments around the Neal-Smith parameter plane are illustrated in Figure 51.

Because the closed-loop, pilot-airplane dynamic system has been modeled as a negative feedback system with unity gain in the feedback path, it is also possible to relate the dynamic characteristics of the elements in the forward loop, $\theta/\theta_\varepsilon = Y_{p_\theta} Y_{c_\theta}$, to the dynamic characteristics of the closed-loop system, $\theta/\theta_c = \frac{Y_{p_\theta} Y_{c_\theta}}{1+Y_{p_\theta} Y_{c_\theta}}$, through use of a Nichols diagram, (Figure 52). This diagram consists of the superposition of two grid systems. The rectangular grid is the magnitude and phase of the forward loop dynamic elements $Y_{p_\theta} Y_{c_\theta}$ and the curved grid system represents the magnitude and phase of the closed-loop system $\theta/\theta_c = \frac{Y_{p_\theta} Y_{c_\theta}}{1+Y_{p_\theta} Y_{c_\theta}}$. Therefore, one can determine the closed-loop dynamic characteristics by plotting the magnitude and phase data of $Y_{p_\theta} Y_{c_\theta}$ for a range of frequency on the rectangular grid.

For the analysis of the shuttle configurations, only a lead term was necessary in the pilot model. The time delay used in the pilot model was .25 sec and included the .02 sec sampling delay.

$$\text{Pilot Model} = K_{p_\theta} e^{-.25s} (\tau_{Lead}\, s + 1)$$

A series of runs were made with each control system/configuration combination to determine the pilot compensation required to achieve closed-loop bandwidths of 1.5, 2.0, 2.5, and 3.0 rad/sec. The bandwidth is the frequency at which the closed-loop phase is -90°. The bandwidth was to be achieved without violating a closed-loop droop boundary of -3 dB. Pilot lead in seconds, τ_{Lead}, and degrees, ϕ_{Lead}, at the bandwidth frequency and maximum resonance, $|\theta/\theta_c|_{max}$, were noted and are presented in Table 9. Results are also plotted on the Neal-Smith parameter plane in Figures 53 through 56 for the four flight configurations. Nichols charts for the compensated Configuration 2 cases with bandwidth = 2 rad/sec are presented in Figures 57, 58, and 59.

TABLE 9

COMPARISON OF CALSPAN, NASA/REVISED AND OFT CONTROL SYSTEMS - ATTITUDE LOOP NEAL-SMITH RESULTS

Configuration		① 240,000 #, 290 Kt, $\gamma = -20°$, AFT C.G.			② 240,000 #, 190 Kt, AFT C.G.			③ 191,000 #, 190 Kt, FWD C.G.			④ 240,000 #, 190 Kt, FWD C.G.		
		CALSPAN	NASA	OFT	CALSPAN	NASA	OFT	CALSPAN	NASA	OFT	CALSPAN	NASA	OFT
$\omega_{BW_\theta} = 1.5$	τ_{Lead}, sec	(No lead req'd for $\omega_{BW} < 1.6$)	.16	.34	.24	.52	.91	.38	.25	.49	.51	.30	.60
	ϕ_{Lead} @ BW, deg		13.2	27.0	200.	37.9	53.7	29.9	20.3	36.5	37.3	24.4	42.13
	$\lvert\theta/\theta_c\rvert_{max}$, dB	1.	-2.9	-2.9	-1.06	-.77	-2.94	-2.13	-1.82	-2.87	-2.24	-1.19	-2.97
$\omega_{BW_\theta} = 2.0$	τ_{Lead}, sec	.24	.35	.57	.56	.89	1.61	.70	.52	.87	.87	.63	1.02
	ϕ_{Lead} @ BW, deg	25.8	34.8	48.5	48.4	60.6	72.8	54.4	46.4	60.0	60.0	51.4	63.8
	$\lvert\theta/\theta_c\rvert_{max}$, dB	.03	-2.88	-2.95	-1.20	-.49	-1.501	-1.63	-1.53	-2.16	-1.76	-1.04	-1.51
$\omega_{BW_\theta} = 2.5$	τ_{Lead}, sec	.44	.54	.83	.86	1.31	2.74	1.04	.77	1.30	1.24	.93	1.60
	ϕ_{Lead} @ BW, deg	47.7	53.3	64.2	65.0	73.0	81.7	68.9	62.6	72.8	72.1	66.6	76.0
	$\lvert\theta/\theta_c\rvert_{max}$, dB	1.04	-2.19	-.32	.24	.76	2.38	-.02	-.11	1.45	.12	.44	2.09
$\omega_{BW_\theta} = 3.0$	τ_{Lead}, sec	.64	.69	1.21	1.20	1.72	4.62	1.52	1.06	2.00	1.82	1.23	2.45
	ϕ_{Lead} @ BW, deg	62.5	64.1	74.6	74.4	79.0	85.9	77.6	72.5	80.6	79.6	74.9	82.3
	$\lvert\theta/\theta_c\rvert_{max}$, dB	3.62	1.89	4.02	3.57	5.24	8.31	3.24	3.82	6.65	3.51	4.66	7.68

Results from the Neal-Smith analysis indicate that generally a specific bandwidth can be achieved with significantly less pilot compensation with both the Calspan and NASA/Revised control systems than with the OFT. The small differences between the Calspan and NASA systems are basically due to the level of the augmented short period mode. For two of the configurations, the Calspan system yields a higher short period frequency while for the other two the NASA system has a slightly higher frequency. From Figures 53 through 56 it can be seen that an attitude bandwidth of 2 to 2.5 rad/sec can be achieved with Level 1 pilot compensation with the Calspan and NASA systems, while only a 1.5 to 2 rad/sec bandwidth is achievabel with the OFT. Another interesting characteristic is the steepness of the resonance versus bandwidth with the OFT system for the low speed configurations (Figures 54, 55, 56). The resonance quickly goes from the Level 1 boundary into the Level 3 area as the desired bandwidth goes from 2 to 3 rad/sec. This is indicative of a PIO situation. This could occur when the pilot's gain increases when an unexpected disturbance forces him to make quick corrections in the flare.

The Neal-Smith analysis was also carried out on an altitude rate loop closure. This was done similarily to the attitude loop closure, except that the $\dot{h}_p/q_{CMD}$ transfer function was used as the controlled element. Only Configuration 2 was analyzed. The bandwidth and phase lag (as defined in the MIL Standard draft) of the open-loop aircraft (no pilot-in-the-loop) were calculated and are presented in Table 10. It is apparent that bandwidth progressively increases and phase delay progressively decreases as one goes from the OFT to NASA/Revised, and then to the Calspan system. The Neal-Smith closed-loop analysis was performed to determine the pilot compensation required to achieve a .5, 1.0, 1.5, and 2.0 rad/sec altitude rate bandwidth. These results are also presented on Table 10 and in Figure 60 on a Neal-Smith parameter plane. No specific criterion levels are currently assigned to altitude rate loop characteristics but it is apparent that significantly less pilot compensation is required with the Calspan system for a given bandwidth. In addition much less resonance in altitude rate results as the pilot drives the system to higher bandwidths.

TABLE 10

COMPARISON OF CALSPAN, NASA/REVISED AND OFT CONTROL SYSTEMS ALTITUDE RATE BANDWIDTH CRITERIA AND NEAL-SMITH RESULTS

	Configuration 2 240,000 # 190 Kt, $\gamma = -3°$ AFT C.G.		
	CALSPAN	NASA	OFT
Bandwidth, open-loop $(\dot{h}_p/q_{CMD})$, ω_{BW} @ 45° phase margin, rad/sec	.7	.6	.4
Phase delay, τ_p, sec	.34	.42	.50
Neal-Smith Results			
$\omega_{BW_{\dot{h}}} = .5$ τ_{Lead}, sec	.01	.14	.89
$\omega_{BW_{\dot{h}}} = .5$ ϕ_{Lead} @ BW, deg	.2	4.0	24.0
$\omega_{BW_{\dot{h}}} = .5$ $\left\|\dot{h}_p/\dot{h}_{p_c}\right\|_{max}$, dB	-2.87	-2.97	-2.97
$\omega_{BW_{\dot{h}}} = 1.0$ τ_{Lead}, sec	1.10	1.49	3.88
$\omega_{BW_{\dot{h}}} = 1.0$ ϕ_{Lead} @ BW, deg	47.8	56.1	75.53
$\omega_{BW_{\dot{h}}} = 1.0$ $\left\|\dot{h}_p/\dot{h}_{p_c}\right\|_{max}$, dB	-2.96	-1.62	-1.66
$\omega_{BW_{\dot{h}}} = 1.5$ τ_{Lead}, sec	2.75	5.26	(No Solution)
$\omega_{BW_{\dot{h}}} = 1.5$ ϕ_{Lead} @ BW, deg	76.4	82.8	
$\omega_{BW_{\dot{h}}} = 1.5$ $\left\|\dot{h}_p/\dot{h}_{p_c}\right\|_{max}$, dB	1.00	4.68	
$\omega_{BW_{\dot{h}}} = 2.0$ τ_{Lead}, sec	10.09	(No Solution)	(No Solution)
$\omega_{BW_{\dot{h}}} = 2.0$ ϕ_{Lead} @ BW, deg	87.2		
$\omega_{BW_{\dot{h}}} = 2.0$ $\left\|\dot{h}_p/\dot{h}_{p_c}\right\|_{max}$, dB	8.12		

6.7 MULTI-LOOP ANALYSIS

A multi-loop analysis was performed to evaluate the characteristics of the various control systems with a control strategy that may be used in the flare. This control structure is shown in Figure 61. There is an inner attitude control loop that was used in the Neal-Smith analysis. The pilot model in this portion of the loop has a gain, delay, and a lead term:

$$Y_{p_\theta} = K_{p_\theta} e^{-.25s} (\tau_{Lead}\, s + 1)$$

Around this inner attitude loop is an altitude loop in which the pilot model is a pure gain:

$$Y_{p_h} = K_{p_h}$$

The pilot senses the altitude at the pilot position and tries to follow some reference altitude trajector, h_c , by controlling the inner attitude loop.

The multi-loop analysis was performed on Configuration 2. As a starting point in this analysis the inner attitude loop was set to achieve a 2 rad/sec bandwidth using the Neal-Smith results. A root locus was performed varying the outer loop pilot gain K_{p_h} . The dominant altitude mode pole is driven to higher frequencies and lighter and then negative damping indicating an altitude PIO as pilot gain increases. The results of this root locus is shown in Figure 62 for the three control systems. Maximum gains achievable (when pole has zero damping) are presented in Table 11. It can be seen that all three control systems achieve similar results. This is primarily due to the inner loop being compensated to the same bandwidth for each control system. However, it should be noted that the pilot compensation or lead used in the inner loop to achieve the 2 rad/sec bandwidth was progressively greater (and perhaps unrealistically high) as one goes from the Calspan to NASA/Revised and OFT control systems.

TABLE 11

COMPARISON OF CALSPAN, NASA/REVISED AND OFT CONTROL SYSTEMS
MULTI-LOOP CLOSURE ANALYSIS

	Configuration ② 240,000 # 190 Kt, $\gamma = -3°$ AFT C.G.			
	CALSPAN Pilot 50 ft Forward	CALSPAN	NASA	OFT
Constant inner-loop bandwidth $\omega_{BW_\theta} = 2$ rad/sec				
τ_{Lead}, sec	.56	.56	.89	1.61
Max K_{p_h} (gain at which altitude pole $\zeta = 0$), rad/ft	(Never goes unstable)	.0085	.0094	.0080
Max ω_{BW_h}, rad/sec	.37	.35	.35	.34
ω @ phase $h/h_\varepsilon = -180$, rad/sec	3.6	.9	1.0	.8
Constant inner-loop pilot compensation $\tau_{Lead} = .563$ sec				
ω_{BW_θ}, rad/sec	2.0	2.0	1.6	1.4
Max K_{p_h}, rad/ft	(Never goes unstable)	.0085	.0075	.0039
Max ω_{BW_h}, rad/sec	.37	.35	.33	.30
ω @ phase $h/h_\varepsilon = -180$, rad/sec	3.6	.9	.8	.6

A second series of root locus runs were then made with the NASA and OFT systems, holding the inner loop pilot lead term equal to that used with the Calspan system. The results are shown in Figure 63 and Table 11. It can be seen that the altitude mode is quickly driven unstable with the OFT mode, and the performance with the NASA system has been reduced somewhat. The inner loop attitude bandwidth has been reduced from 2 rad/sec to 1.6 and 1.4 rad/sec with the NASA and OFT systems, respectively.

Also included in this analysis was the effect of moving the pilot 50 feet forward. This puts the pilot well in front of the instantaneous center of rotation. It can be seen from the root locus for the Calspan control system in Figure 63 that the altitude mode never goes unstable for any pilot gain. This would indicate that a primary cause of an altitude PIO is the pilot position relative to the center of rotation. This characteristic was verified in an in-flight simulation program (Reference 4) in which identical airplane dynamical models were flown with varying pilot position. As the pilot position was moved aft and approached, the center of rotation of the aircraft became much more PIO prone.

The open-loop h_p/h_ϵ transfer functions were plotted on Nichols charts and the gain, K_{p_h} was varied until the maximum altitude bandwidth that was achievable without producing a resonance greater than 3 dB was determined. These results are shown on Table 11. Again very small differences between the control systems were obtained when identical inner loop bandwidths were used. However, when the inner loop compensation was held fixed at the Calspan system's pilot compensation, lower altitude bandwidths were obtained with the OFT and NASA systems. Higher altitude bandwidth was obtained with the pilot 50 feet forward. The Nichols plots of these latter cases are shown in Figures 64 through 67. All are done with identical inner loop compensation and the differences in the closed-loop bandwidth can be seen. The major benefit with the pilot 50 feet forward is that the open-loop phase does not pass through -180 degrees until 3.6 rad/sec while for the nominal pilot position it passes through -180 degrees at approximately 1 rad/sec.

In summary, it is apparent form the Neal-Smith analysis that though some improvement is seen in pitch attitude control as one goes from the OFT to NASA/Revised and then to Calspan system, a more dramatic improvement in altitude control is seen.

6.8 SIMPLIFIED CALSPAN CONTROL SYSTEM

Analysis was carried out on the various configurations with a simplified Calspan control system. In this simplification the pitch rate feedback filter time constants were held fixed at the values calculated for the most unstable configuration: 2 (190 KEAS, heavy weight, aft C.G.). This control system would only require scheduling K_q and Z_I with flight configuration. Table 12 lists the results of this analysis. The augmented short period mode became more heavily damped (Configuration 1 was over-damped) and frequency remained approximately the same for each configuration. The open-loop attitude bandwidth criteria parameters of bandwidth and phase delay remained the same, and only small changes are seen in the Neal-Smith solution for a closed-loop bandwidth of 2 rad/sec. Time histories to a one degree/sec pitch rate command were run and are presented in Figures 68, 69, and 70 for the Configurations 1, 2, and 3 for the constant feedback filter cases. They are very close to the scheduled filter time histories of Figures 13, 19, and 22.

6.9 INCREASED LOOP GAIN IN OFT CONTROL SYSTEM

An additional piece of analysis was done to see the effect of increasing the loop gain in the OFT control system. The *GDQ* gain was doubled and step input time histories run for Configuration 2. The resulting time histories are shown in Figure 71. It can be seen that the pitch rate response is much quicker than that with the nominal gain (Figure 18). However, the amount of pitch rate overshoot and the effective time constant of the angle of attack response is similar to what they were at the lower gain. The angle of attack continuously ramps off without coming to a steady state. Precise flight path control would still be a problem with this system. This again

TABLE 12

COMPARISON OF CALSPAN SYSTEM WITH SCHEDULED q FEEDBACK FILTER VERSUS CONSTANT q FEEDBACK FILTER

(P_F & Z_F held fixed at Configuration 2 values)

Configuration	① 240,000# 290 Kt, $\gamma = -20°$ AFT C.G.		③ 191,000# 190 Kt, $\gamma = -3°$ FWD C.G.		④ 240,000# 190 Kt, $\gamma = -3°$ FWD C.G.	
	P_F & Z_F Scheduled	P_F & Z_F Constant	P_F & Z_F Scheduled	P_F & Z_F Constant	P_F & Z_F Scheduled	P_F & Z_F Constant
q Feedback Constants P_F	.52	.41	.45	.41	.36	.41
q Feedback Constants Z_F	1.1	.7	.8	.7	.7	.7
Augmented Short Period ω	1.74	1.69	1.22	1.19	1.07	1.14
Augmented Short Period ζ	.71	1.02	.72	.76	.71	.78
Pitch Attitude Bandwidth, open-loop a/c ω_{BW}, rad/sec	2.1	2.2	1.5	1.5	1.4	1.4
Phase Delay, τ_p sec	.11	.11	.10	.10	.10	.10
Neal-Smith, θ/θ_c, Solution $\omega_{BW_\theta} = 2.0$ rad/sec						
τ_{Lead}, sec	.24	.30	.70	.73	.87	.75
ϕ_{Lead} @ BW, deg	25.8	31.3	54.4	55.8	60.0	56.3
$\lvert\theta/\theta_c\rvert_{max}$, dB	.03	-2.63	-1.63	-2.23	-1.76	-2.19

points out the importance of preserving the numerator zero at $1/T_{\theta_2}$ in the pitch rate transfer function. Gain alone will not do this, but proper placement of the integrator zero and pole/zero of the feedback filter will, as in the Calspan design control system.

6.10 EVALUATION OF CALSPAN'S PITCH RATE CONTROL SYSTEM IN THE VARIABLE-STABILITY LEARJET

An evaluation of the Calspan pitch rate control system was made in the variable-stability Learjet. The control system implemented was similar to that recommended for the shuttle except that no lead/lag filter was used on the pitch rate feedback. Very favorable pilot comments were obtained from the land-approach and touchdown evaluations. The following discussion describes the setup of the Learjet and the results of the evaluation.

The variable-stability Learjet was augmented with α and $\dot{\alpha}$ feedback to provide a statically unstable baseline aircraft about which the Calspan pitch rate control system was implemented. At the flight condition of interest (125 KIAS, 20° flaps, gear down) the pitch rate transfer function was:

$$\frac{q}{\delta_e} = -\frac{3.72(s + .756)(s + .057)s}{(s - .42)(s + 1.54)\left[s^2 + 2(.06)(.11)s + .11^2\right]}$$

The unstable pole at $+.42$ yields a fairly rapid time to double amplitude of $\frac{(.693)}{.42} = 1.65$ sec which is more unstable than any of the shuttle configurations. The control system implemented about this unstable Learjet configuration in shown below:

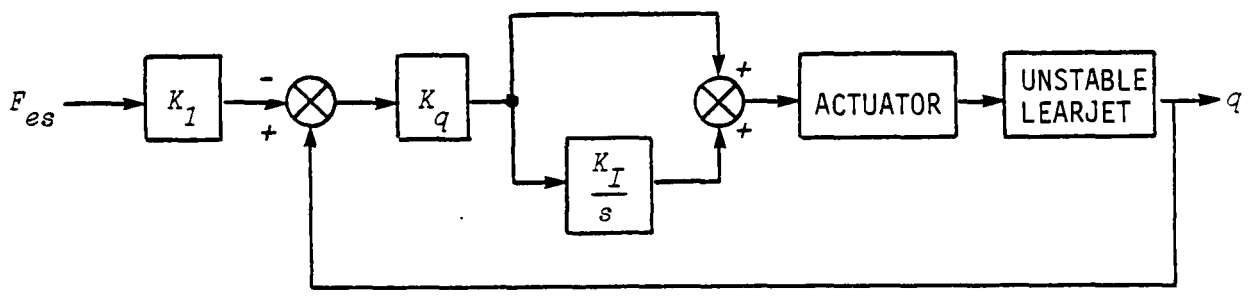

K_I was chosen equal to $-\lambda_2 = 1.54$ (the stable pole)

K_1 was pilot-selected for good sensitivity

K_q was chosen to yield a good short period frequency and damping:

$$\frac{\omega_n^2}{n_z/\alpha} = .35 \text{ for Level 1, Category C Flight Phase}$$

$$\omega_n^2 = .35 \frac{n_z}{\alpha} \simeq .35 \frac{V}{g} \frac{1}{T_{\theta_2}} = .35 \frac{(210)}{(32.17)} (.756) = 1.73$$

$$\left.\begin{aligned} \omega_n &= 1.31 \\ \zeta &= .7 \end{aligned}\right\} \text{ Select } K_q \text{ to yield these values.}$$

Neglecting actuator and low frequency terms, the system reduces to:

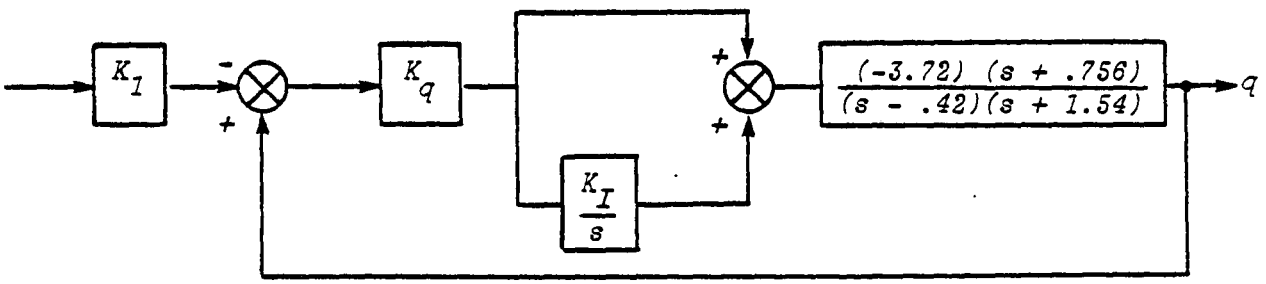

Denominator in root locus form is:

$$1 + \frac{K_q(3.72)(s+.756)(s+K_I)}{(s-.42)(s+1.54)s}$$

Let $K_I = -\lambda_2 = 1.54$, then

$$1 + \frac{K_q(3.72)(s+.756)}{s(s-.42)} = 0$$

$$s^2 - .42s + 3.72\,K_q\,s + 3.72\,K_q\,(.756) = 0$$

$$\omega_n^2 = 3.72\,K_q\,(.756) \equiv (-M_{\delta_e})(K_q)\left(\frac{1}{T_{\theta_2}}\right)$$

$$K_q = \frac{\omega_n^2}{(3.72)(.756)} \equiv -\frac{\omega_n^2}{M_{\delta_e}}\,T_{\theta_2}$$

since $\omega_n^2 = (1.31)$:

$$K_q = .61$$

$$2\zeta\omega_n = 3.72\,K_q - .42 \equiv -M_{\delta_e}\,K_q - \lambda_1$$

$$\zeta = \frac{3.72(.61)-.42}{2(1.31)}$$

$$\zeta = .7$$

Therefore, with $K_I = 1.54$ and $K_q = .61$ the augmented closed-loop Learjet had a Level 1 short period root with:

$$\omega_{sp} = 1.31 \text{ rad/sec}$$

$$\zeta = .7$$

The Calspan control system was implemented in the Learjet on the analog computer. The aircraft was trimmed up at the desired flight condition of 125 KIAS, 20° flaps, gear down and handed over to the evaluation pilot in level flight. Several approaches were made with two pilots. Evaluations included turns with rapid rollout to investigate the possibility of any pitch up in this maneuver. There was none noticed. Low and high gain approaches were made. The pilots had no problems with pitch attitude control and no overshoot tendency was noticed. The only problem encountered was the tendency to get low on airspeed during the first approach due to the lack of speed stability with this configuration. The pilot had to watch his airspeed and correct with throttle; an autothrottle would have improved this condition. There was also a slight floating tendency noted after flare, which was attributed by the pilots to an inherent float tendency in the Learjet with 20° flaps and light fuel load. However, this might have been due to the attitude hold tendency of this control system.

A transcription of the pilot comments recorded in flight follows.

Learjet Flight 507, 3 September 1982
Parrag and Berthe
Evaluation of Calspan's pitch rate control system

Parrag made one approach and landing. On initiation of go-around, after advancing throttle, the system dumped. The airplane pitched nose down after the dump and may have touched nose gear before Berthe could check the pitch down. Pilots did not note the cause of the system dump.

After the pilots changed seats, Berthe made three approaches and landings and recorded evaluation comments.

Berthe: downwind 125 kt.

Little heavy command gain. Can we lighten those gains up Mike?

Parrag: Which ones?

Berthe: Both, lighten them up about the same (pitch and roll).

Parrag: Are you talking about the feel or the command gain?

Berthe: The (ah) I got plenty of motion, I would just like to lighten the forces.

Berthe: That's all right. O.K., we just reset the command gains for lighter forces. I'm in a fairly steep turn here for final. I'm going to roll out fairly smartly.

Parrag: That was a 40% increase in command gain.

Berthe: That's good.

O.K., roll out went very normally, no drifting in either axis.
Rollout for final, really smart rollout with no apparent problems in the pitch axis.

We're on a simulated ILS approach now. Airspeed control looks good.

Parrag: Turning up the roll command gains. That better?

Berthe: Yeah, that's better. (Marker Beacon)

It's fairly low gain at this point but airspeed control, glide path control is no problem.

I've got a 3-degree glide slope going so there should be a significant roundout and we will see what that task looks like. O.K., starting a preflare here without any problem.

Parrag: Watch your speed!

Berthe: Little bit slow.

Parrag: I'll dump it off here.

Berthe: Pitch response - (Dump beeper)
O.K., you got it.

Force sluggish in pitch response on flare, and tendency to -- (overlaid by radio transmissions) get slow. The safety pilot took it over at about 110 kt.

Technique was - flying it normal closed-loop airplane. I'll try one more of those and then I'll try an open-loop type approach.

Berthe: Approach No. 2. Going to try a normal closed pattern. (Radio over) ---- Shooting for 130 kt in turn (Radio over). Wind 25 gusting over thirty right down the runway. Three green, 20 flaps. O.K., I'm going to save some rollout here. Going to make some correction on final. No apparent problem with roll attitude change - stopping the heading and starting it again looks to be no problem. (Marker Beacon)
Now I'm going to try getting it down - and getting it right on 125 kts.
O.K., I'm going to start a little preflare here. Well now, we are getting close to the ground, seems to be no problem holding the attitude I want.
Touchdown - O.K. you got it. (Beeper).
O.K., that was a successful landing. No problem on glide path control, however, throughout the pattern you have a feeling that you don't want to mess with it too much. You're making your inputs pretty low gain. I'll try to be a little more aggressive.

Third Approach

Berthe: O.K., coming off the 180° on the last approach. It's a closed pattern type approach. On this one I'm going to try to hold 125 kts all through the pattern. I'm going to try to be a little more aggressive with the airplane. Rolling out here at the 90° rather aggressively to see what the response is. No coupling in the pitch axis on the rollout at all. It has about a 30° bank into the final. I'll roll that out rather smartly also. O.K. that one went very nominally too. No problem in rolling out of headings.
I'm going to try some corrections to the glide slope here. I'm going to get a little low. Then level out and work myself high again. Didn't seem to be any problem with that.

The thing just floats with 20° of flaps. That's the problem.
(Beeper for dump). O.K., you got it? O.K. I found that a very well behaved airplane, no problem through the whole approach. Good touchdown (Radio overlay) ---- so my premonition of having to back off on it was not true. I can be as aggressive as I need to on a conventional landing approach. I had no tendency to overcontrol or overshoot or anything; (ah) any control problems in nose position in the flare? The big problem I had was, we're shooting these with 20° of flaps and we're getting light and the airplane tends to float quite a bit in that condition. But even with the floating condition, there was no problem in holding the nose where I wanted it. END.

Section 7
CONCLUDING SECTION

7.1 INTRODUCTION

This section contains a summary of the results described in more detail in the previous section. The conclusions derived from these results are then presented and recommendations are given.

7.2 SUMMARY OF RESULTS

1. A control system which uses filtered pitch rate feedback with proportional plus integral paths in the forward loop was designed which stabilized the shuttle and produced near Level 1 flying qualities over a variety of flight configurations.

2. This Calspan-designed system has four parameters:

   K_q - loop gain

   Z_I - integral path gain

   Z_F and P_F - zero and pole of q feedback filter. The K_q and Z_I gains can be easily scheduled with velocity, weight, and C.G. The Z_F and P_F parameters can be left fixed at values chosen for the most critical flight condition with little deterioration in characteristics.

3. Time histories to pitch rate command step inputs show that the Calspan and NASA/Revised control system have generally similar characteristics. They both have larger pitch rate overshoots and faster angle of attack response than the OFT design. Some ringing in the elevon rate can be seen with the NASA/Revised control system which is not seen with the Calspan

system. The OFT control system yields only a very slight pitch rate overshoot and a slow angle of attack response which continuously ramps up and does not level off. Ringing can also be seen in the OFT elevon rate. Maximum elevon rates occuring immediately following the step input for the OFT design are approximately one-third those for the Calspan and NASA/Revised systems.

4. There is a significant reduction in effective time delay (maximum slope intercept) of the pitch rate response to a step command for the Calspan system and the NASA/Revised system relative to the OFT. In addition, the Calspan design has less delay than the NASA/Revised system. This is also seen in the phase delay parameter of the open-loop bandwidth criterion. The reduced time delay results from the placement of the body bending filter in the feedback path for the Calspan and NASA systems, and replacing the smoothing filter with a notch filter in the Calspan system.

5. Discrete vertical gust responses are similar for all control systems.

6. Typical flare profile time histories indicate that flight path angle can be precisely controlled with the Calspan control system with little ballooning or floating tendency. Similar simple flare inputs used with the NASA/Revised system and OFT system yield progressively larger ballooning tendencies. To yield a good non-floating flare profile with the NASA or OFT control system requires a more complex pilot control technique which could lead to a PIO. The non-overshooting pitch rate characteristic of the OFT system causes a slow responding angle of attack and flight path response which makes tight control of the flare difficult.

7. In the frequency domain, the pitch attitude control-loop dynamics of the Calspan and NASA/Revised control systems are similar to each other with small variations between them depending upon flight configuration. They are both significantly better than the OFT system in open-loop bandwidth and closed-loop bandwidth Neal-Smith analyses results.

8. When compared to the proposed open-loop bandwidth/phase delay criteria requirement for the MIL Standard, the Calspan configurations are generally in the middle Level 2 region, NASA/Revised in the upper Level 2, and OFT on the Level 2/3 boarder.

9. When compared to the Neal-Smith parameter plane, significantly less pilot compensation is required to achieve a given closed-loop attitude bandwidth with the Calspan or NASA/Revised system than with the OFT system. Closed-loop resonance also increases more rapidly with the OFT system as bandwidth is increased.

10. The Neal-Smith analysis technique was applied to a model assuming direct pilot control of flight path angle or altitude rate. The results indicate higher bandwidth for the Calspan system and the NASA/Revised than for the OFT.

11. Multi-loop analysis of an inner pitch attitude and outer altitude loop closure shows that all three control systems yield similar closed loop altitude bandwidth if the inner loop is compensated to equivalent bandwidth. The NASA and OFT systems require unrealistically high pilot compensation to do this. When the inner-loop pilot compensation is held fixed at the valve chosen for the Calspan system, the Calspan system achieves higher attitude and altitude bandwidths than the NASA or OFT systems. With the Calspan system the pilot can go to higher gain before the altitude mode goes unstable.

With the pilot shifted 50 feet forward, the altitude mode remains stable at any gain and significantly higher altitude bandwidth is possible.

12. In-flight evaluation of the Calspan-designed control system in the variable stability Learjet showed promising results. The Learjet was artificially de-stabilized to yield a statically unstable airframe. A proportional plus integral pitch rate control system designed similarly to that investigated in this study was programmed in the Learjet's flight control computer. Favorable pilot comments were received on pitch attitude and flight path control during approach and landing evaluations.

7.3 CONCLUSIONS

1. The analysis conducted in this program shows that both the Calspan-designed control system and the NASA/Revised system significantly improve the approach and landing flying qualities of the shuttle.

2. The Calspan and NASA/Revised systems produced better characteristics than the OFT system in the following respects:

   - Higher pitch attitude, altitude rate, and altitude bandwidth
   - Less pilot compensation required
   - Less time delay
   - More precise flight path and flare control.

3. The Calspan system was similar to the NASA/Revised system in the following respects:

   - Pitch attitude bandwidth and pilot compensation
   - Pitch rate and angle of attack response to step inputs
   - Vertical gust response.

4. The Calspan system was better than the NASA/Revised system in the following respects:

   - Less time delay
   - Simpler mechanization
   - Reduced ringing in elevon rate to sharp inputs.

5. Any improved control system such as the Calspan or NASA/Revised systems must contend with the relatively low rate limit capability of the elevons. Pilots often force the elevons to their rate limits during PIO encounters with the OFT system. The improved control systems must be evaluated through pilot in the loop simulation to determine whether or not the shuttle surface rate capability is adequate.

7.4 RECOMMENDATIONS

1. **The Calspan designed control system and the NASA/Revised system should be evaluated further in piloted simulations using the TIFS facility.**

2. The flying qualities of the Calspan control system should be investigated without the PIO suppressor.

3. The effect of Shuttle elevon rate limits on the performance of the Calspan designed control system should be determined from piloted in-flight simulation tests.

4. Analysis of the proposed flight control systems should be extended to include ground effect and wheel reaction effects at touchdown. The study would determine control law changes required such as gain changes, and placing the integrator in HOLD as a function of weight on wheels and/or nose wheel rotation rate.

Section 8

REFERENCES

1. Weingarten, N. C., "In-Flight Simulation of the Space Shuttle (STS-1) During Landing Approach With Pilot-Induced Oscillation Suppressor," Calspan Report No. 6339-F-2, December 1979.

2. Military Specification - Flying Qualities of Piloted Airplanes, MIL-F-8785C, November 1980.

3. Chalk, C. R., "Calspan Recommendations for SCR Flying Qualities Design Criteria," NASA CR-159236, April 1980.

4. Weingarten, N. C. and Chalk, C. R., "In-Flight Investigation of the Effects of Pilot Location and Control System Design on Airplane Flying Qualities for Approach and Landing," NASA CR-163115, December 1981.

5. Mitchell, D. and Hoh, R., "Review and Interpretation of Existing Longitudinal Flying Qualities Criteria for Use in the MIL Standard Handbook," STI Working Paper No. 1163-1, December 1980.

6. Neal, T. P. and Smith, R. E., "An In-Flight Investigation to Develop Control System Design Criteria for Fighter Airplanes," AF FDL-TR-70-74, December 1970.

7. Radford, R. C., et al., "Landing Flying Qualities Evaluation Criteria for Augmented Aircraft," NASA CR-163097, August 1980.

A = Amplitude/Steady State Amplitude

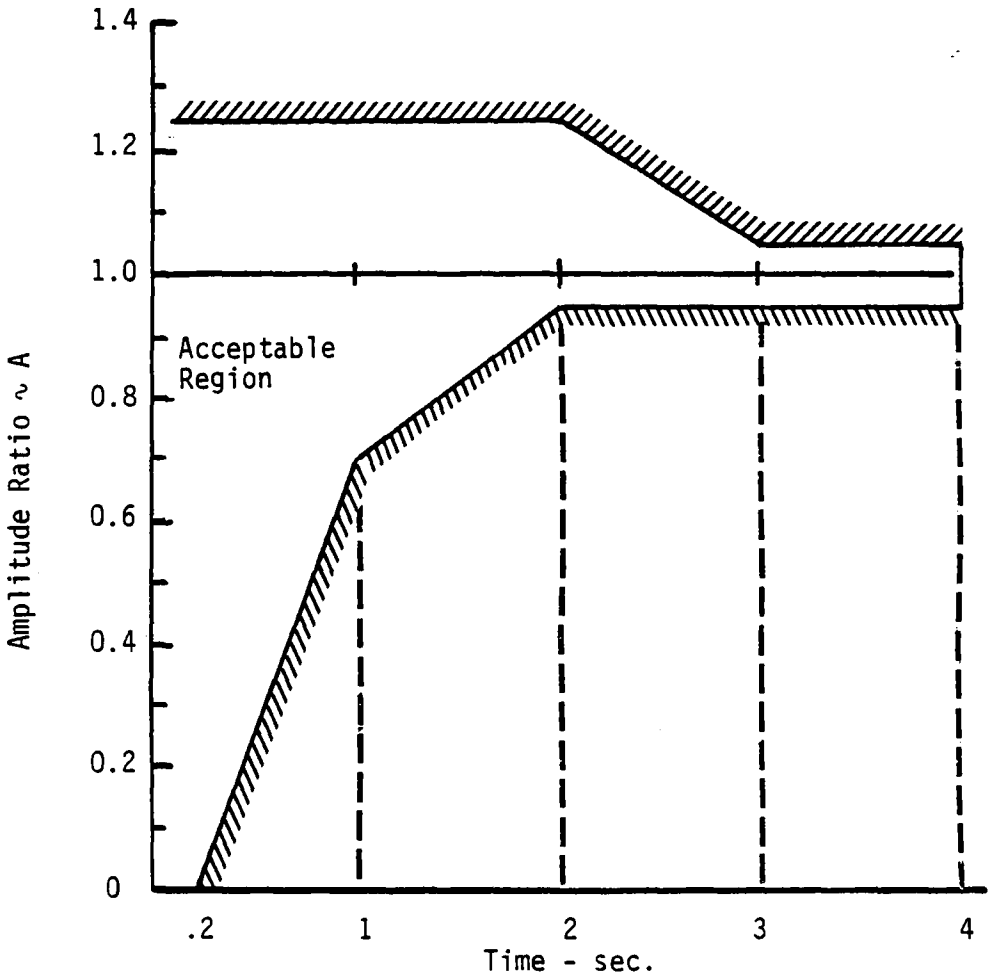

Figure 1. GENERALIZED PITCH RATE TRANSIENT RESPONSE CRITERIA FOR SPACE SHUTTLE

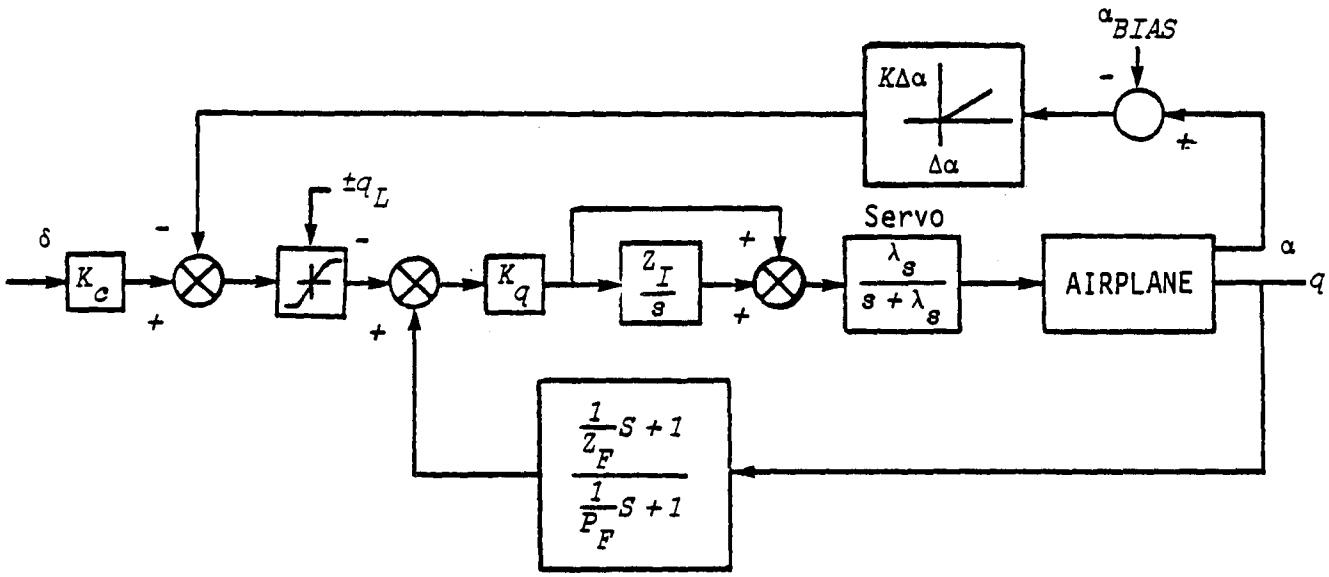

where $\pm q_L = \frac{g}{V_T}\left[n_z - (\pm n_L)\right] + q$

Figure 2. BLOCK DIAGRAM OF SHUTTLE CONTROL SYSTEM PROPOSED BY CALSPAN

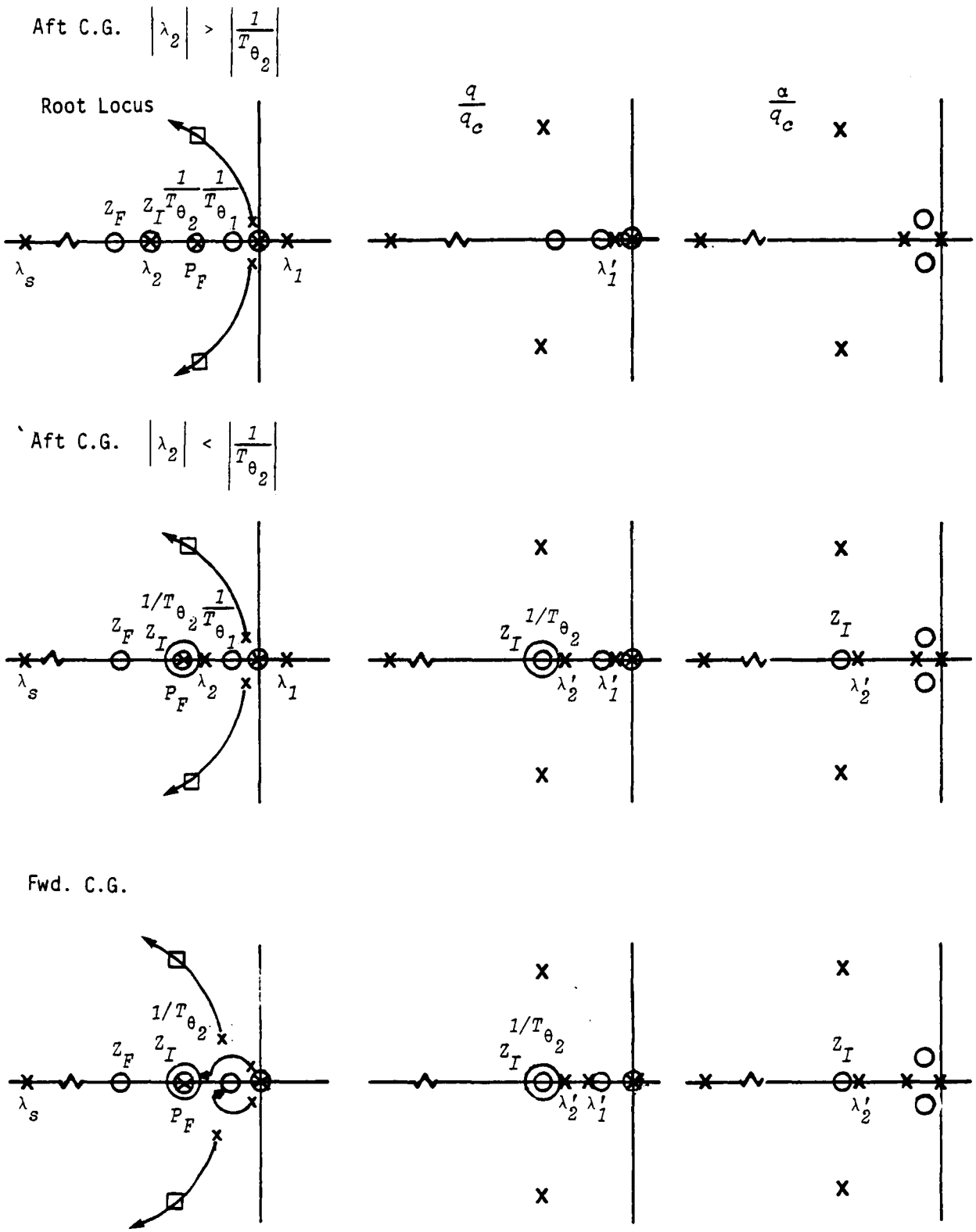

Figure 3. ROOT LOCUS AND CLOSED LOOP POLE-ZERO CONFIGURATIONS

$$\frac{\delta_e}{q_c} = \frac{K_q P_F}{Z_F} \frac{S+Z_F}{S+P_F} \frac{S+Z_I}{S}$$

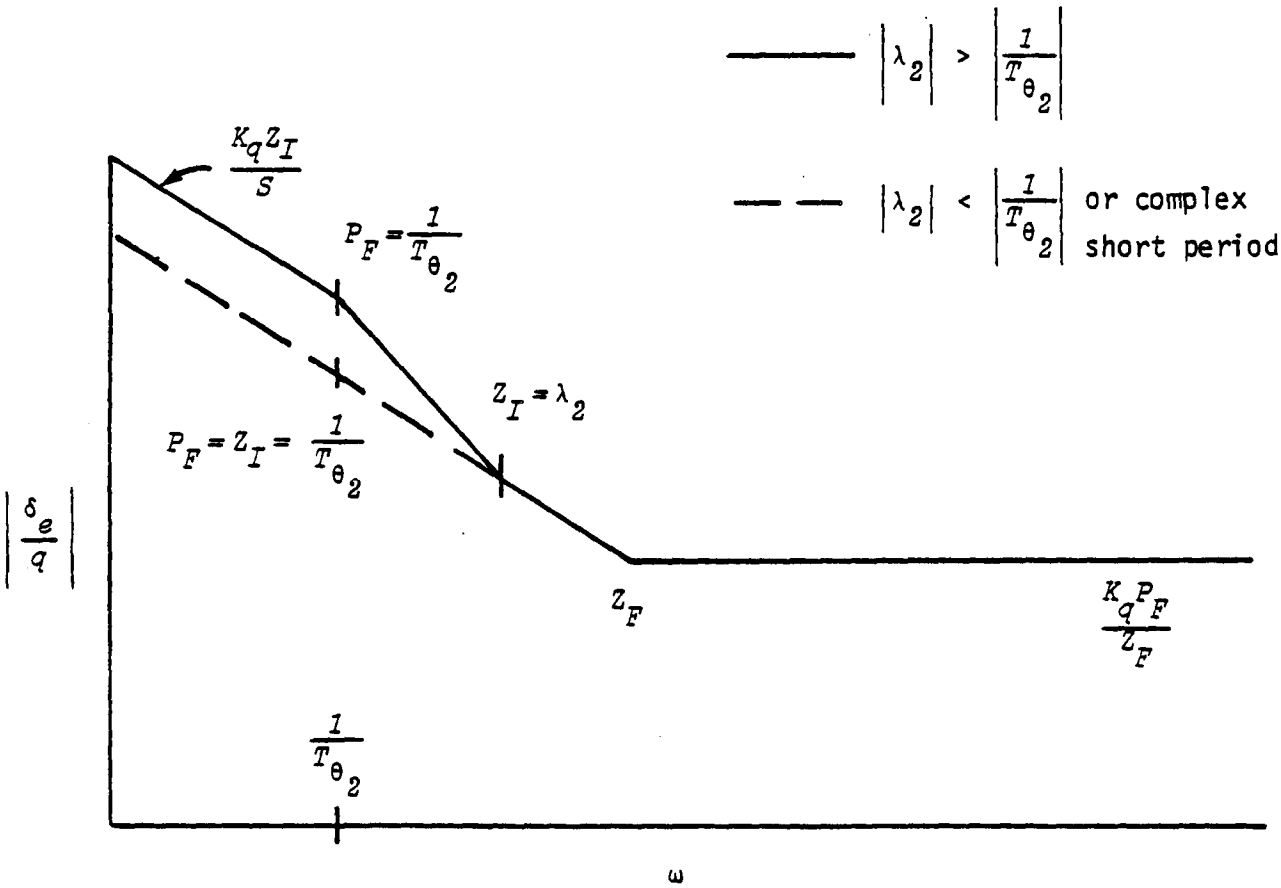

Figure 4. FREQUENCY RESPONSE OF δ_e/q FOR CALSPAN SYSTEM

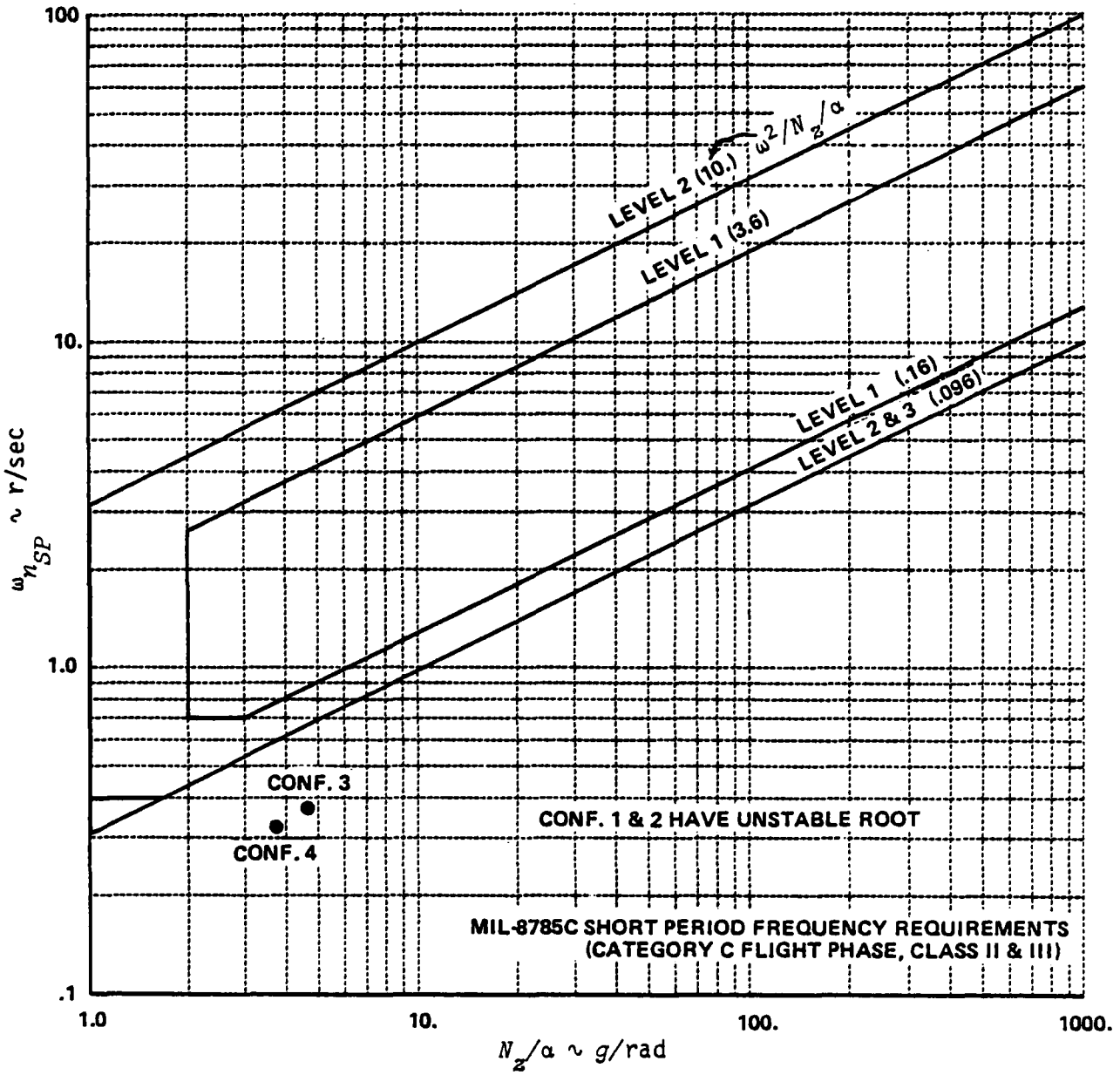

Figure 5. UNAUGMENTED CONFIGURATIONS VERSUS SHORT PERIOD REQUIREMENTS

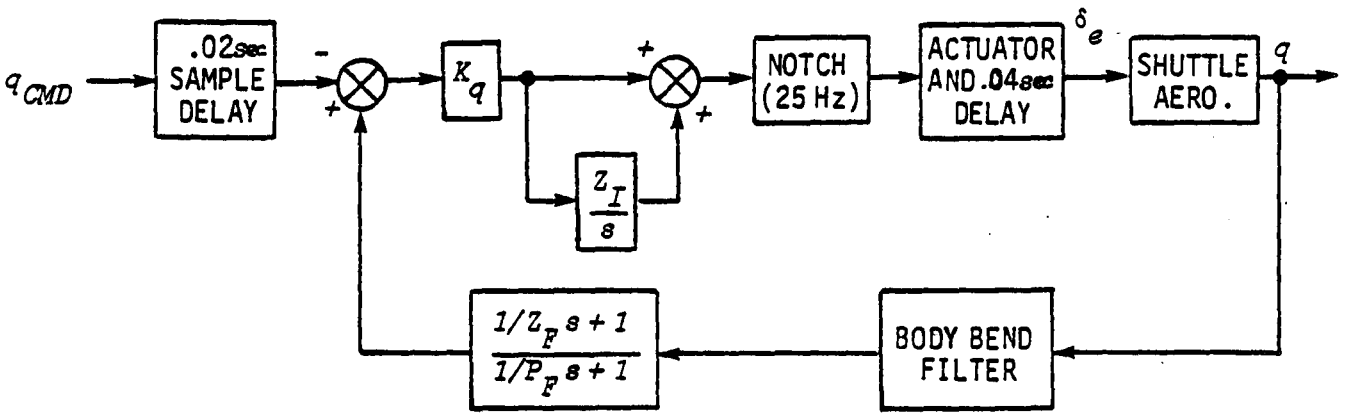

K_q, Z_I, Z_F, P_F - System gains and filter time constants function of flight condition.

$$\text{Notch (25 Hz)} = \frac{[s^2 + 157^2]}{[s^2 + 2(.5)(157)s + 157^2]}$$

$$\text{Actuator} = \frac{(27.65)(36^2)}{(s + 27.65)[s^2 + 2(.707)(36)s + 36^2]}$$

$$\text{Body Bending Filter} = \left(\frac{20}{32.75}\right)^2 \frac{[s^2 + 2(.04)(32.75)s + 32.75^2]}{[s^2 + 2(.4)(20)s + 20^2]}$$

Figure 6. CALSPAN CONTROL SYSTEM

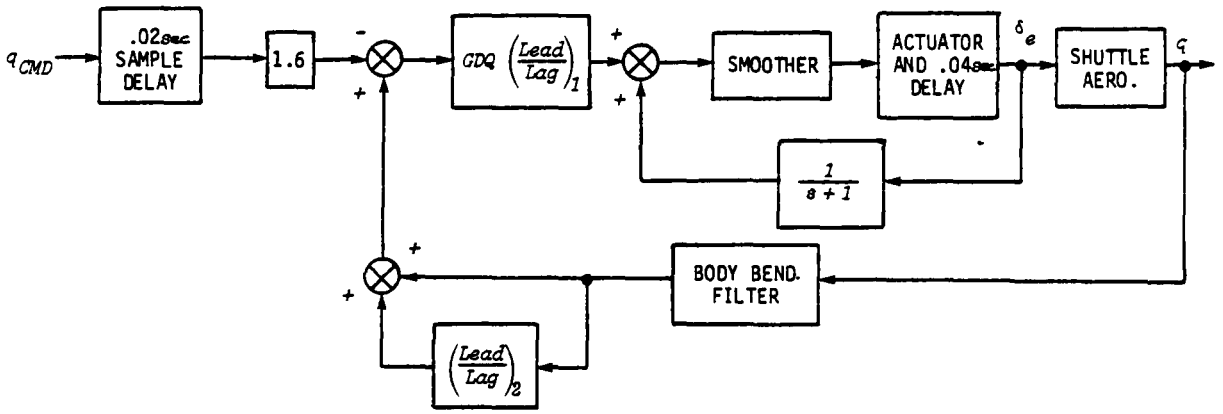

$$GDQ = 16/\sqrt{\bar{q}}$$

$$\left(\frac{Lead}{Lag}\right)_1 = 1.5\left(\frac{s+2}{s+3}\right)$$

$$\text{Smoother} = \frac{36^2}{[s^2 + 2(.7)(36)s + 36^2]}$$

$$\text{Actuator} = \frac{(27.65)(36^2)}{(s+27.65)[s^2 + 2(.707)(36)s + 36^2]}$$

$$\text{Body Bending Filter} = \left(\frac{20}{32.75}\right)^2 \frac{[s^2 + 2(.04)(32.75)s + 32.75^2]}{[s^2 + 2(.4)(20)s + 20^2]}$$

$$\left(\frac{Lead}{Lag}\right)_2 = (.6)(-7.81)\frac{(s-3.2)(s+2)}{(s+100)(s+.5)}$$

Figure 7. NASA/REVISED CONTROL SYSTEM

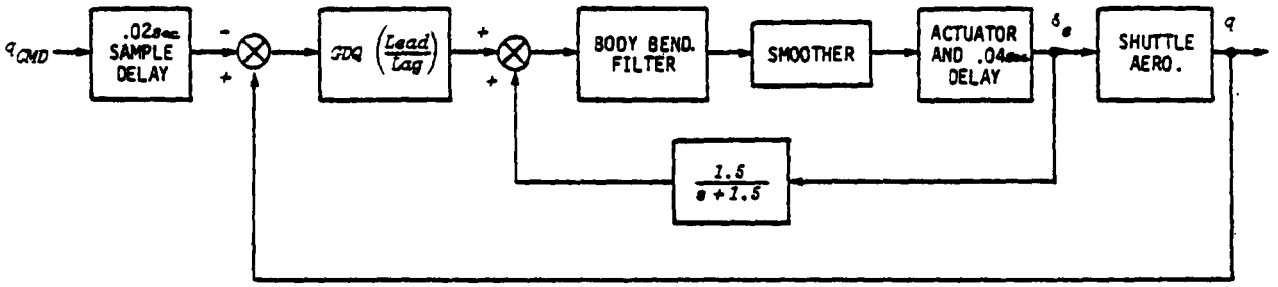

$$GDQ = 16/\sqrt{\bar{q}}$$

$$\left(\frac{Lead}{Lag}\right) = 1.42\left(\frac{s + .588}{s + .833}\right)$$

$$\text{Body Bending Filter} = \left(\frac{20}{32.75}\right)^2 \frac{[s^2 + 2(.04)(32.75)s + 32.75^2]}{[s^2 + 2(.4)(20)s + 20^2]}$$

$$\text{Smoother} = \frac{36^2}{[s^2 + 2(.7)(36)s + 36^2]}$$

$$\text{Actuator} = \frac{(27.65)(36^2)}{(s + 27.65)[s^2 + 2(.707)(36)s + 36^2]}$$

Figure 8. OFT CONTROL SYSTEM

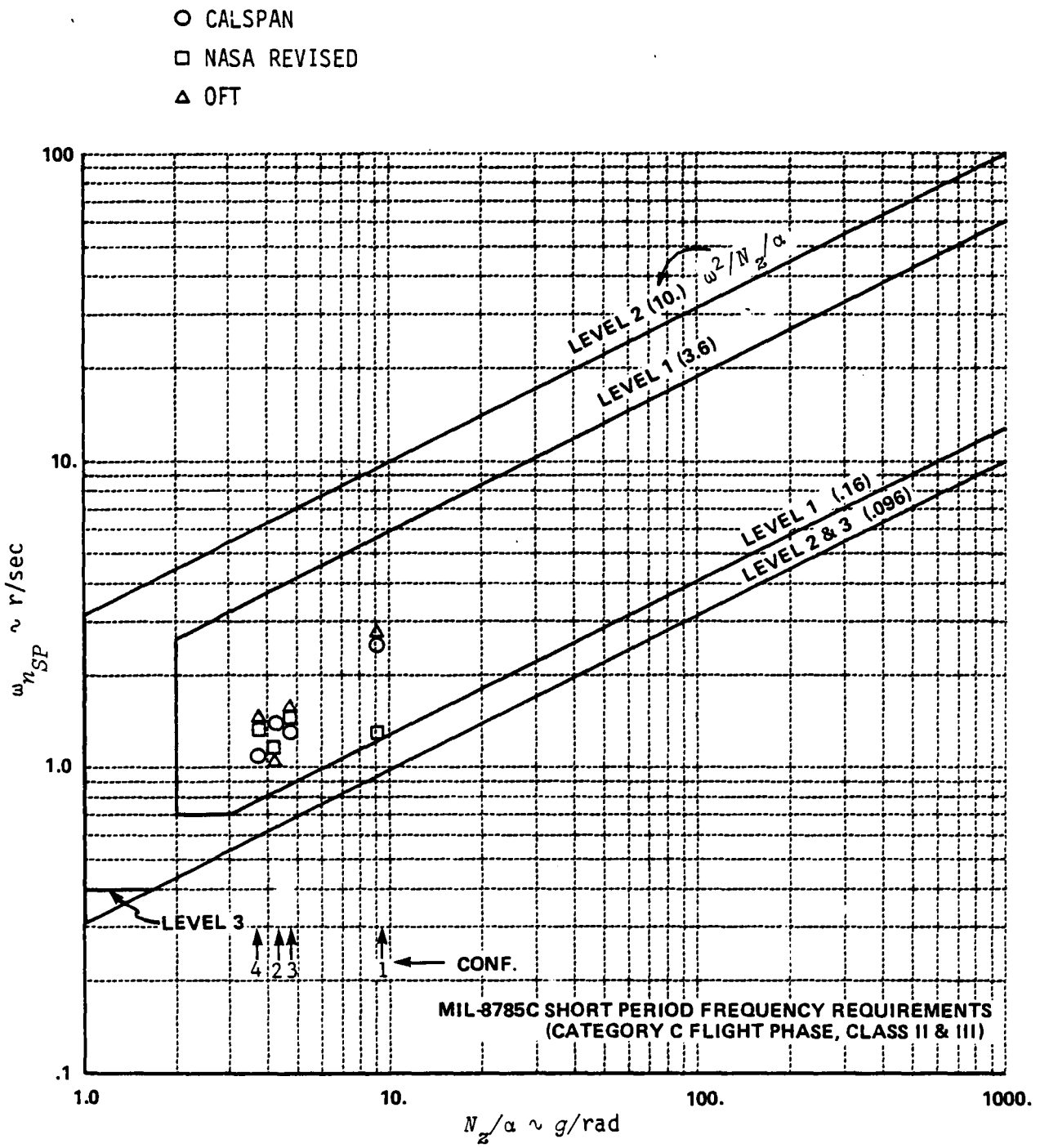

Figure 9. AUGMENTED CONFIGURATIONS VERSUS SHORT PERIOD REQUIREMENTS

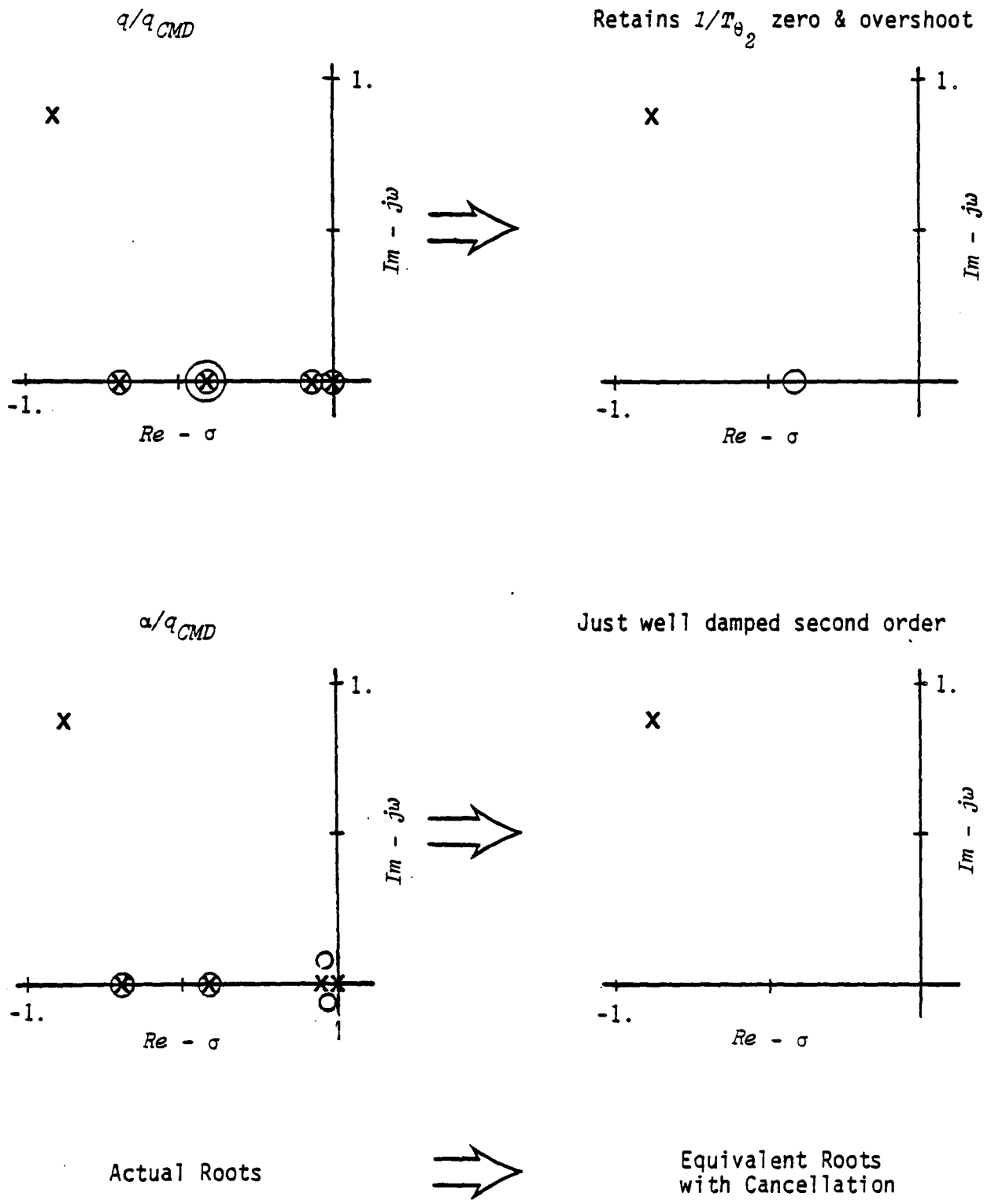

Figure 10. POLE-ZERO LOCATIONS - CALSPAN CONFIGURATION 2

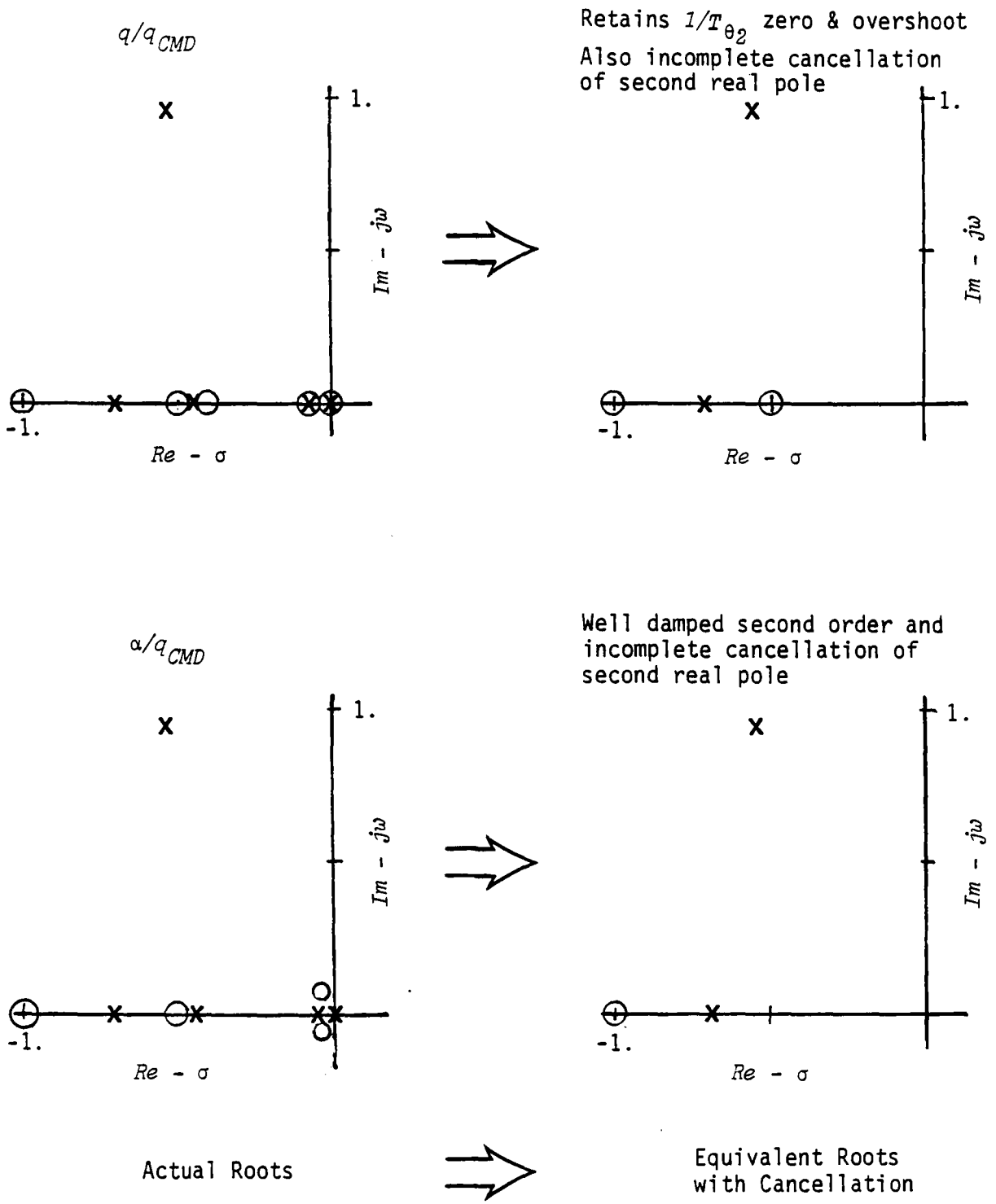

Figure 11. POLE-ZERO LOCATIONS - NASA, REVISED CONFIGURATION 2

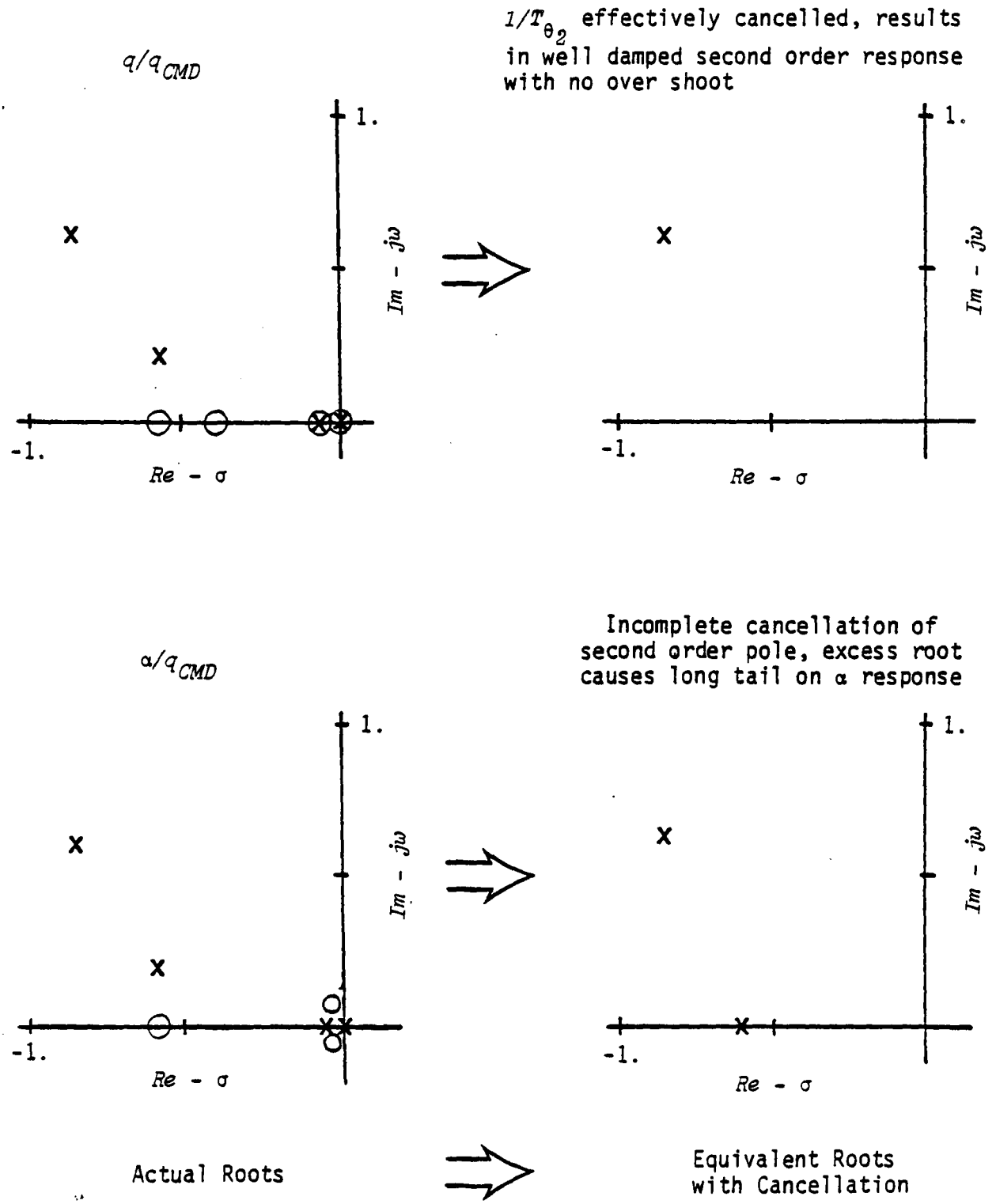

Figure 12. POLE-ZERO LOCATIONS - OFT CONFIGURATION 2

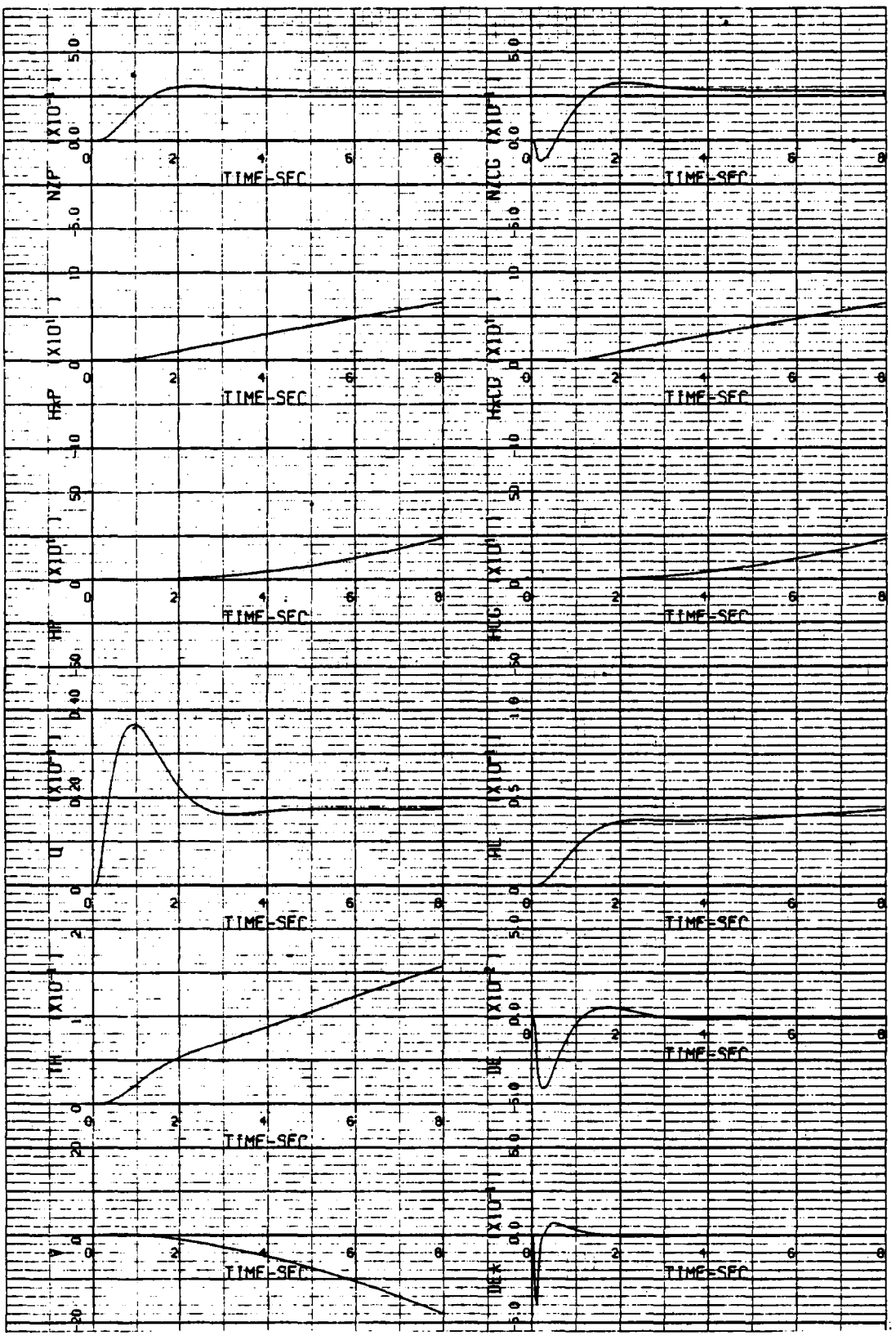

Figure 13. CALSPAN CONFIGURATION 1, q_{CMD} STEP RESPONSE

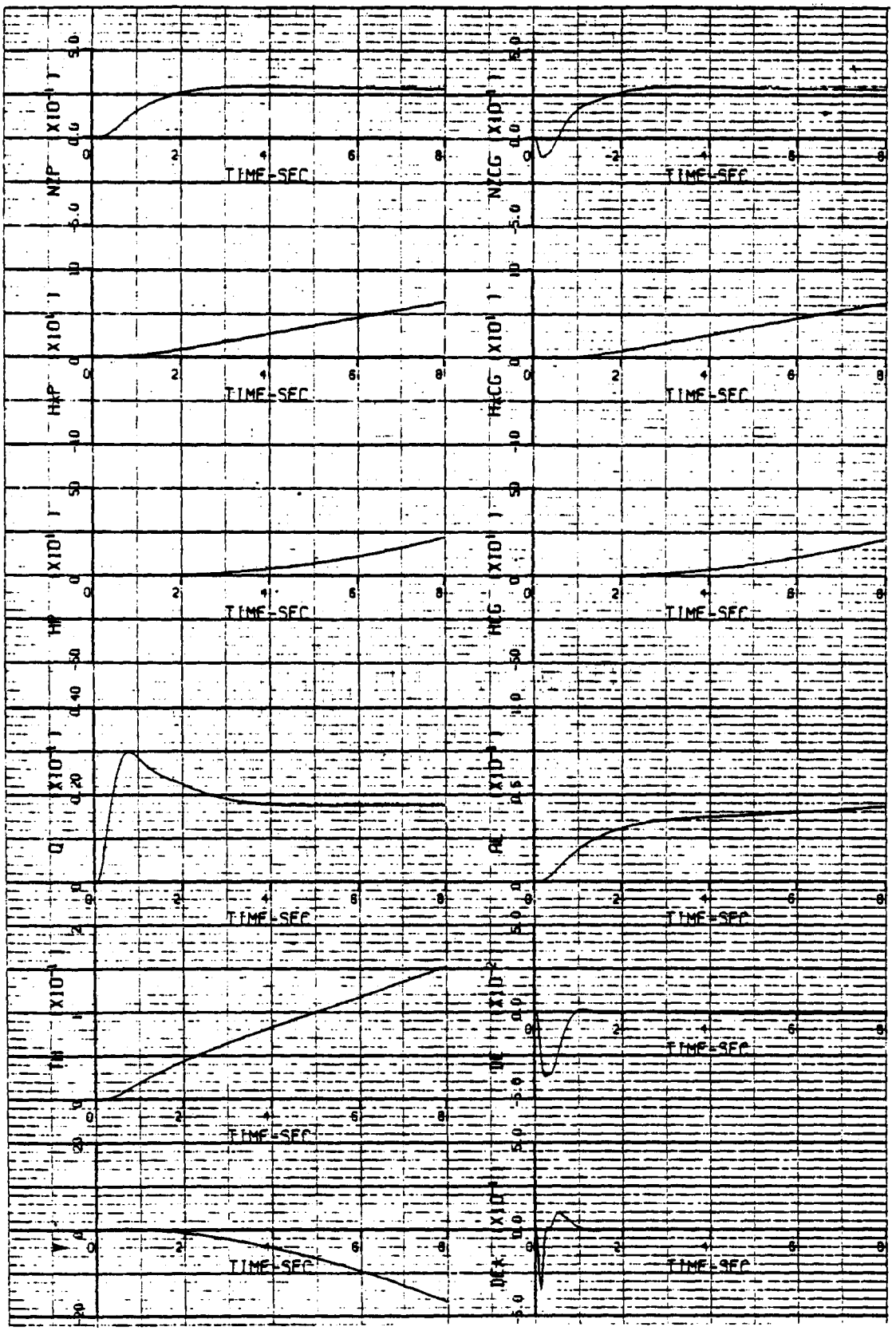

Figure 14. NASA/REVISED CONFIGURATION 1, q_{CMD} STEP RESPONSE

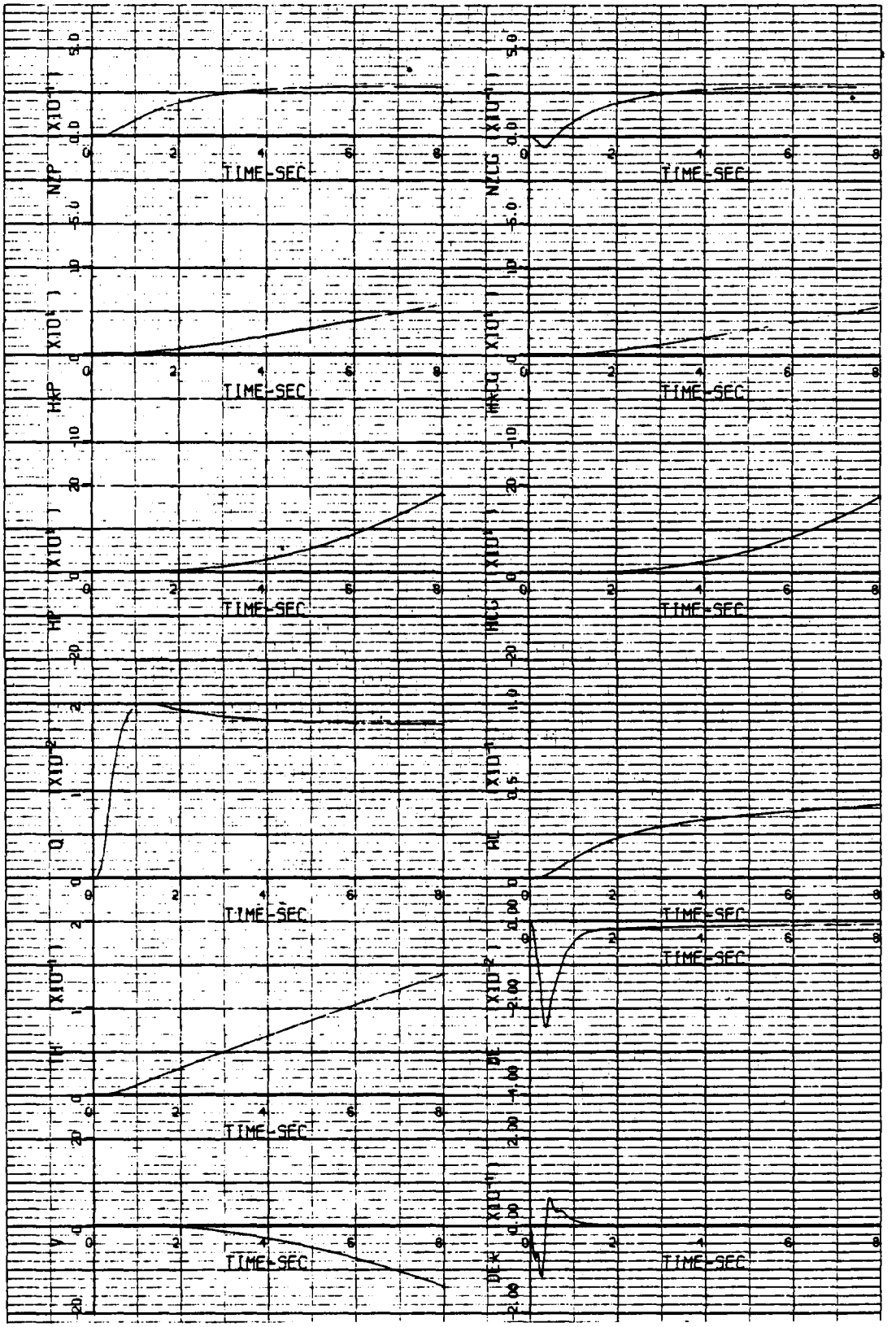

Figure 15. OFT CONFIGURATION 1, q_{CMD} STEP RESPONSE

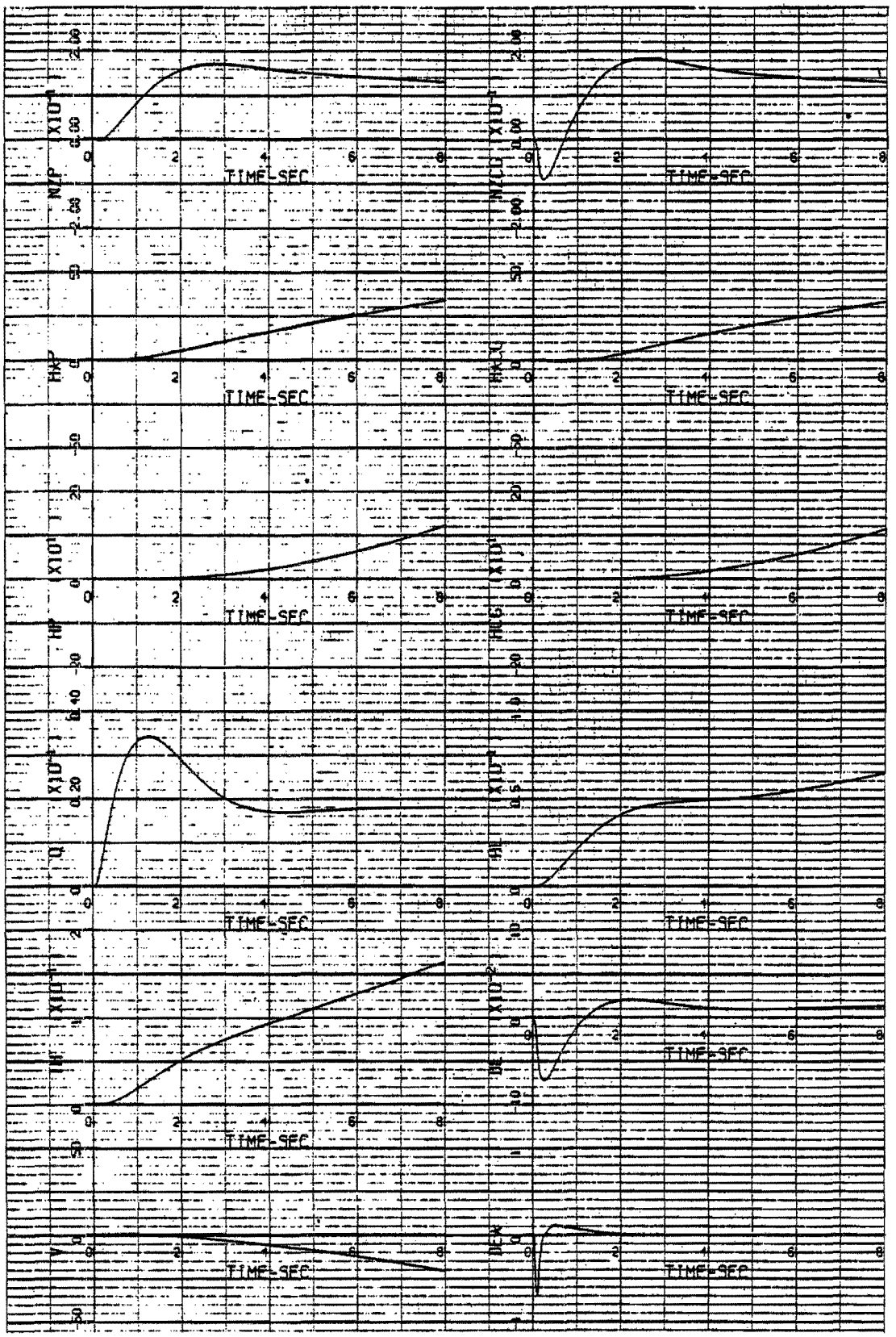

Figure 16. CALSPAN CONFIGURATION 2, q_{CMD} STEP RESPONSE

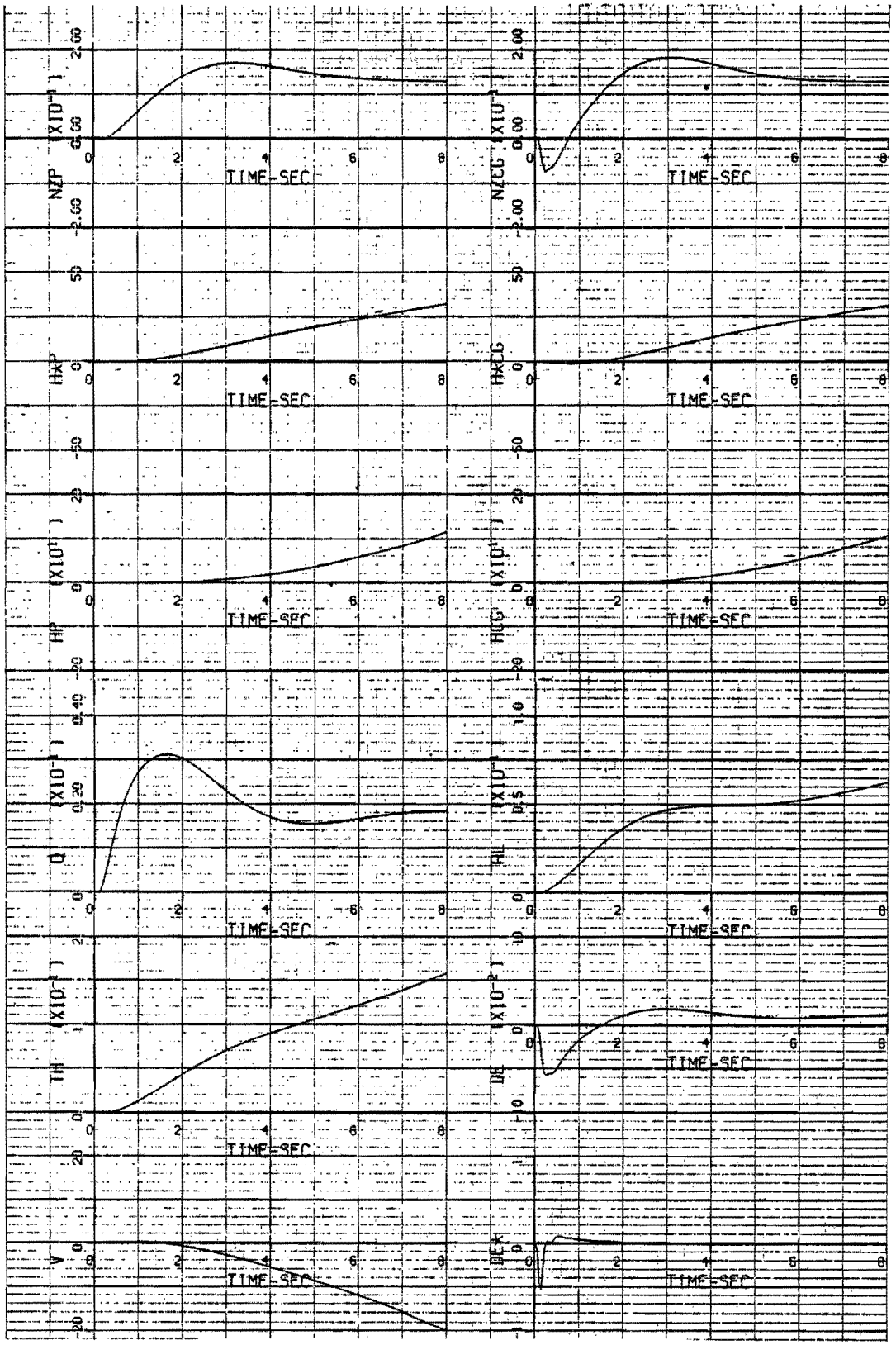

Figure 17. NASA/REVISED CONFIGURATION 2, q_{CMD} STEP RESPONSE

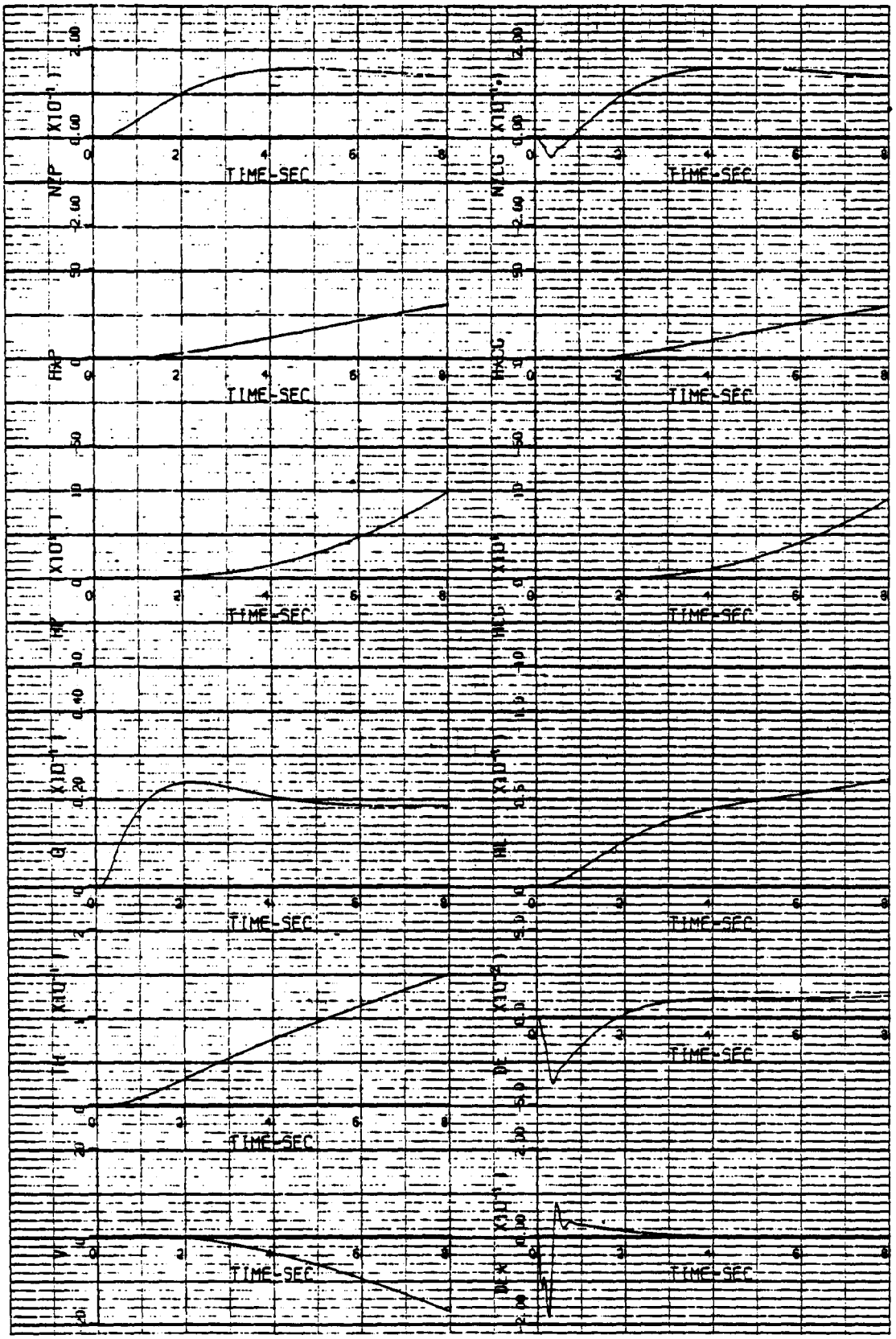

Figure 18. OFT CONFIGURATION 2, q_{CMD} STEP RESPONSE

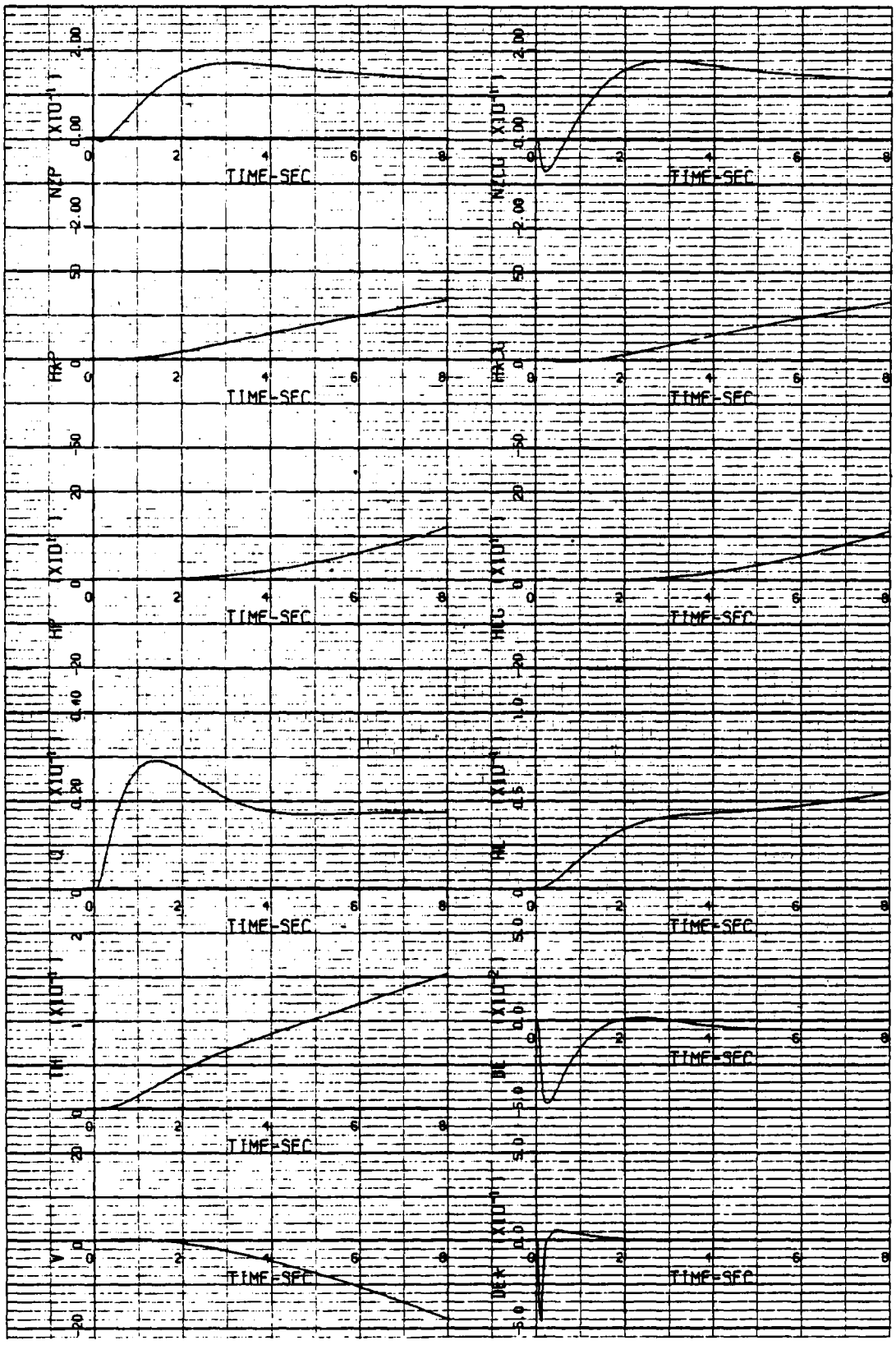

Figure 19. CALSPAN CONFIGURATION 3, q_{CMD} STEP RESPONSE

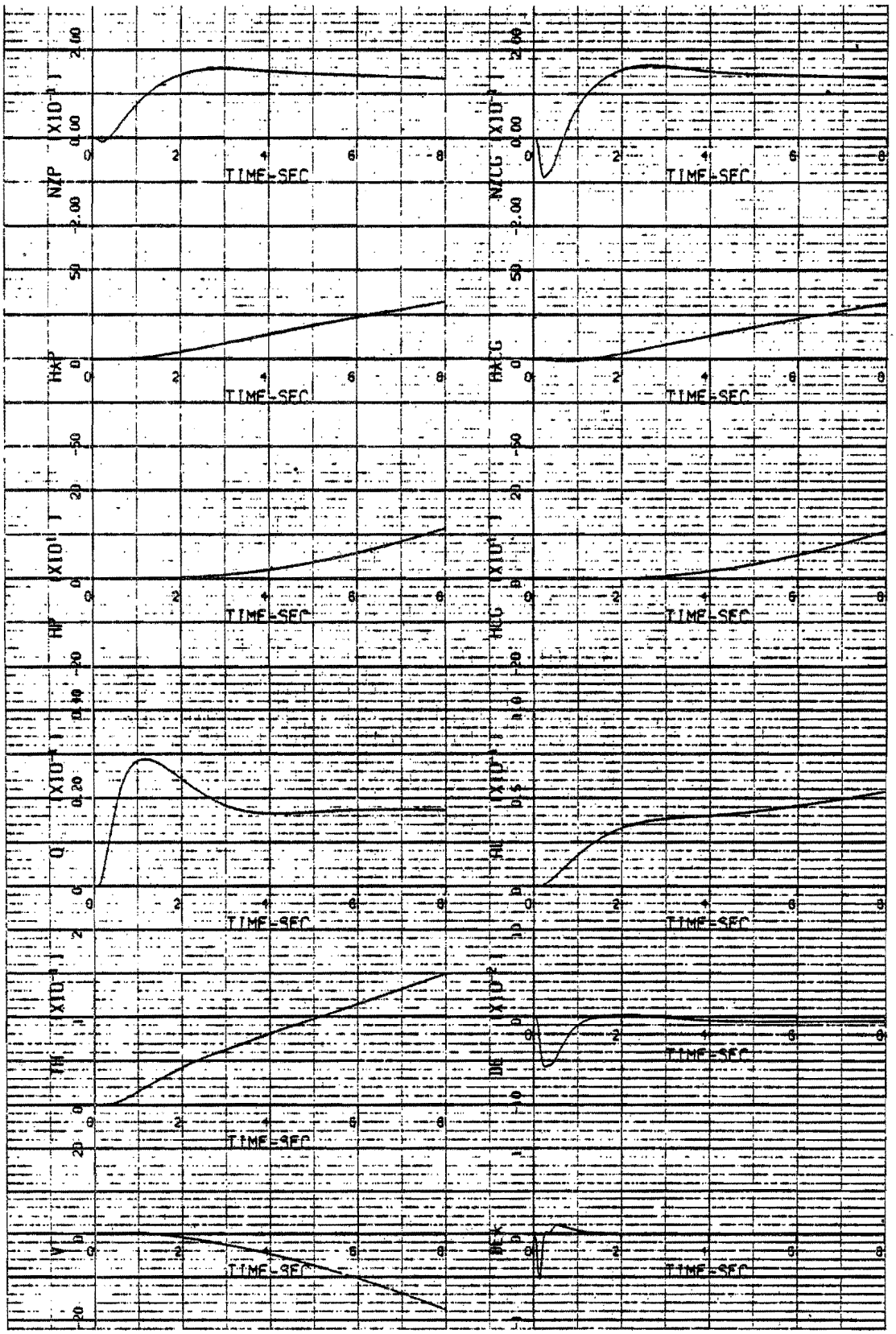

Figure 20. NASA/REVISED CONFIGURATION 3, q_{CMD} STEP RESPONSE

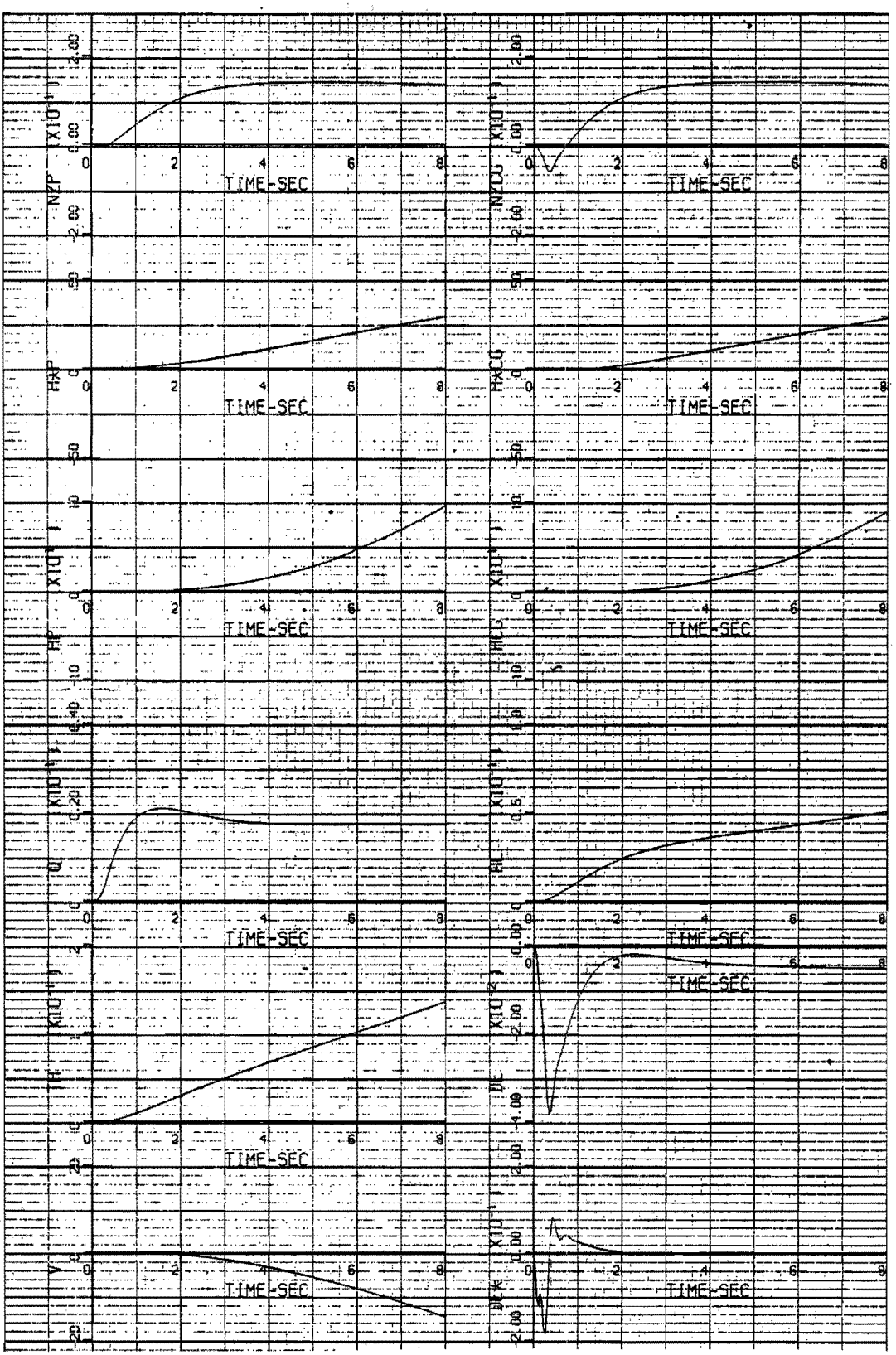

Figure 21. OFT CONFIGURATION 3, q_{CMD} STEP RESPONSE

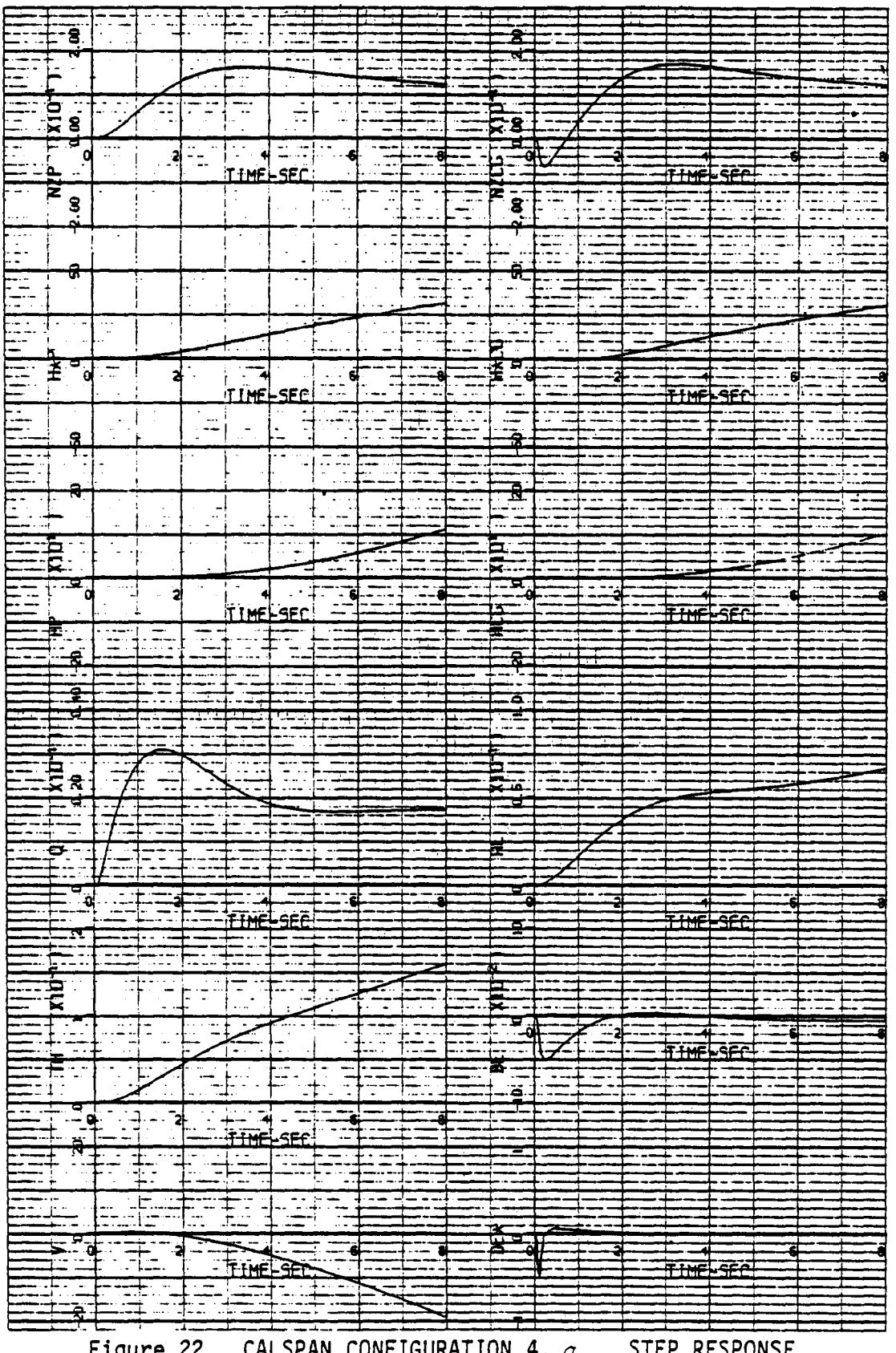

Figure 22. CALSPAN CONFIGURATION 4, q_{CMD} STEP RESPONSE

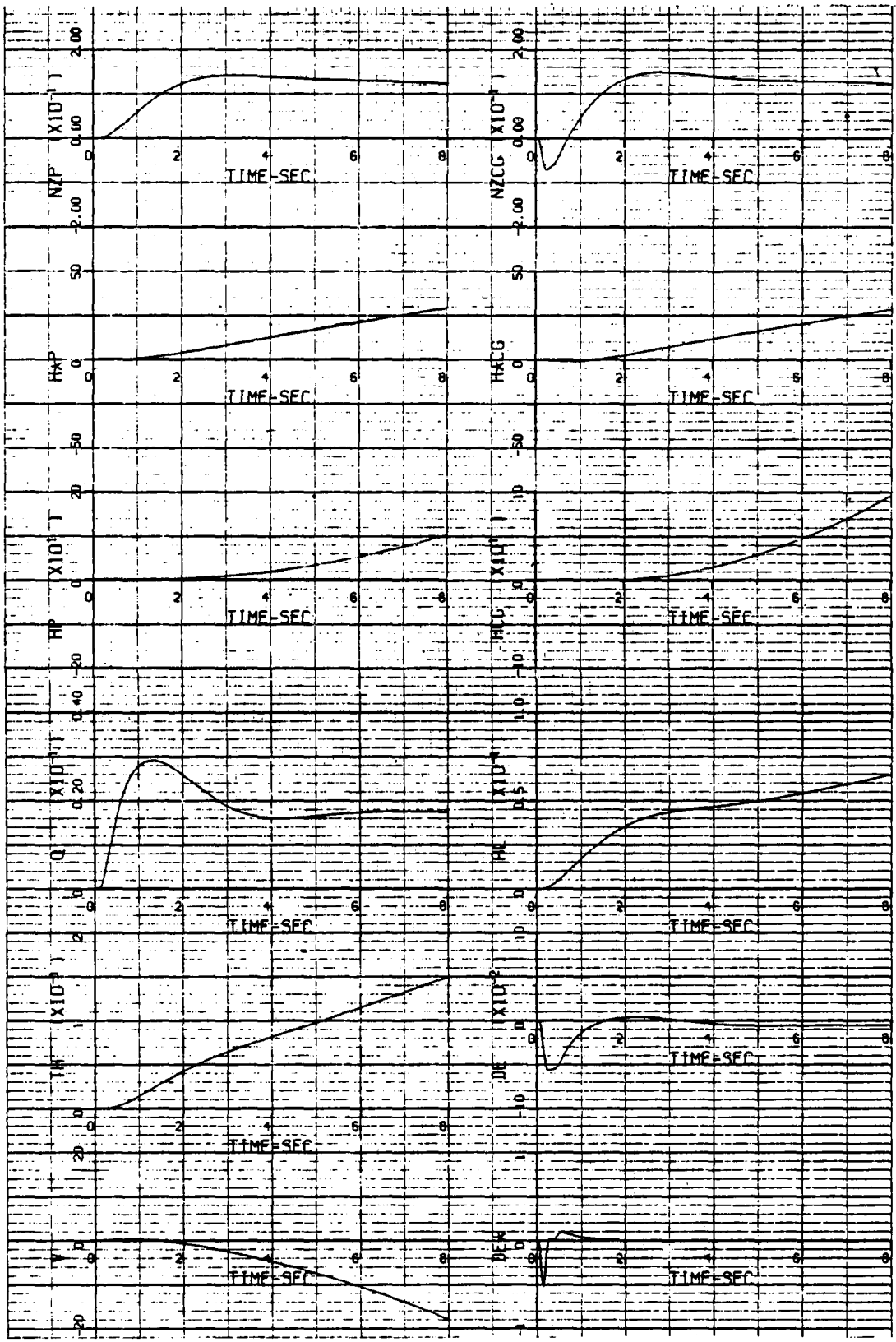

Figure 23. NASA/REVISED CONFIGURATION 4, q_{CMD} STEP RESPONSE

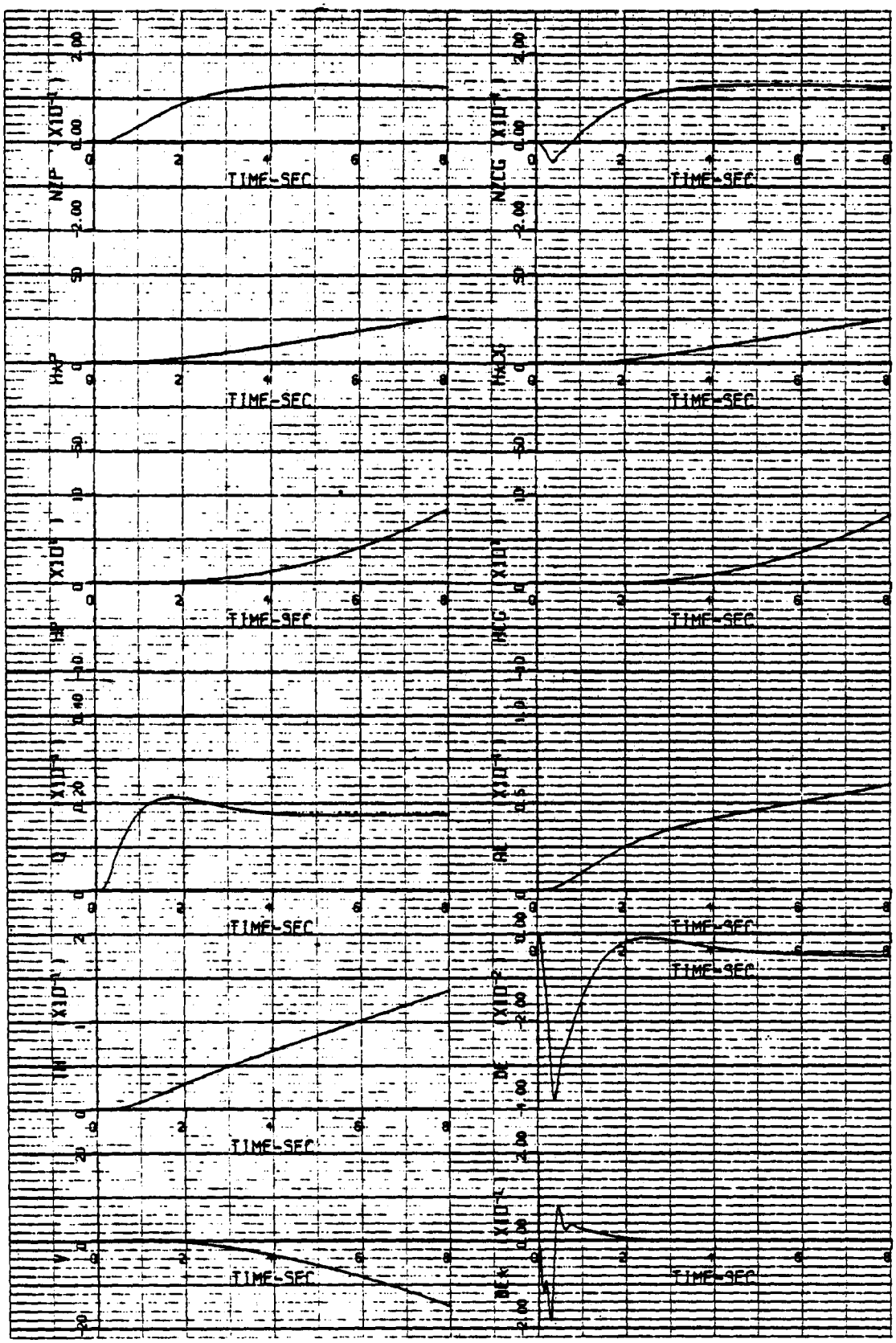

Figure 24. OFT CONFIGURATION 4, q_{CMD} STEP RESPONSE

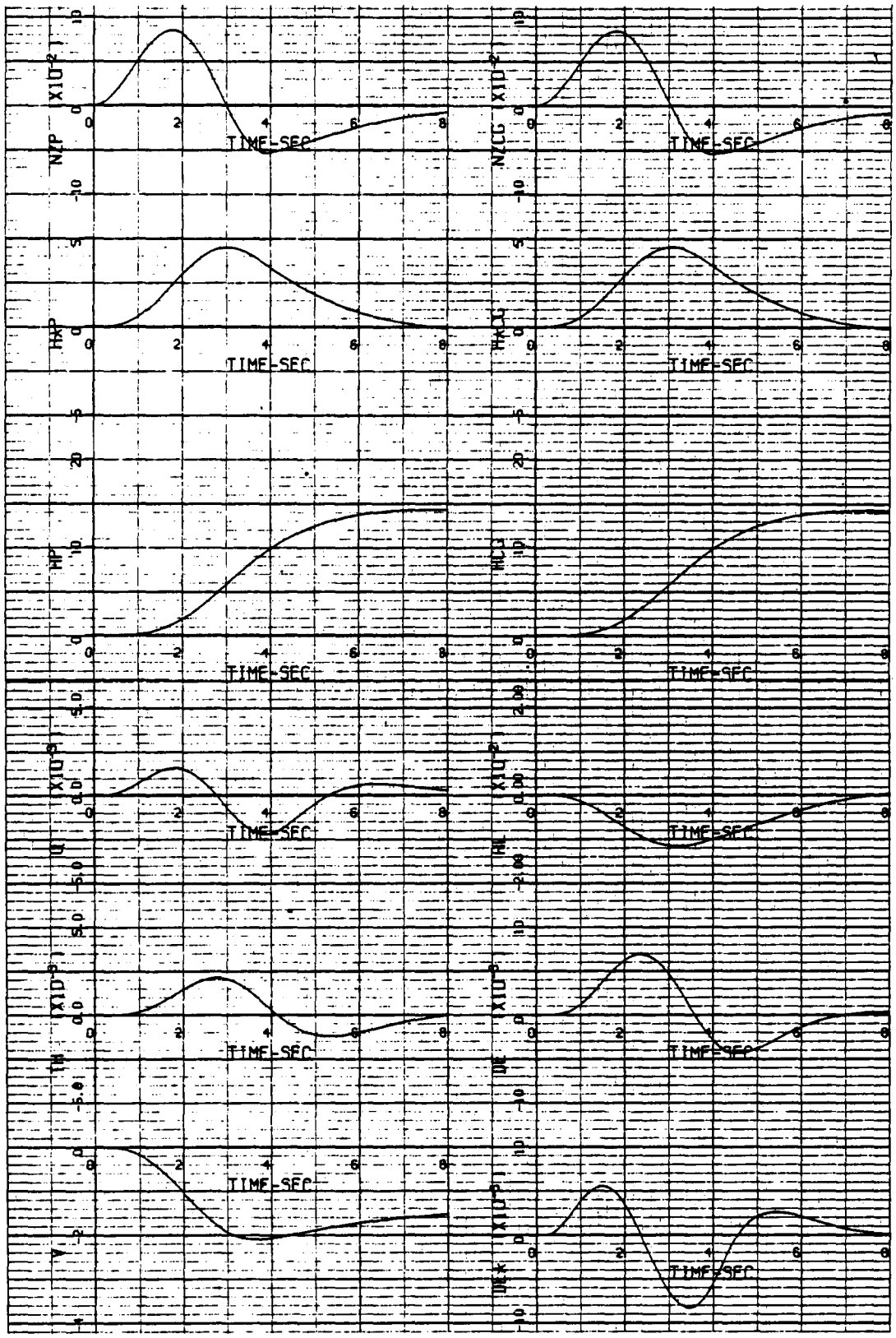

Figure 25. CALSPAN CONFIGURATION 2, DISCRETE VERTICAL GUST RESPONSE

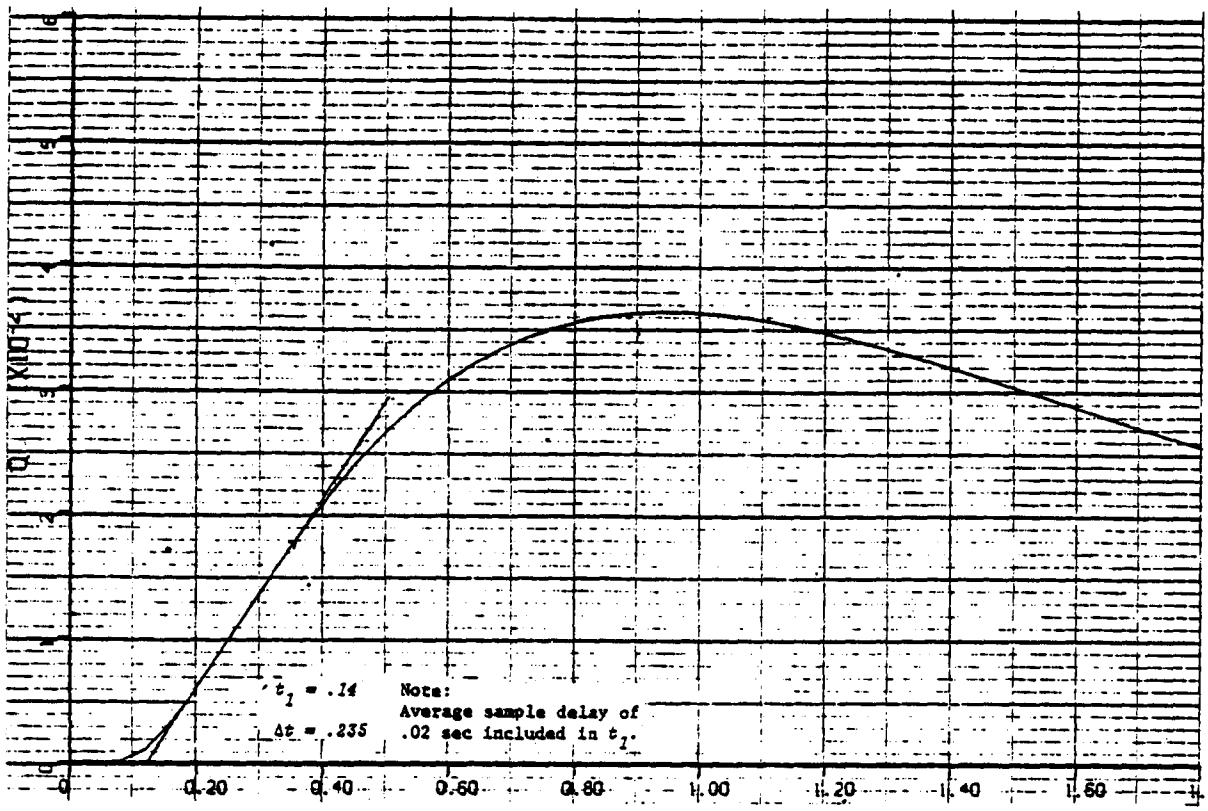

Figure 26. EXPANDED PITCH RATE RESPONSE - CALSPAN CONFIGURATION 1

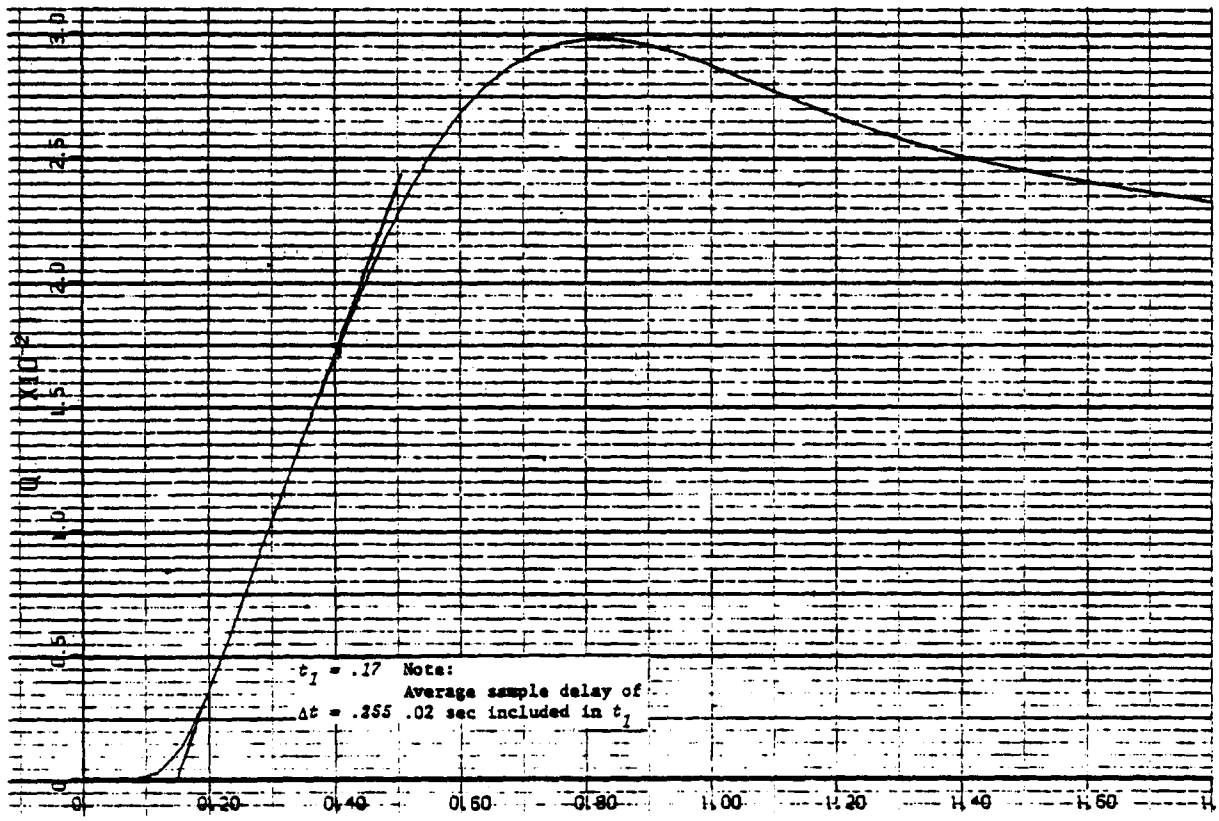

Figure 27. EXPANDED PITCH RATE RESPONSE - NASA/REVISED CONFIGURATION 1

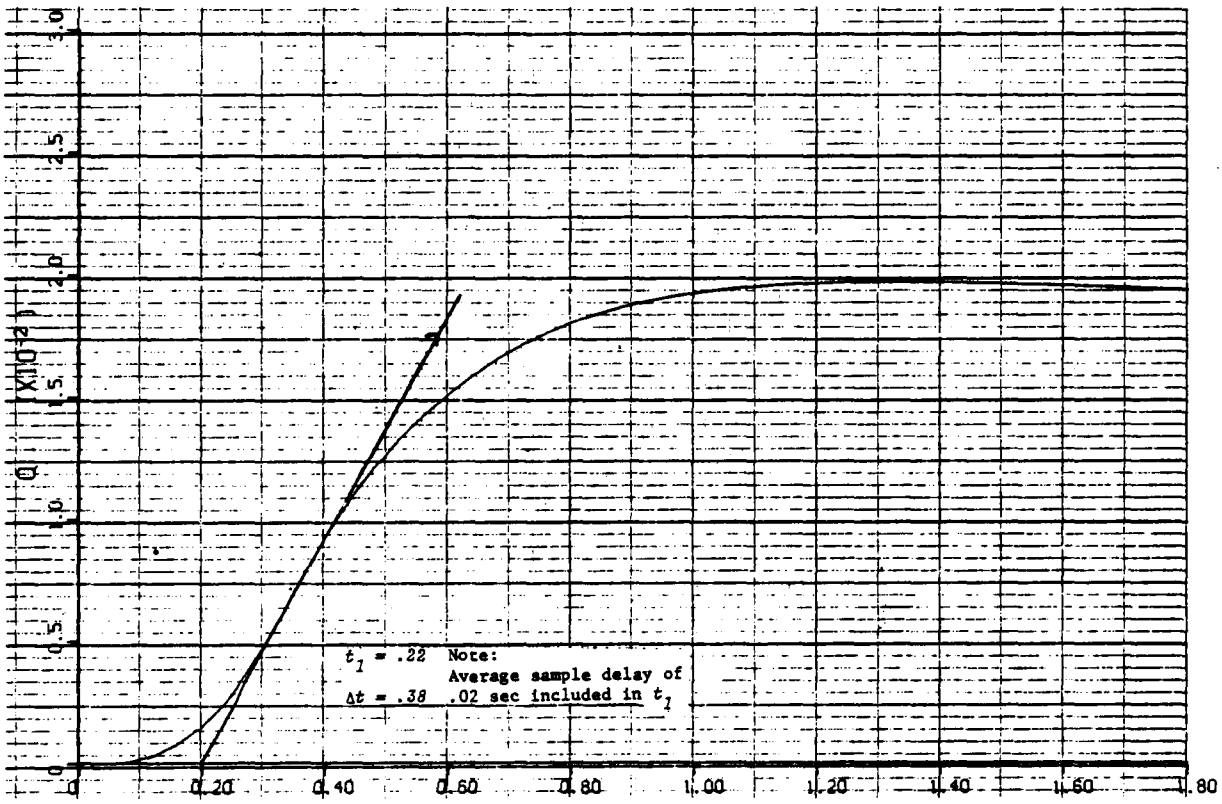

Figure 28. EXPANDED PITCH RATE RESPONSE - OFT CONFIGURATION 1

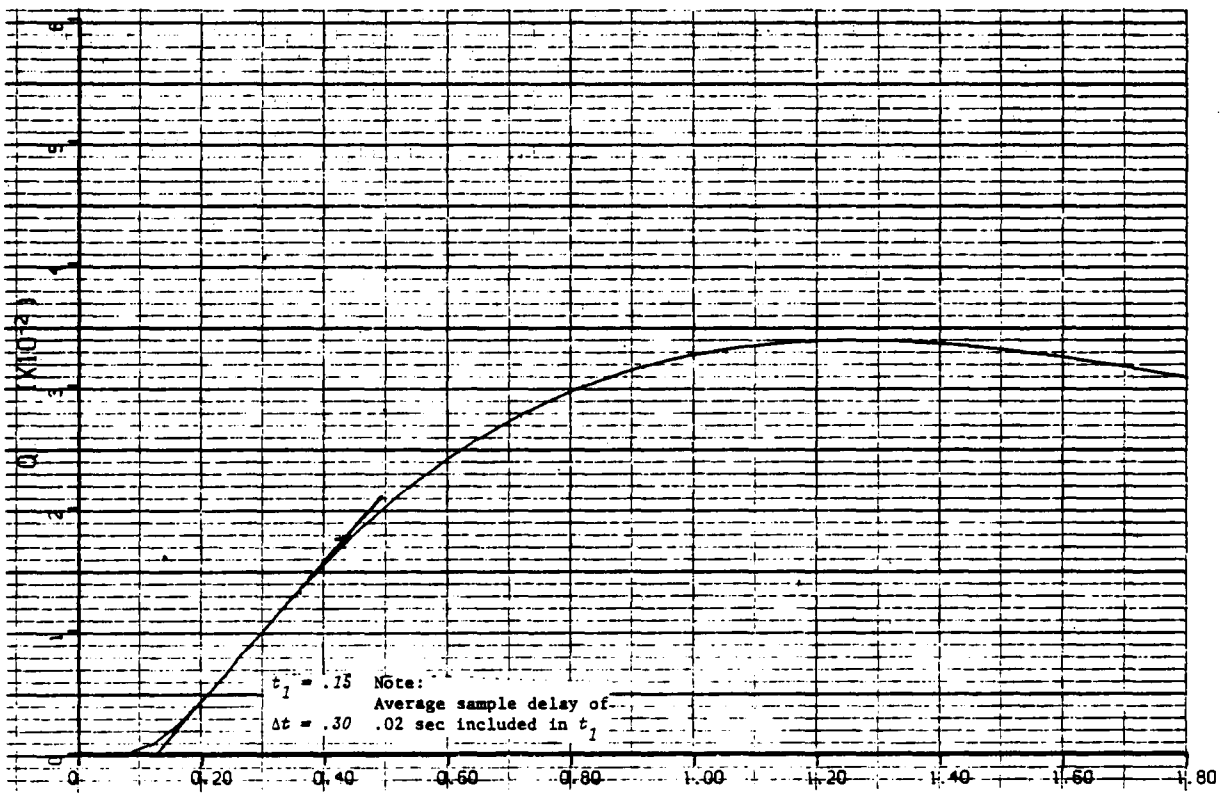

Figure 29. EXPANDED PITCH RATE RESPONSE - CALSPAN CONFIGURATION 2

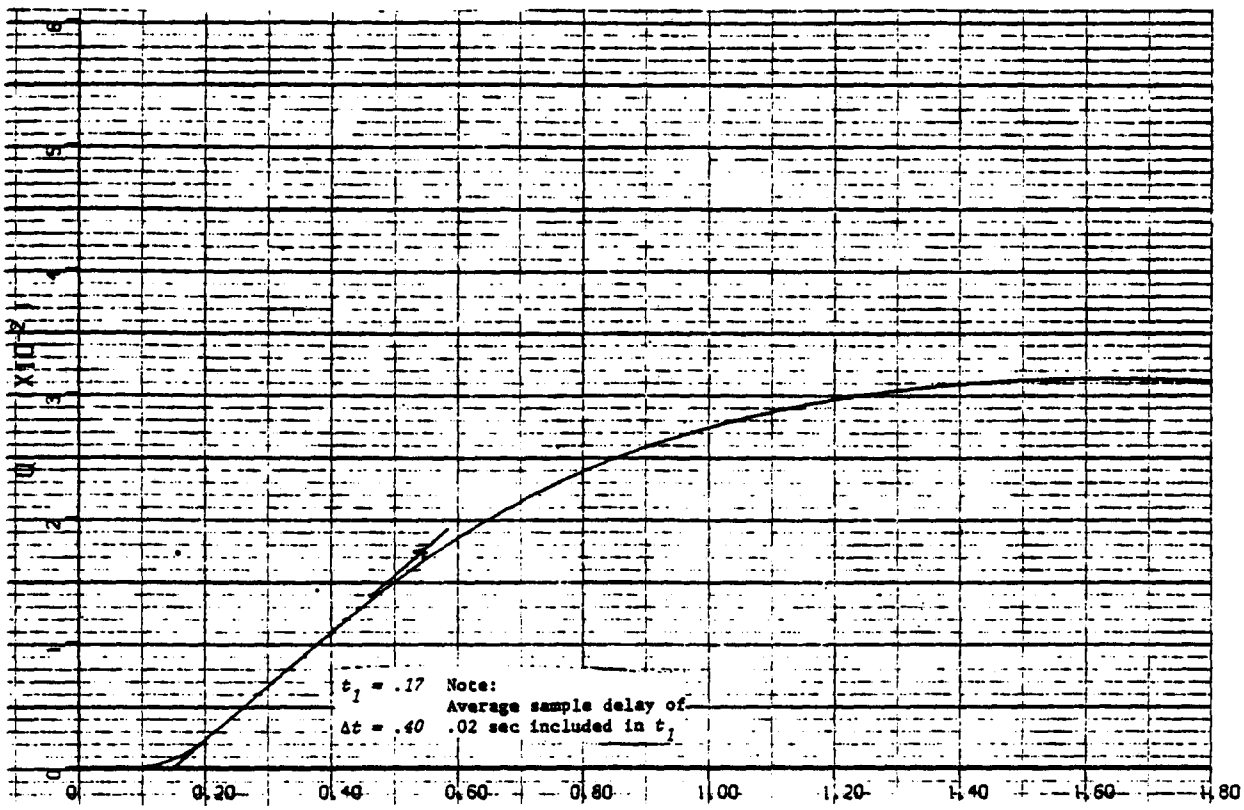

Figure 30. EXPANDED PITCH RATE RESPONSE - NASA/REVISED CONFIGURATION 2

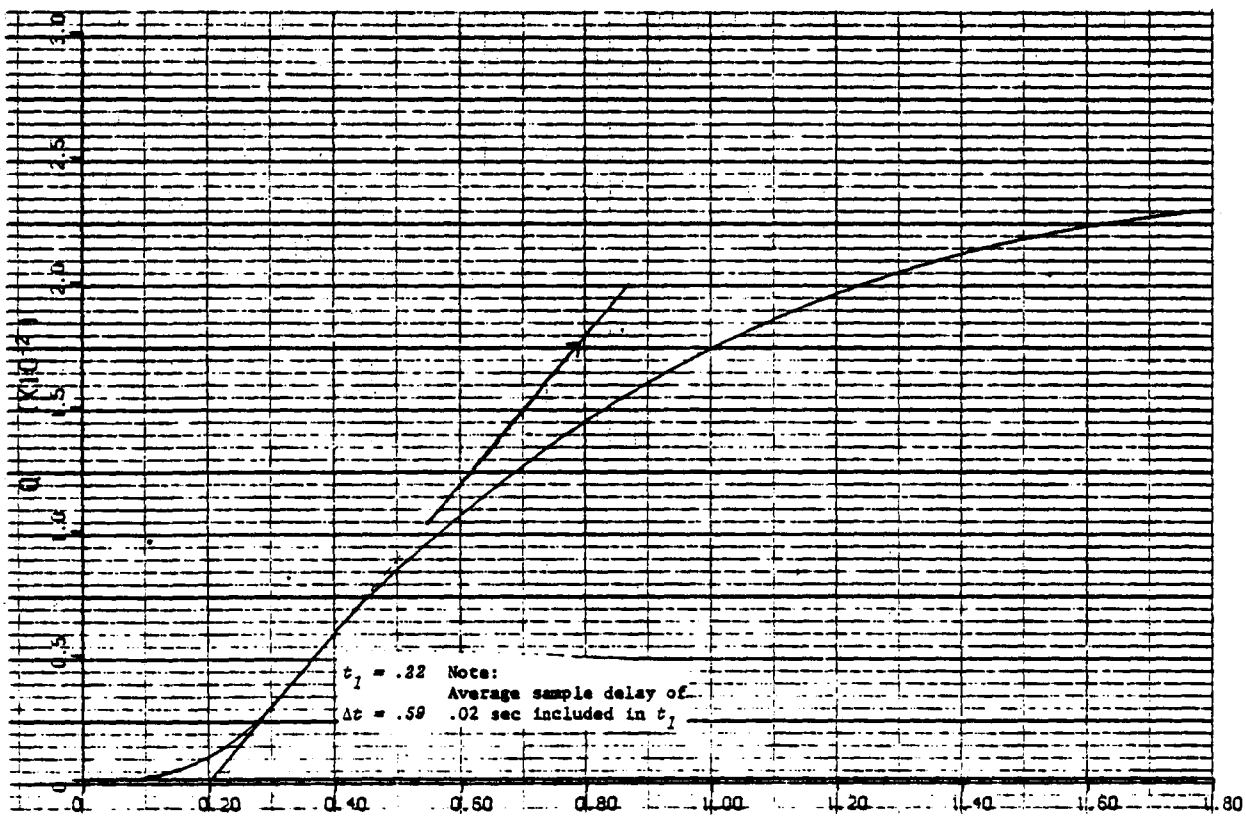

Figure 31. EXPANDED PITCH RATE RESPONSE - OFT CONFIGURATION 2

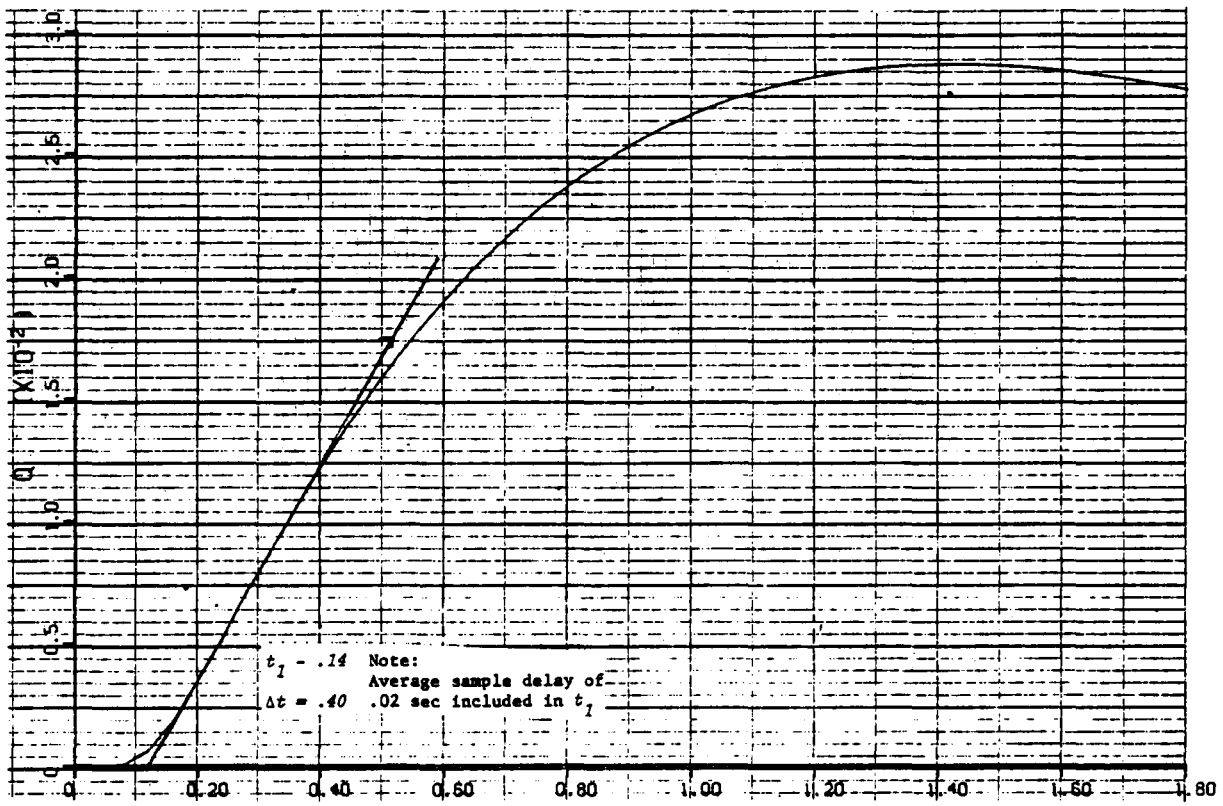

Figure 32. EXPANDED PITCH RATE RESPONSE - CALSPAN CONFIGURATION 3

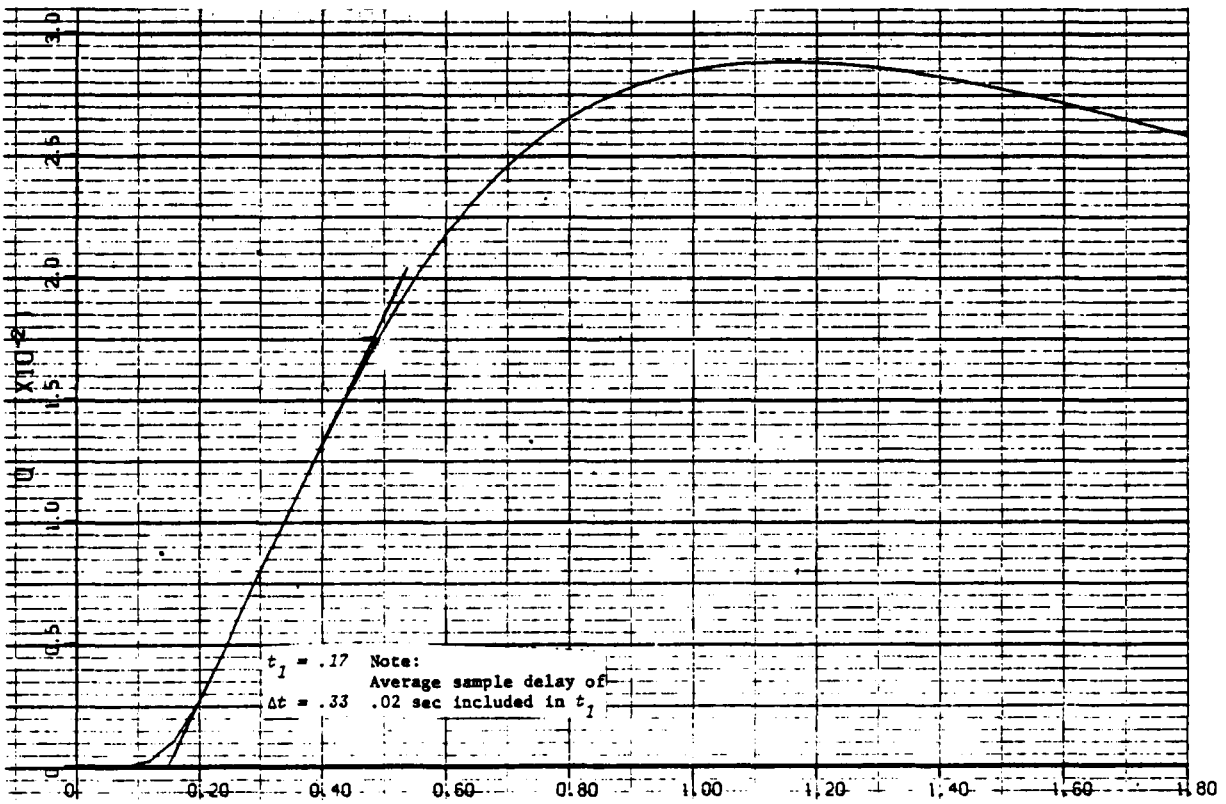

Figure 33. EXPANDED PITCH RATE RESPONSE - NASA/REVISED CONFIGURATION 3

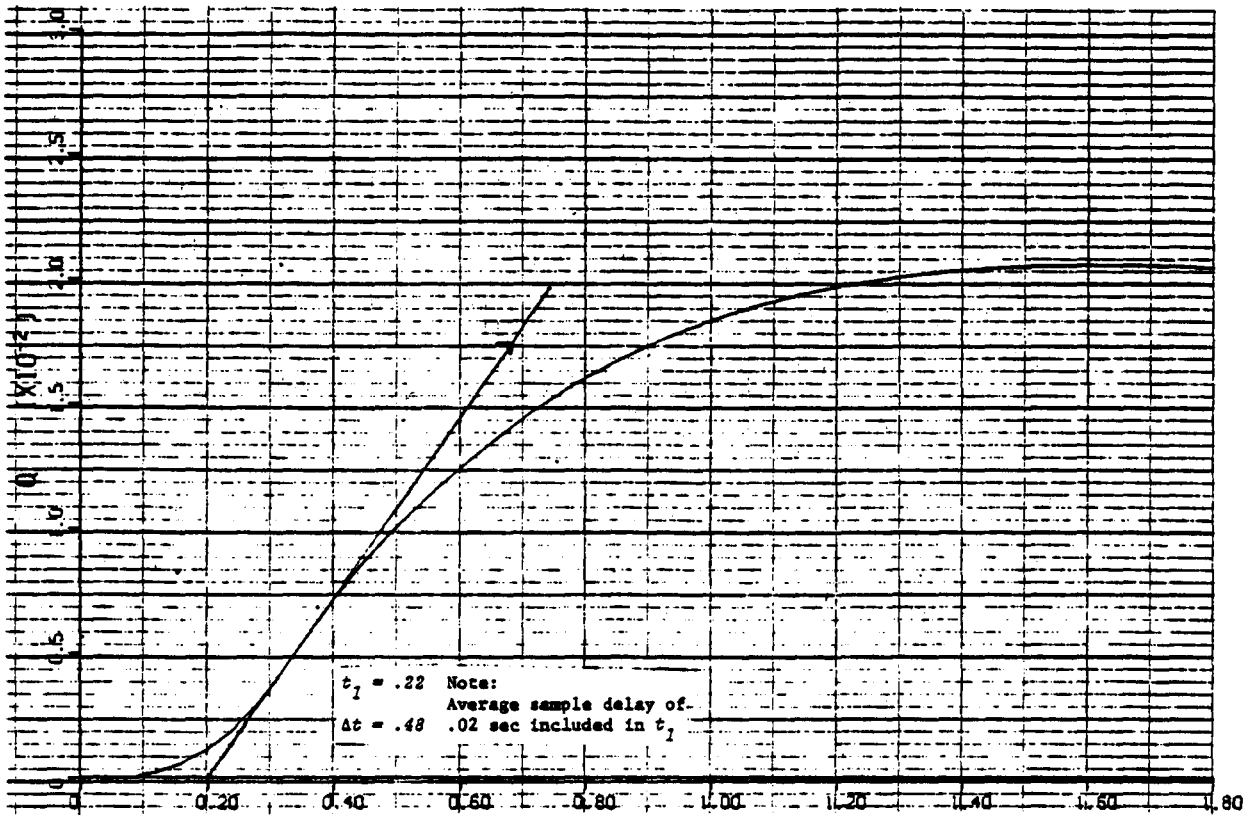

Figure 34. EXPANDED PITCH RATE RESPONSE - OFT CONFIGURATION 3

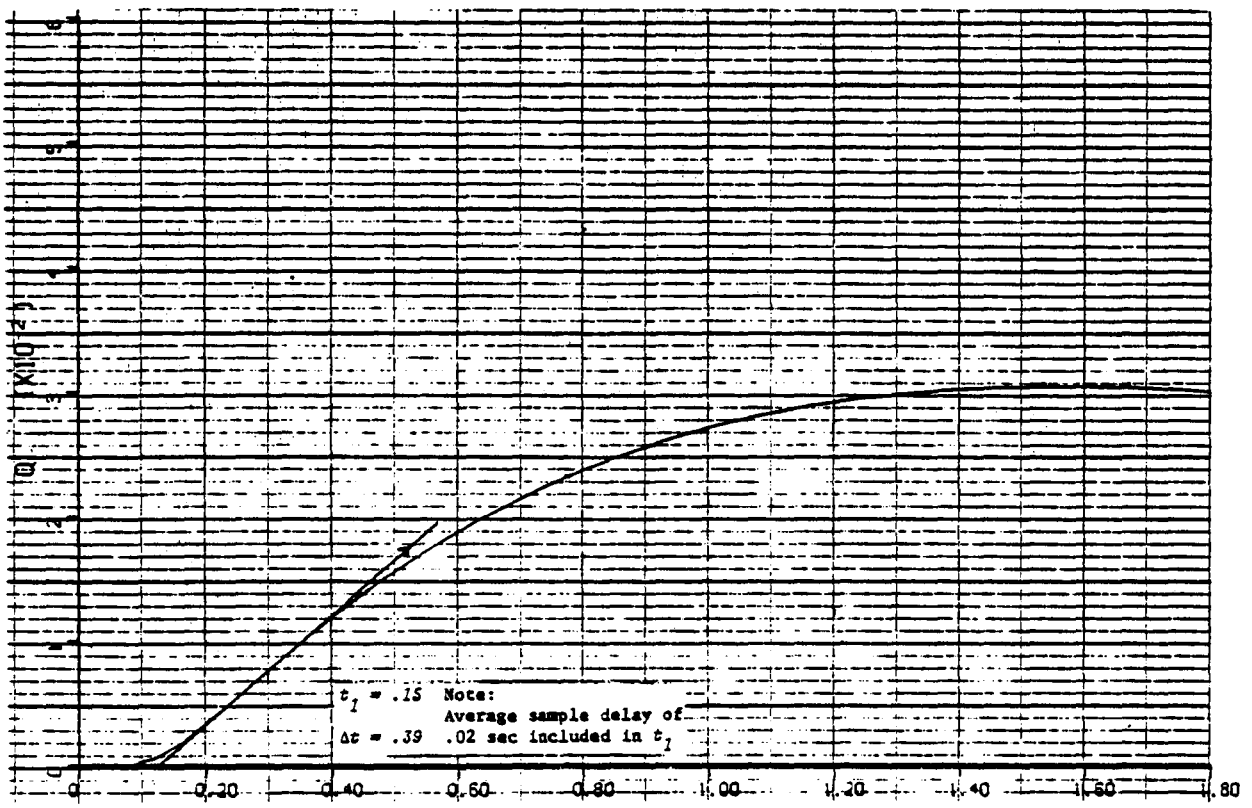

Figure 35. EXPANDED PITCH RATE RESPONSE - CALSPAN CONFIGURATION 4

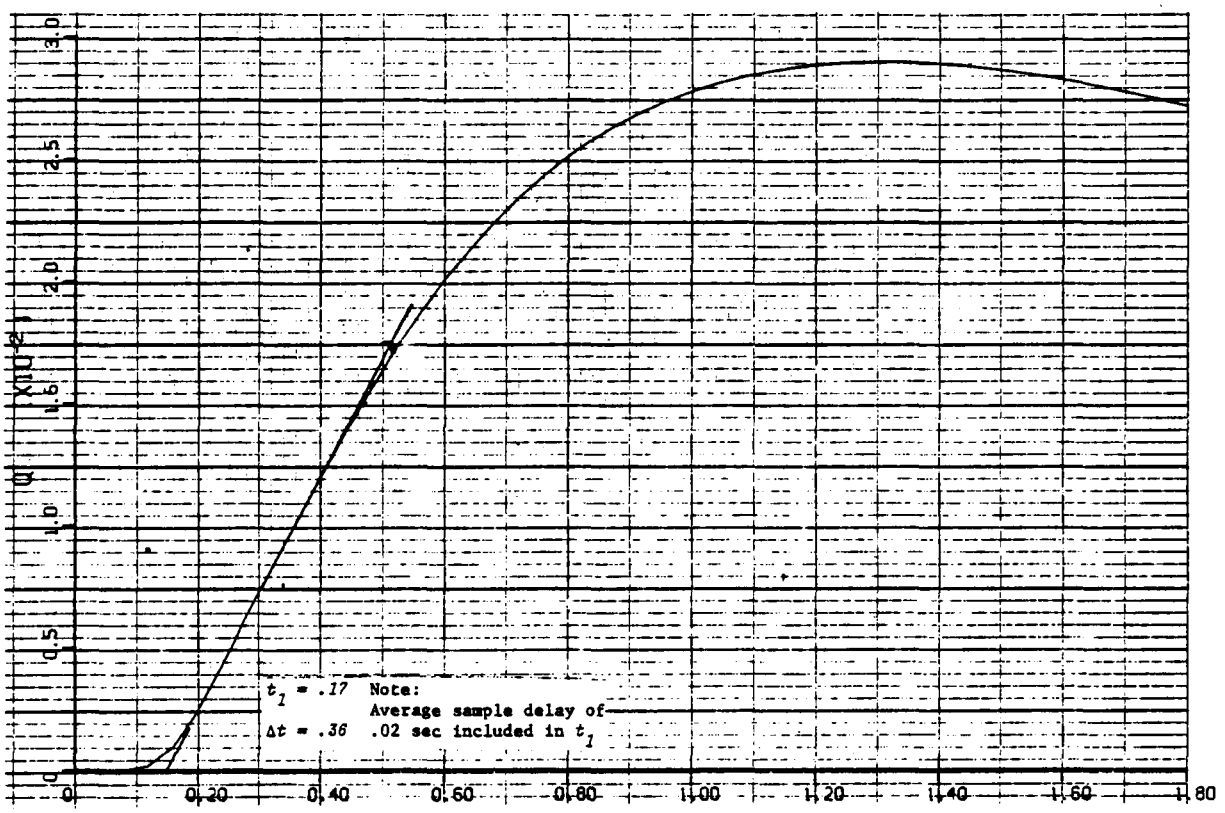

Figure 36. EXPANDED PITCH RATE RESPONSE - NASA/REVISED CONFIGURATION 4

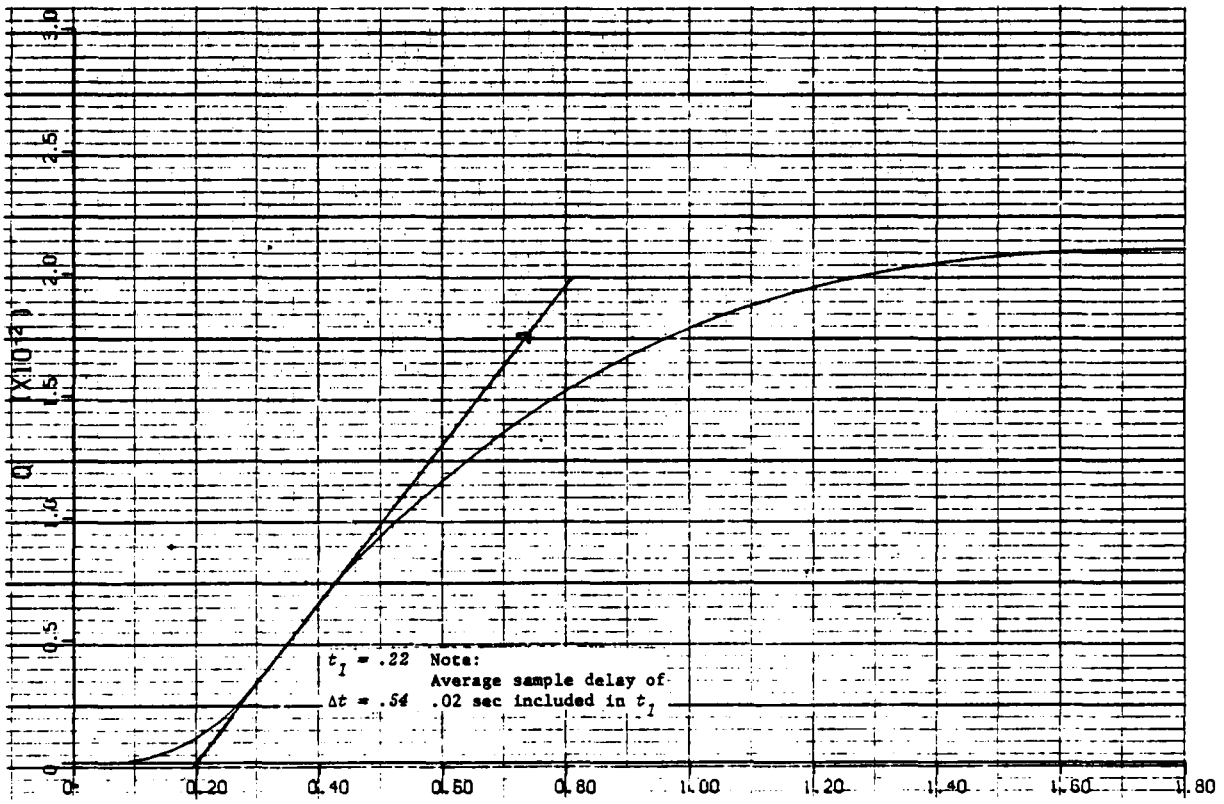

Figure 37. EXPANDED PITCH RATE RESPONSE - OFT CONFIGURATION 4

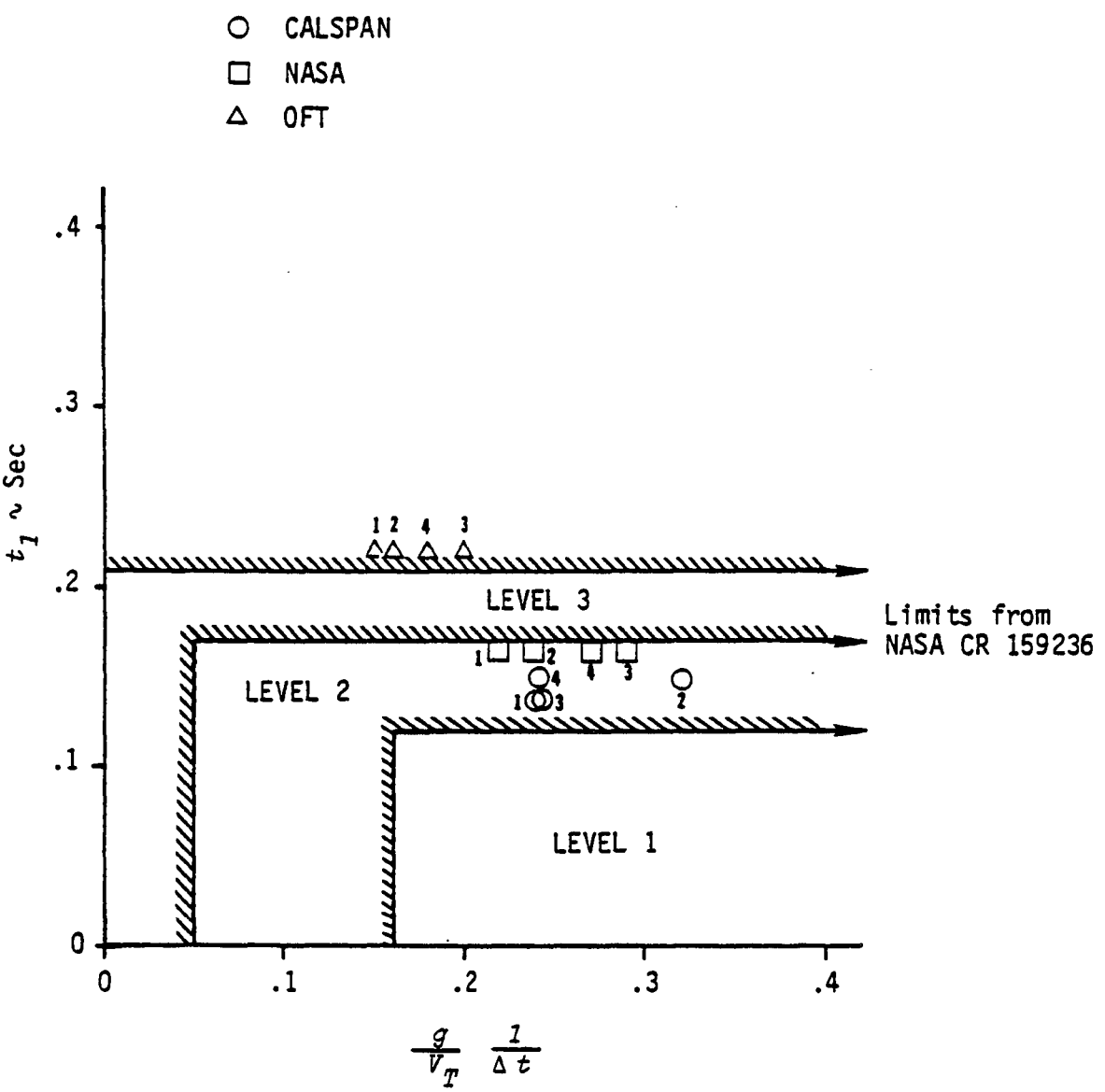

Figure 38. EFFECTIVE TIME DELAY AND RISE TIME PARAMETERS

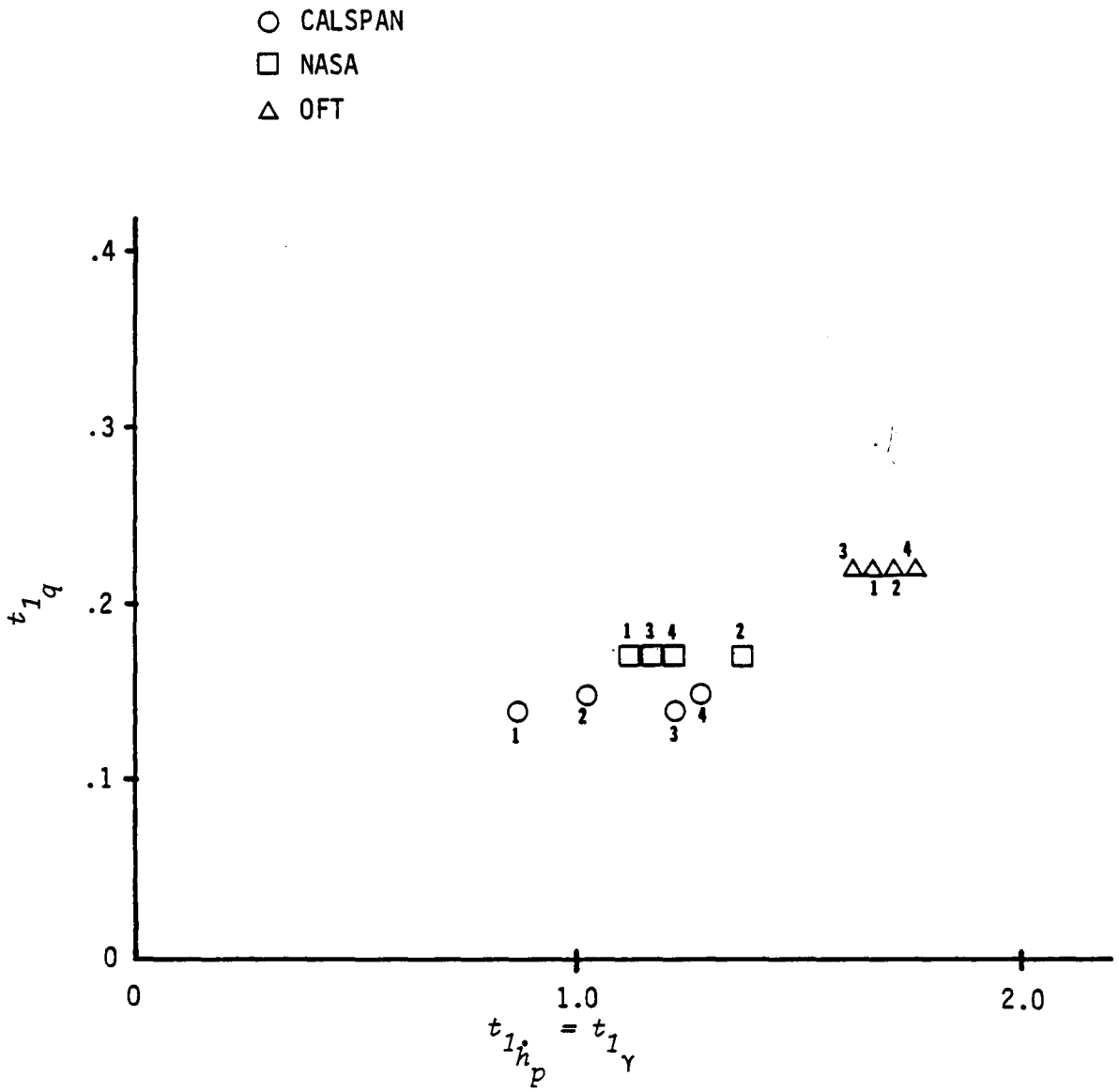

Figure 39. PITCH RATE AND FLIGHT PATH TIME DELAY

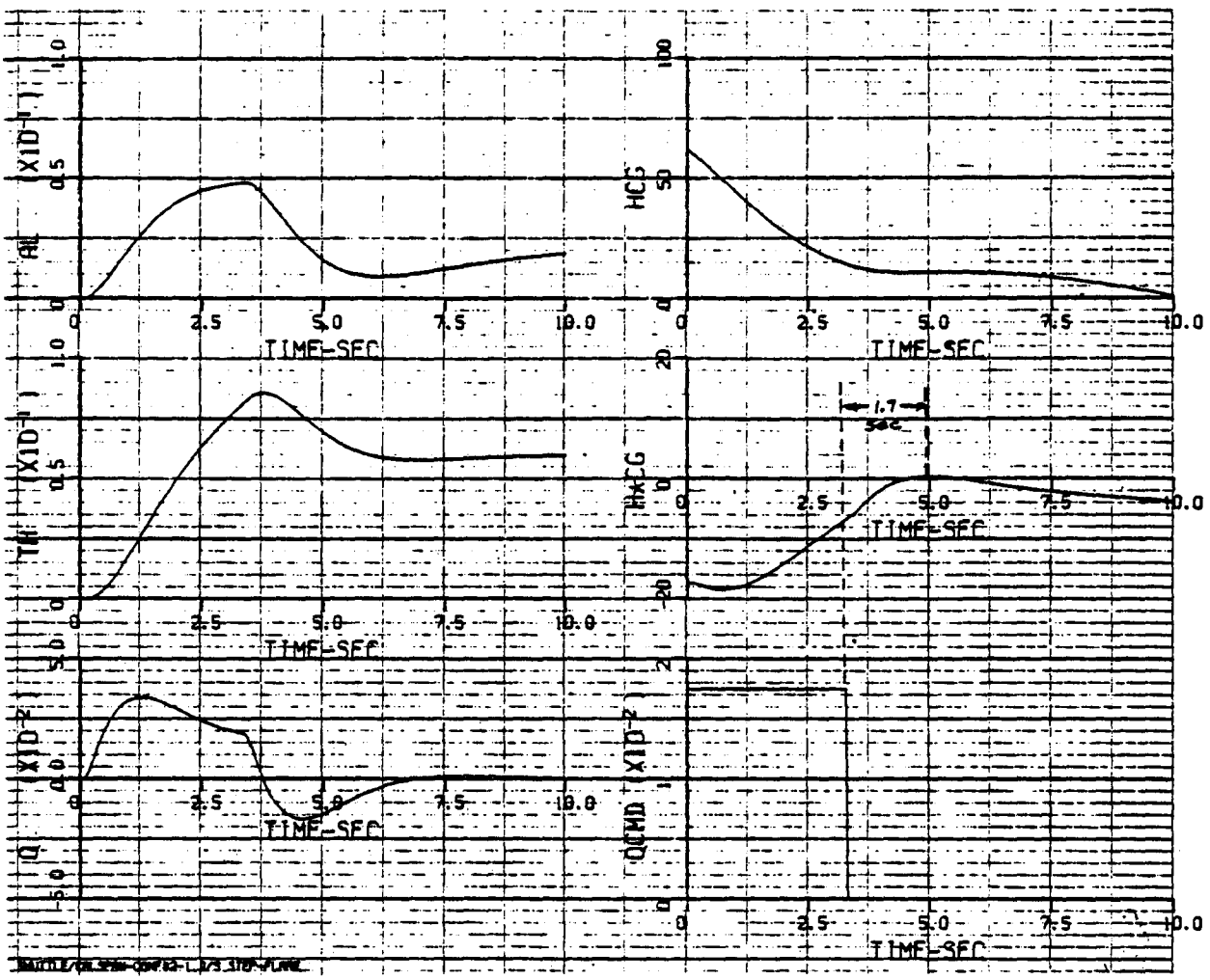

Figure 40. FLARE TIME HISTORY - CALSPAN CONFIGURATION 2

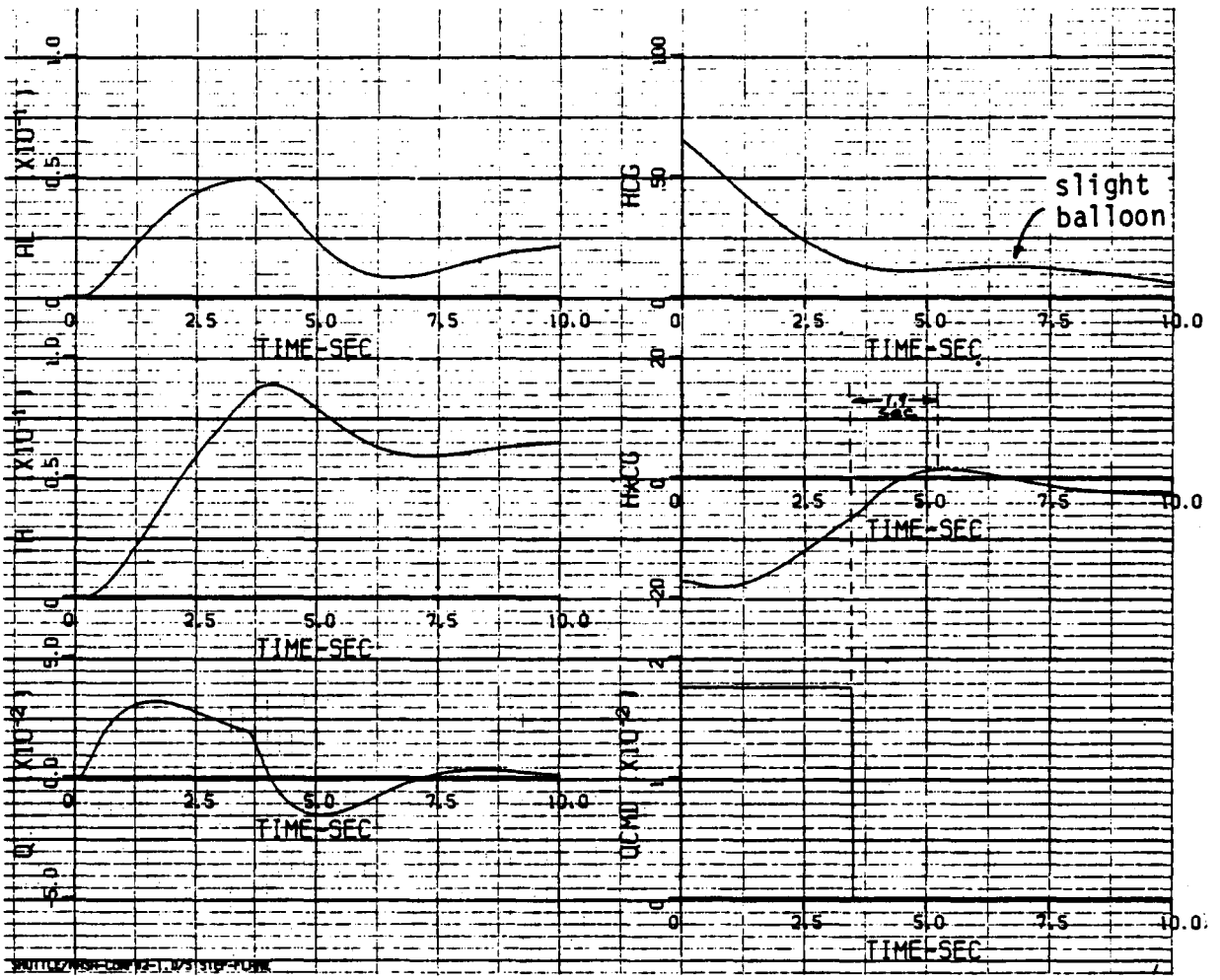

Figure 41. FLARE TIME HISTORY - NASA/REVISED CONFIGURATION 2

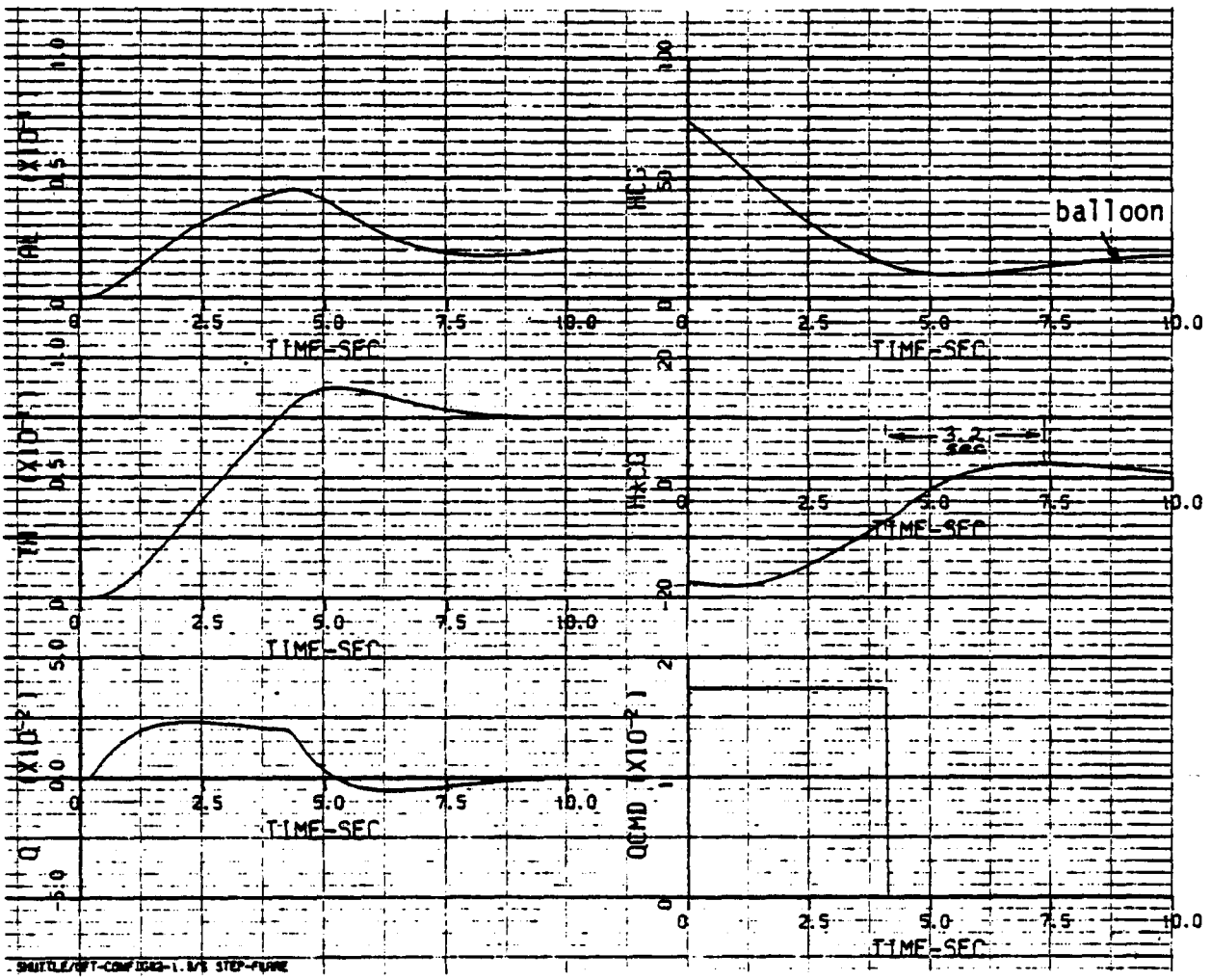

Figure 42. FLARE TIME HISTORY - OFT CONFIGURATION 2

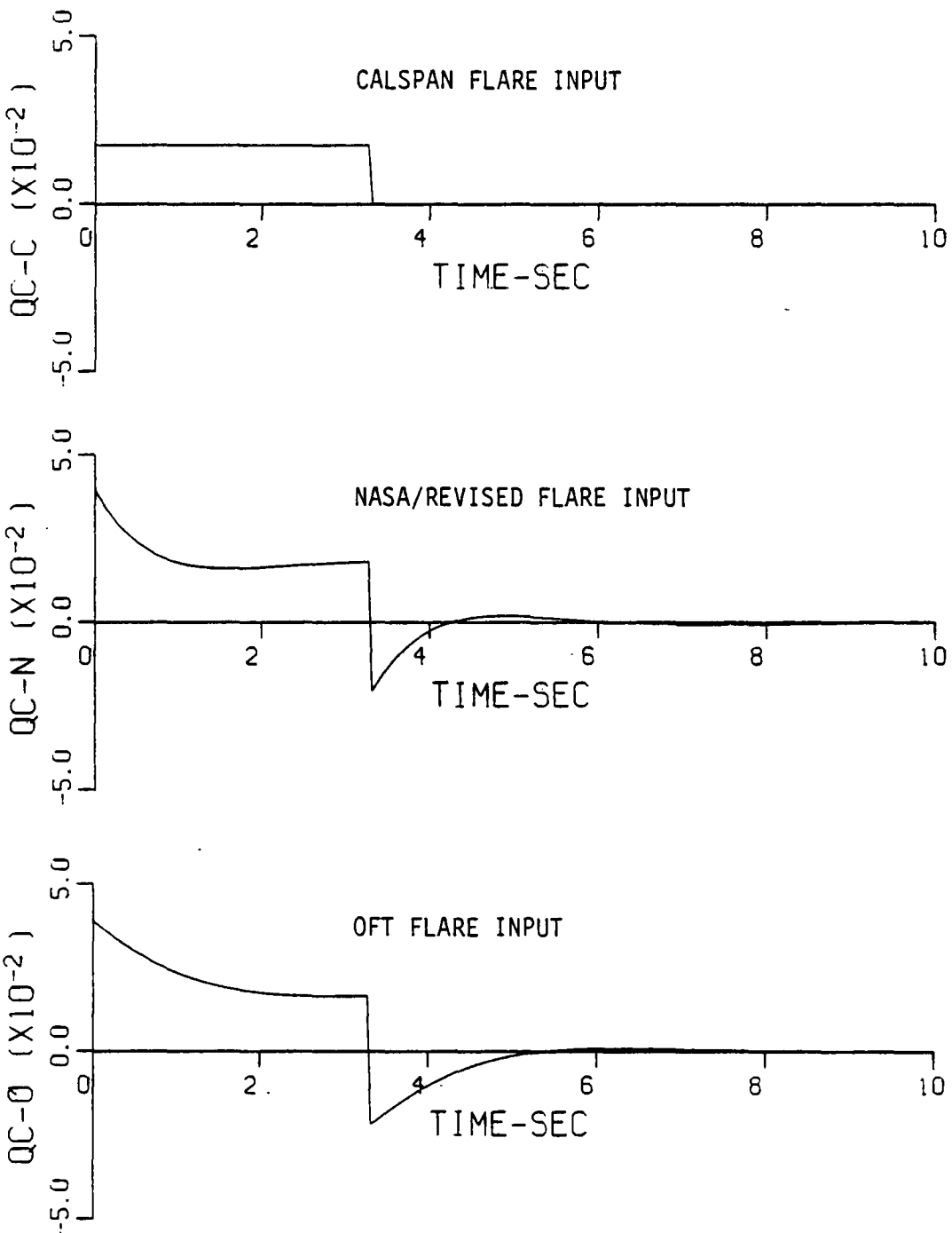

Figure 43. FLARE INPUT REQUIRED TO MATCH CALSPAN FLARE RESPONSE

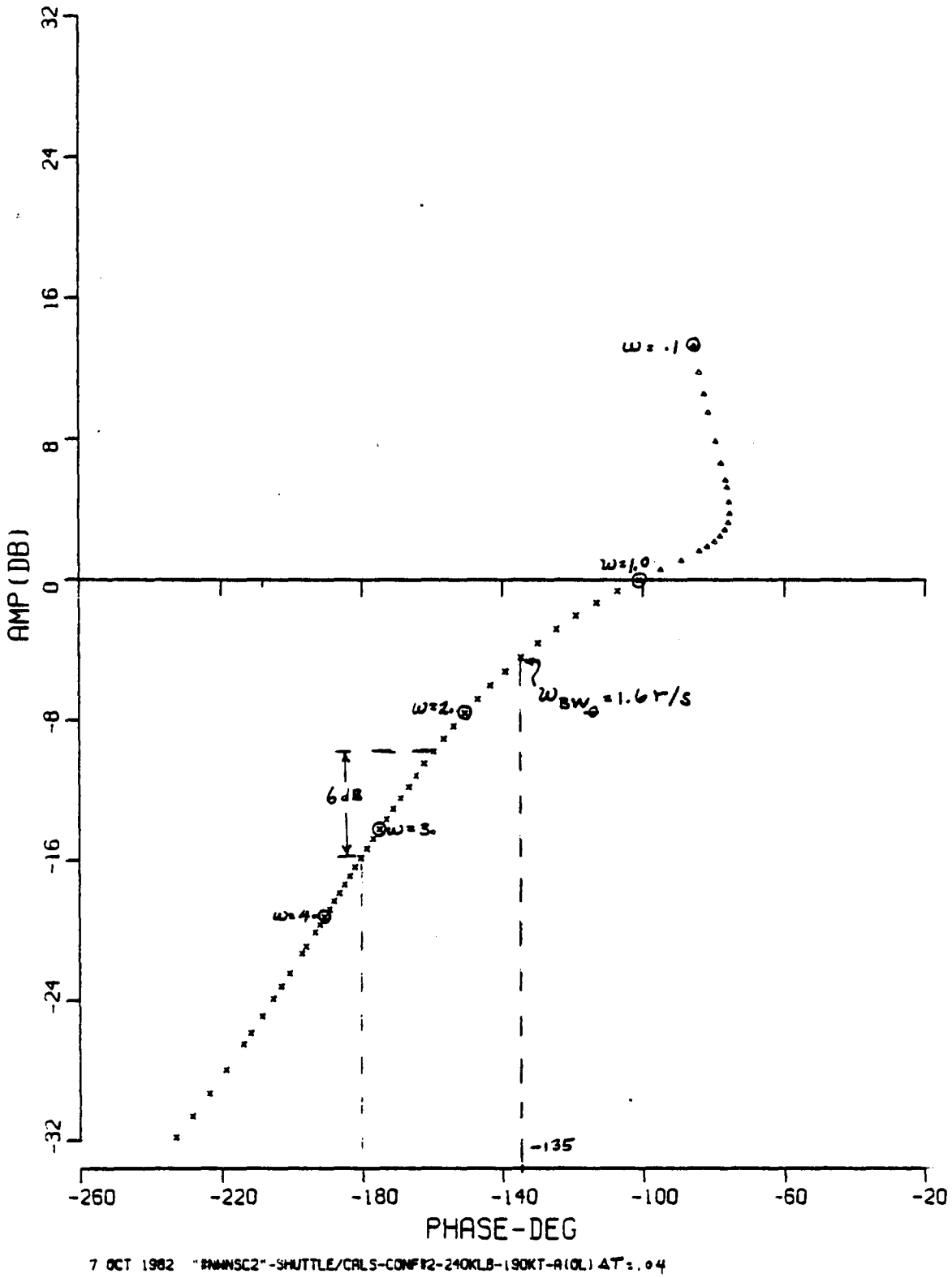

Figure 44. OPEN-LOOP ATTITUDE FREQUENCY RESPONSE AND BANDWIDTH CALSPAN CONFIGURATION 2

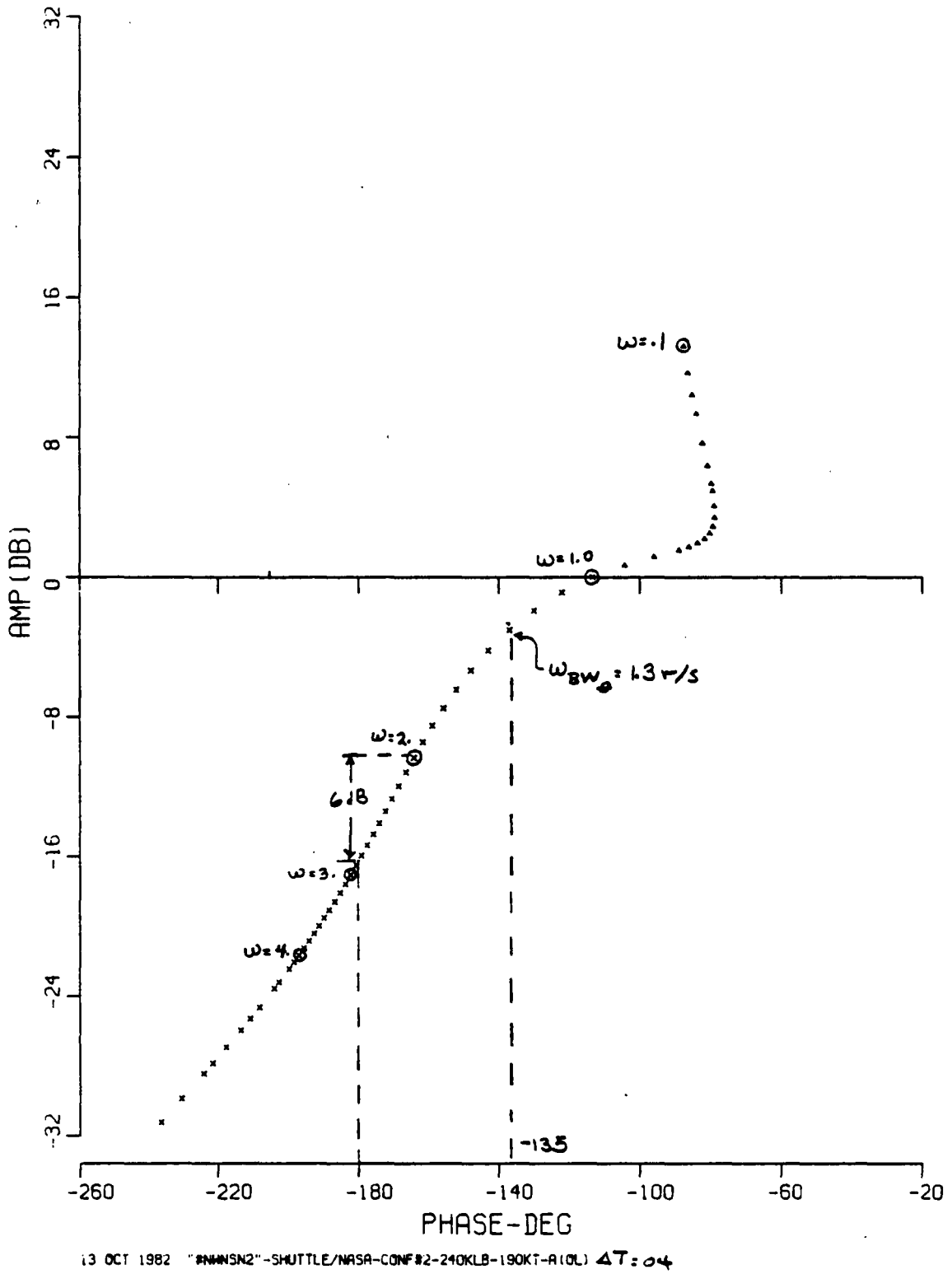

Figure 45. OPEN-LOOP ATTITUDE FREQUENCY RESPONSE AND BANDWIDTH NASA/REVISED CONFIGURATION 2

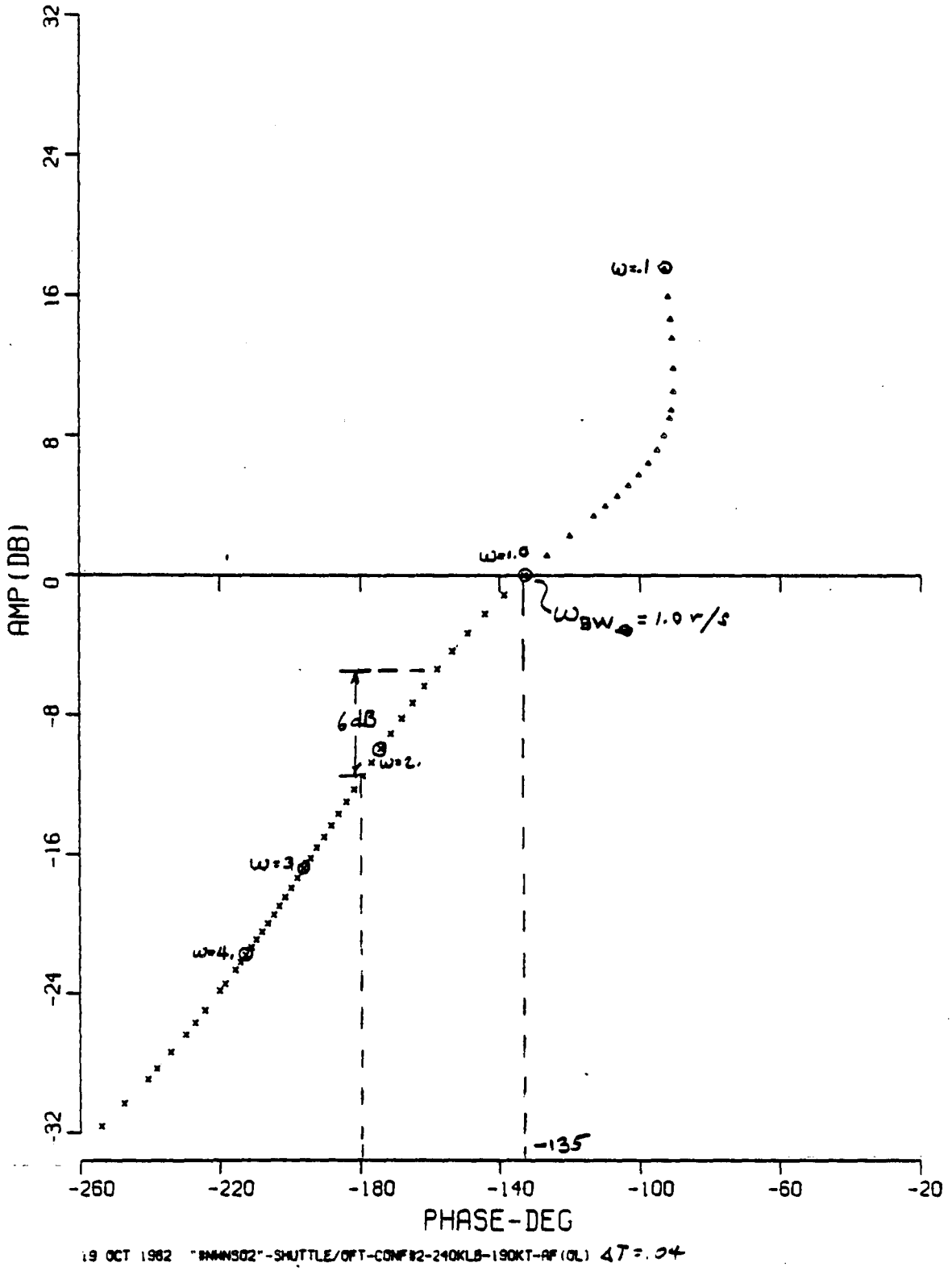

Figure 46. OPEN-LOOP ATTITUDE FREQUENCY RESPONSE AND BANDWIDTH OFT CONFIGURATION 2

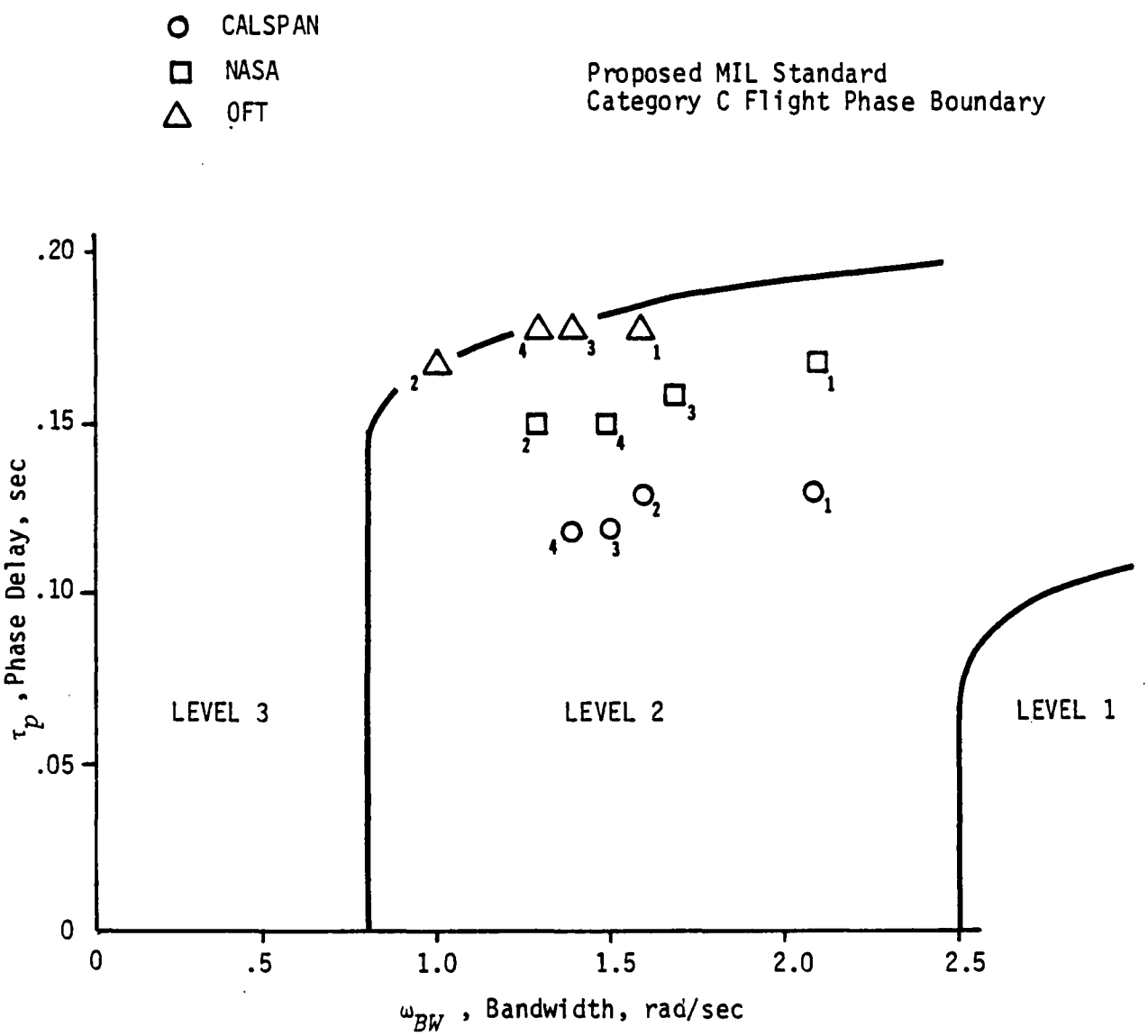

Figure 47. OPEN-LOOP BANDWIDTH (θ/q_{CMD}) AND PHASE DELAY

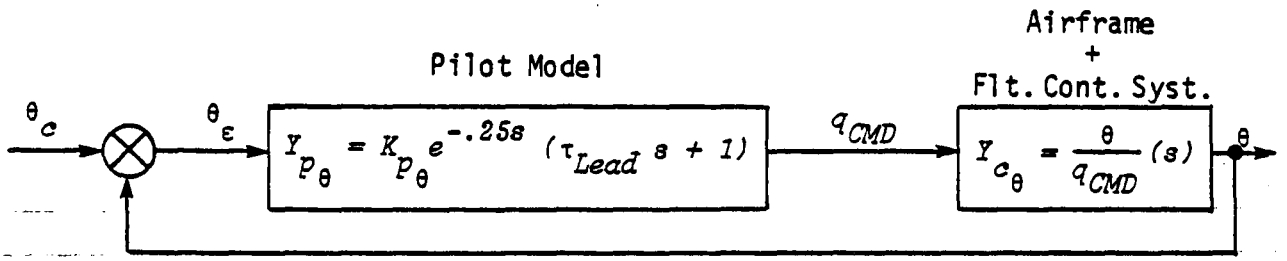

$$\text{Open-Loop} \quad \frac{\theta}{\theta_\varepsilon} = Y_{p_\theta} Y_{c_\theta}$$

$$\text{Closed-Loop} \quad \frac{\theta}{\theta_c} = \frac{Y_{p_\theta} Y_{c_\theta}}{1 + Y_{p_\theta} Y_{c_\theta}}$$

Figure 48. PITCH ATTITUDE TRACKING LOOP

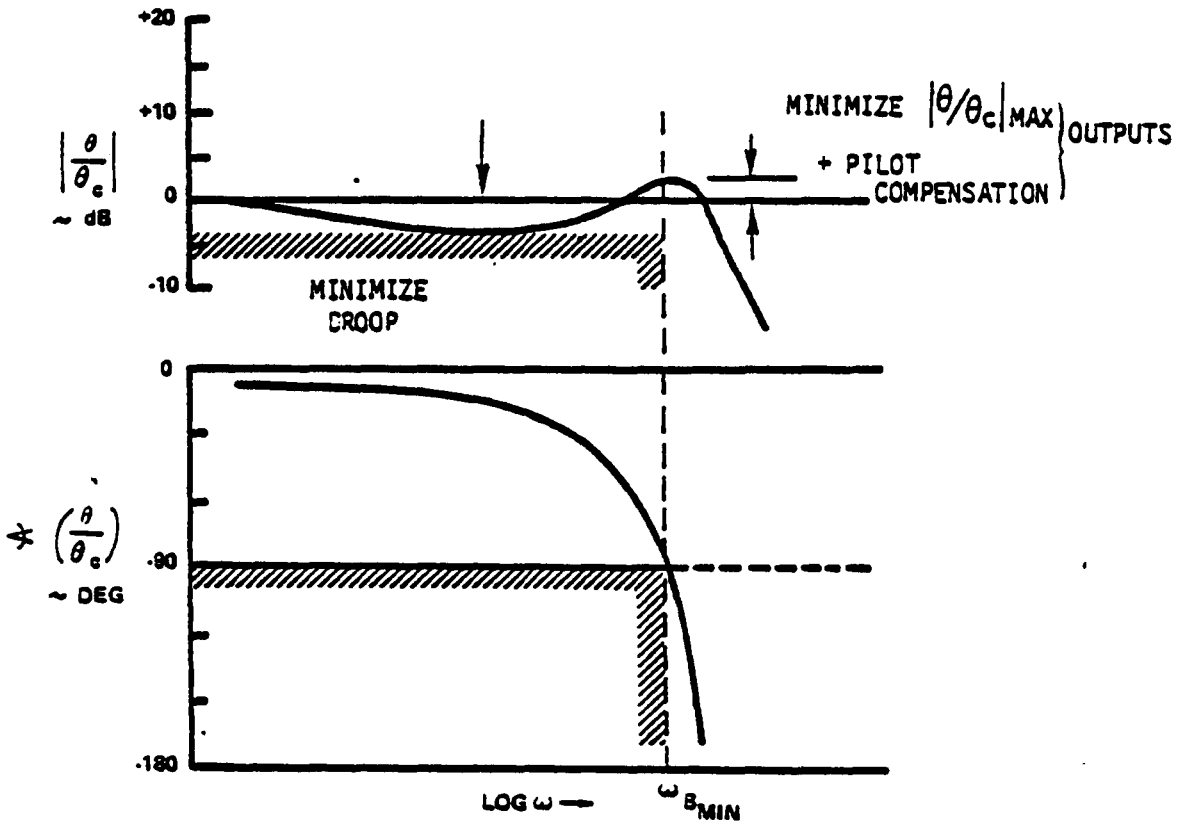

Figure 49. NEAL SMITH CRITERION PARAMETERS

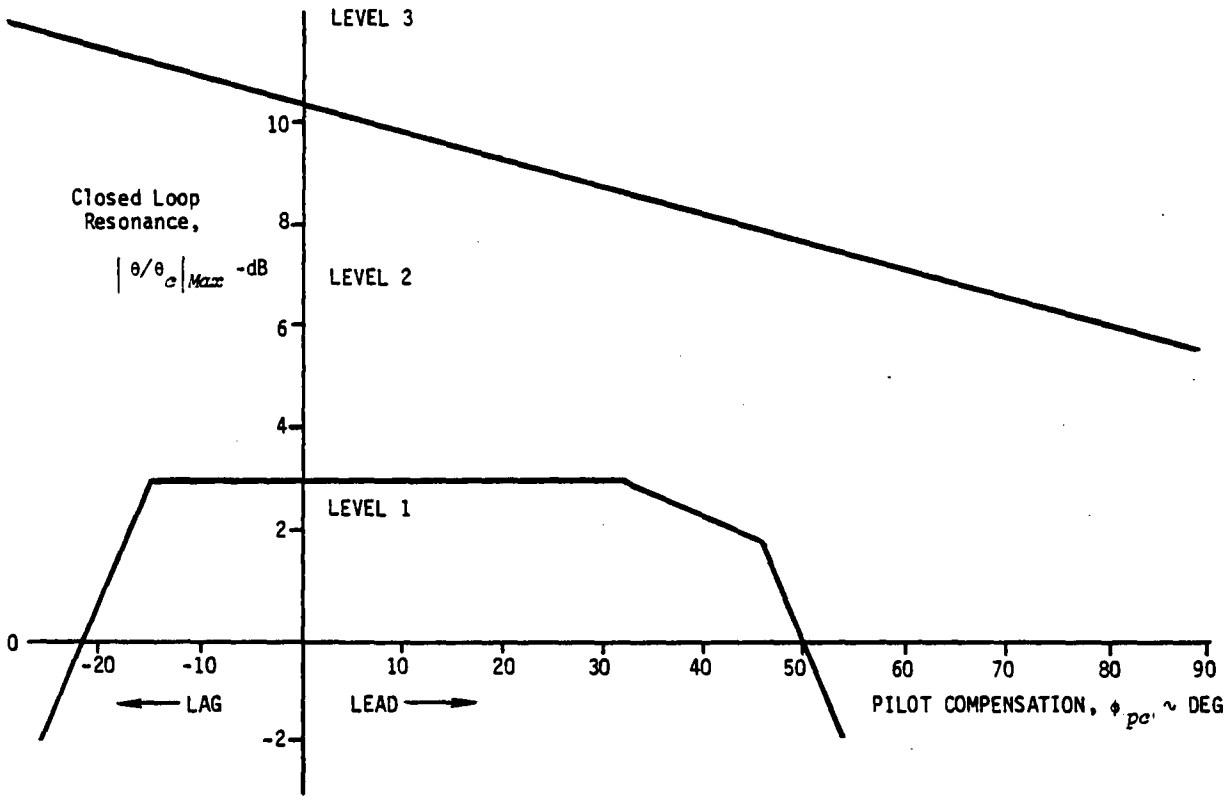

Figure 50. NEAL-SMITH PARAMETER PLANE

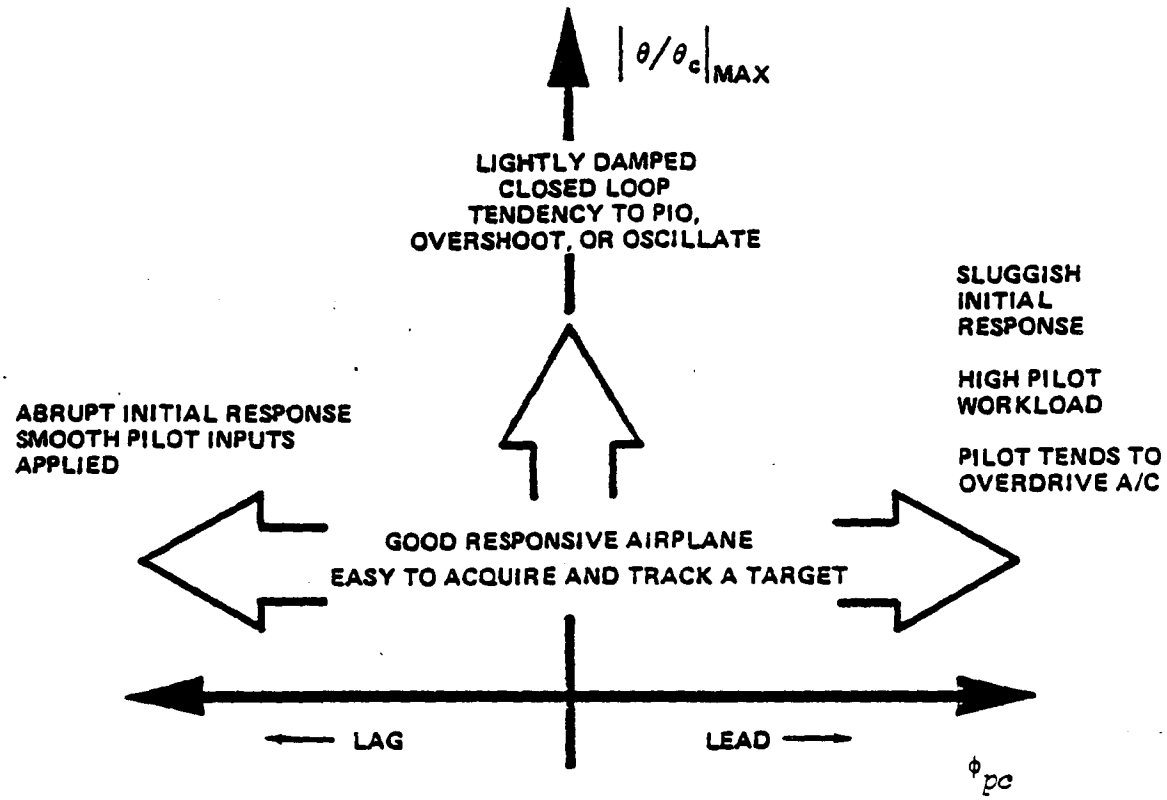

Figure 51. TYPICAL PILOT COMMENTS

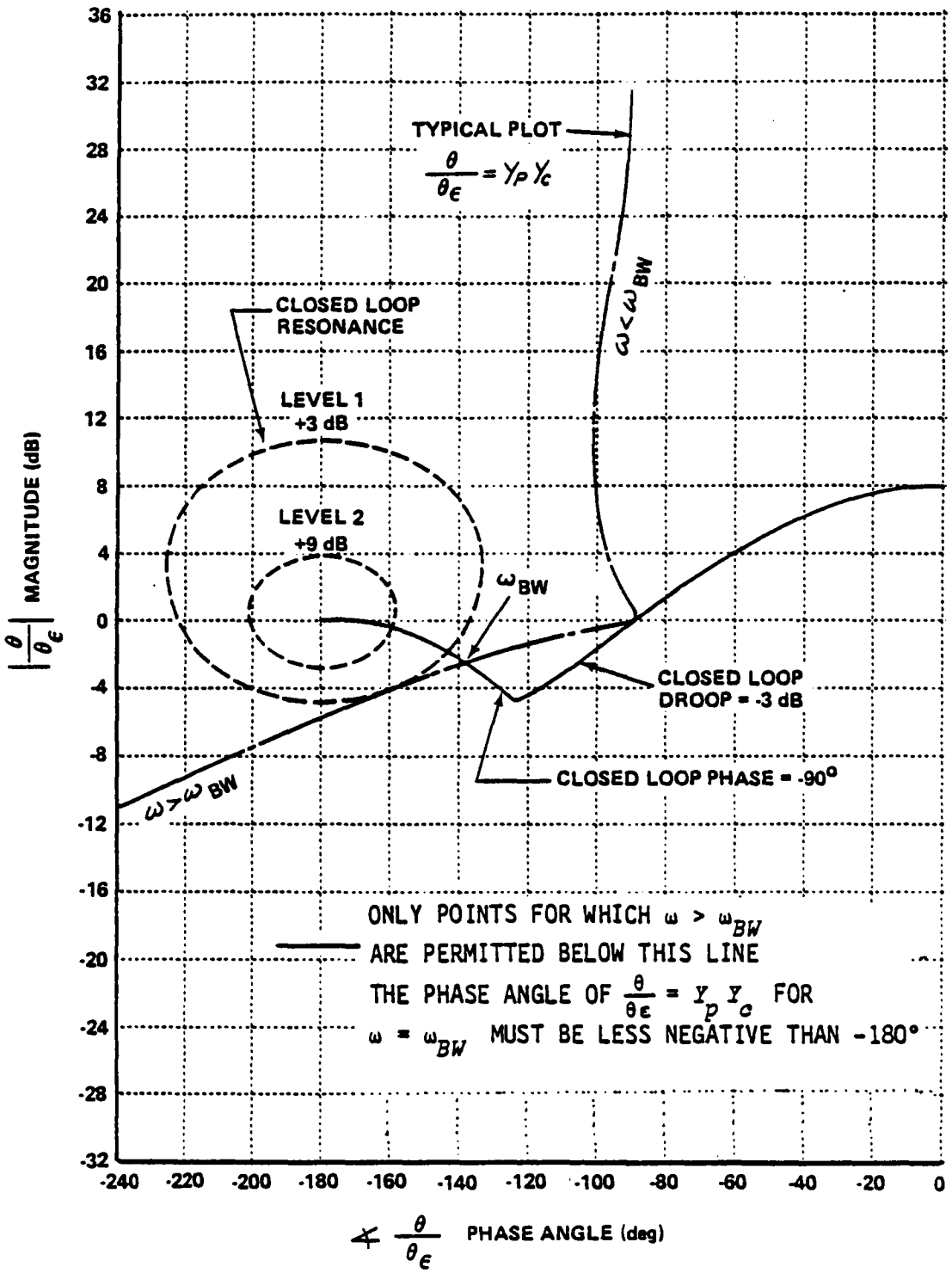

Figure 52. DESIGN CRITERIA FOR PITCH DYNAMICS WITH THE PILOT IN THE LOOP

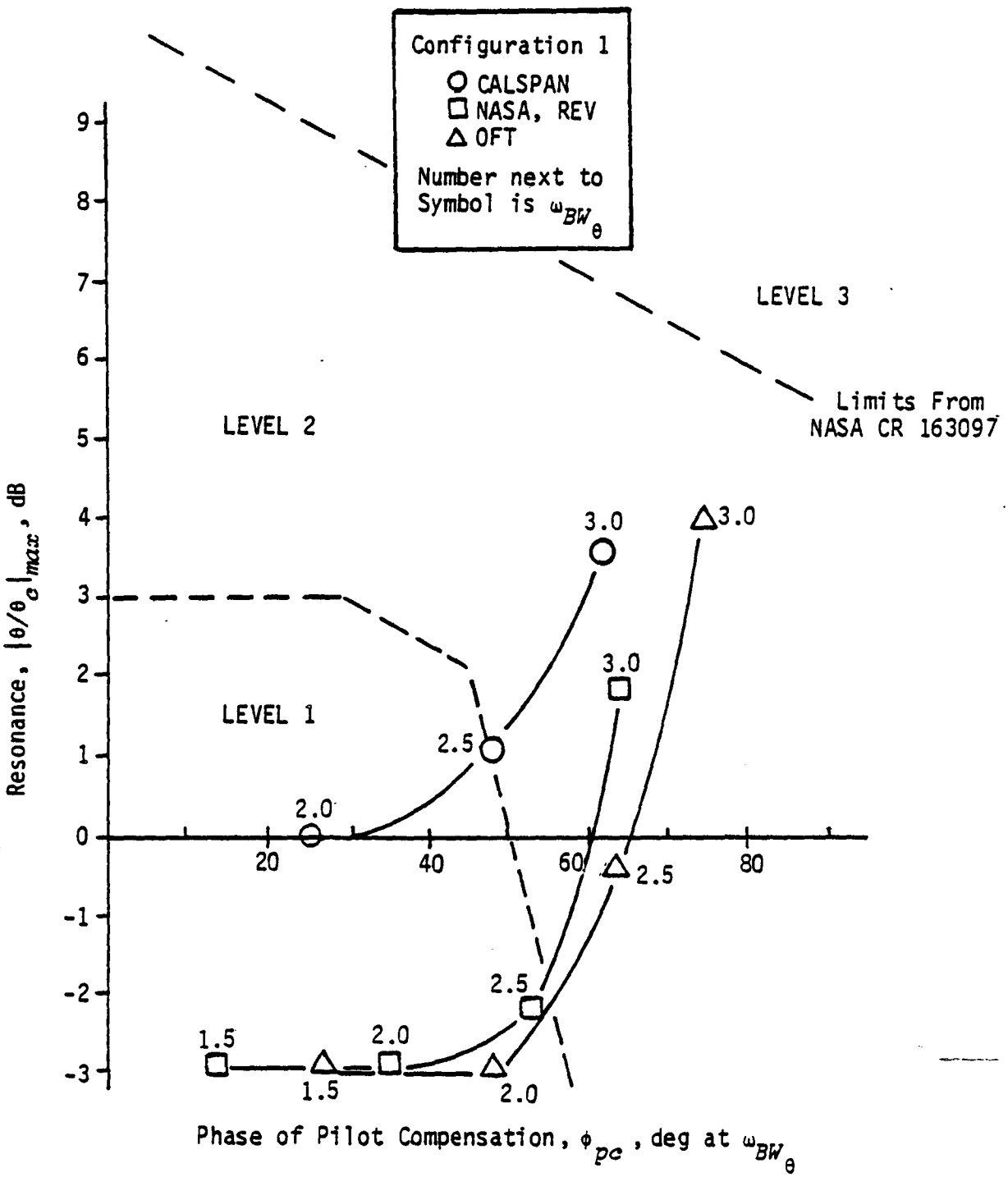

Figure 53. NEAL-SMITH ATTITUDE LOOP RESULTS CONFIGURATION 1

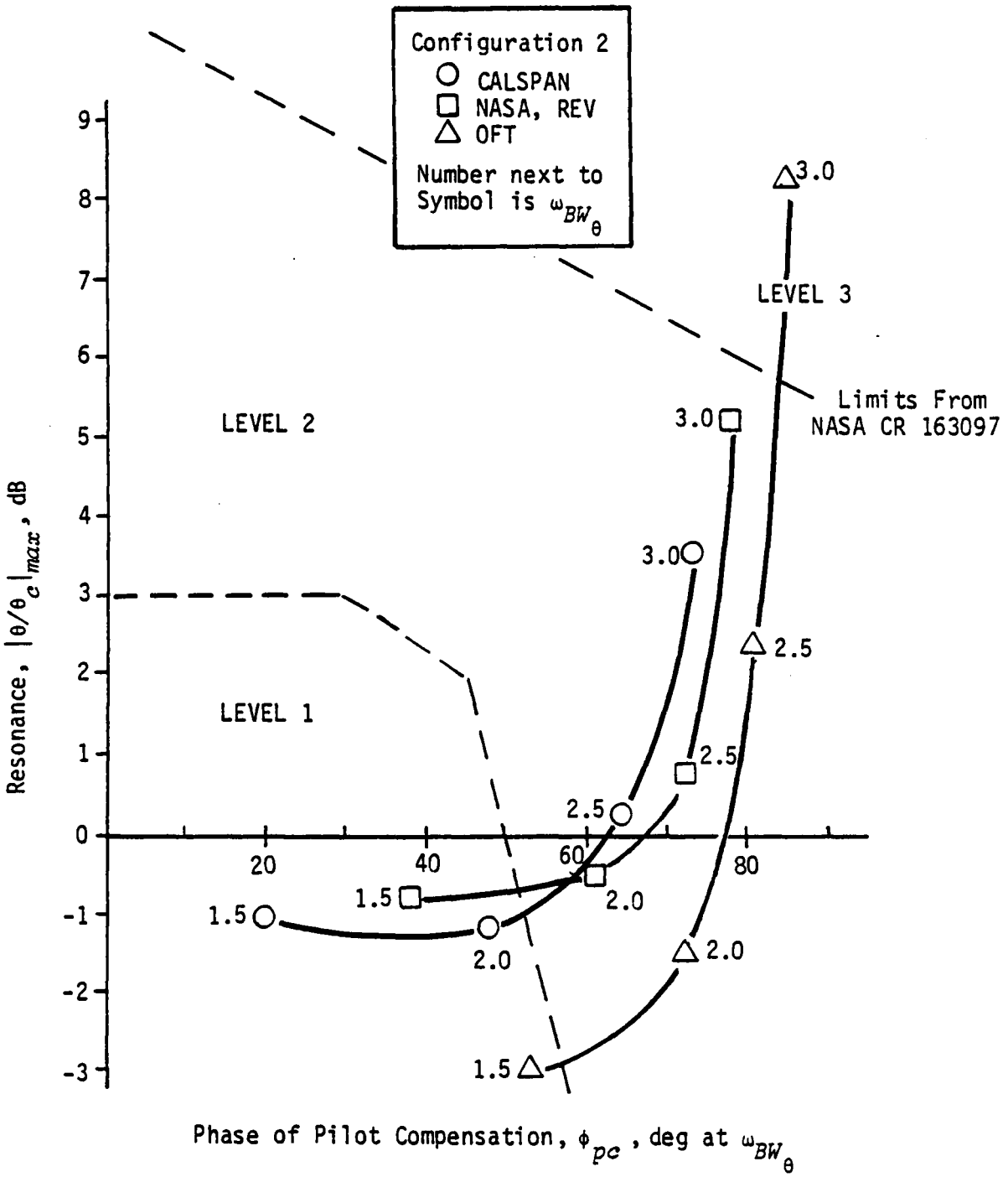

Figure 54. NEAL-SMITH ATTITUDE LOOP RESULTS CONFIGURATION 2

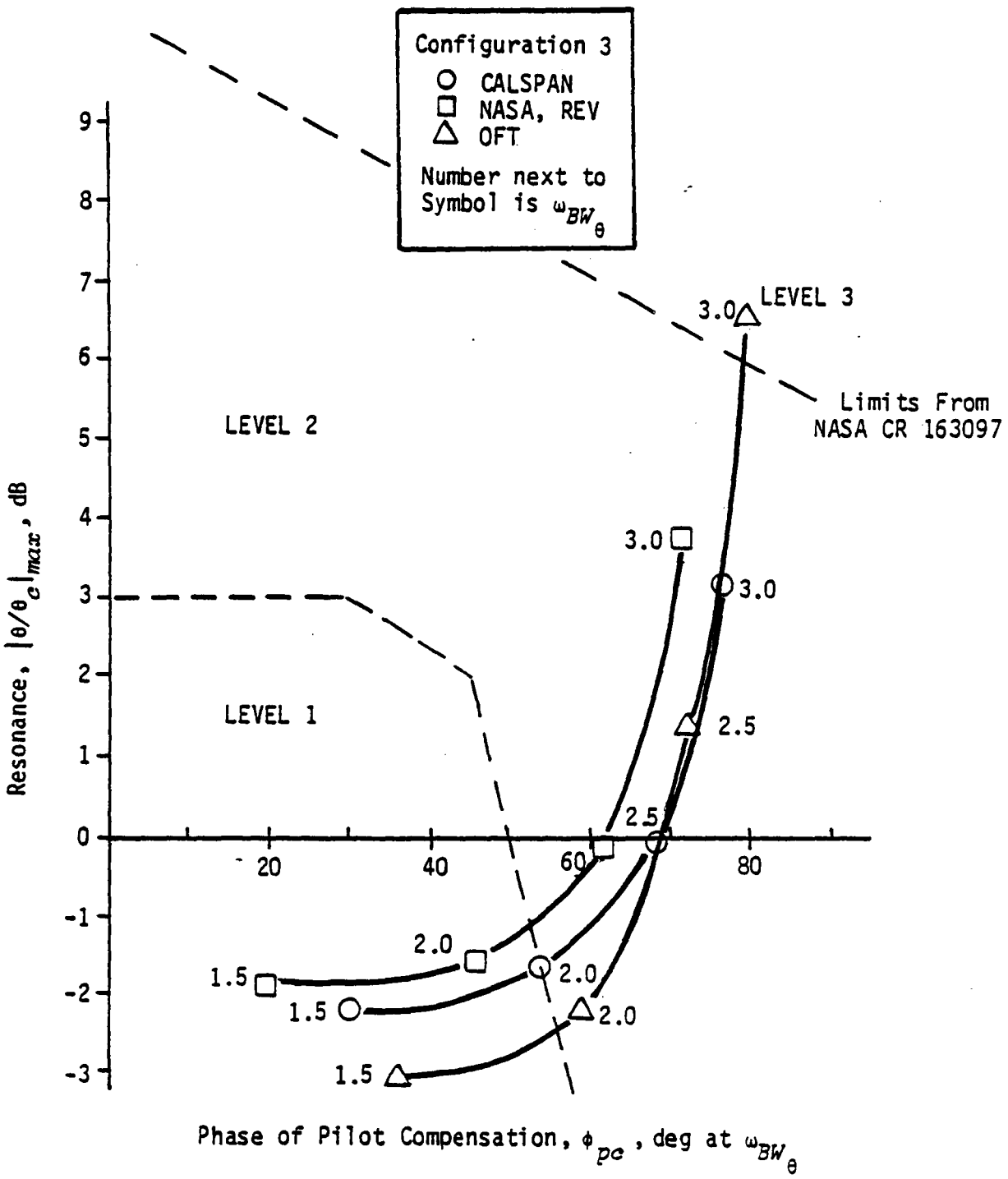

Figure 55. NEAL-SMITH ATTITUDE LOOP RESULTS CONFIGURATION 3

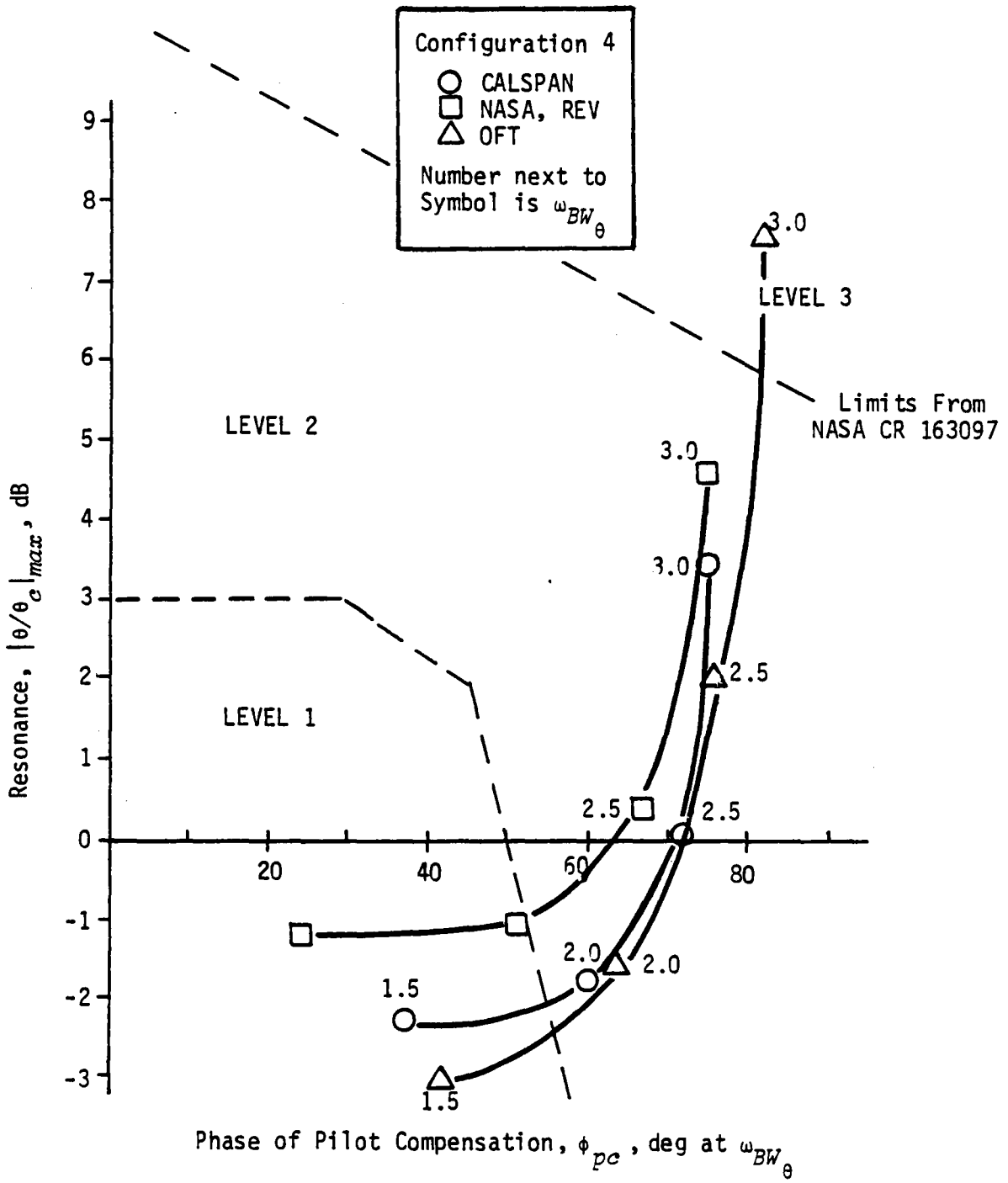

Figure 56. NEAL-SMITH ATTITUDE LOOP RESULTS CONFIGURATION 4

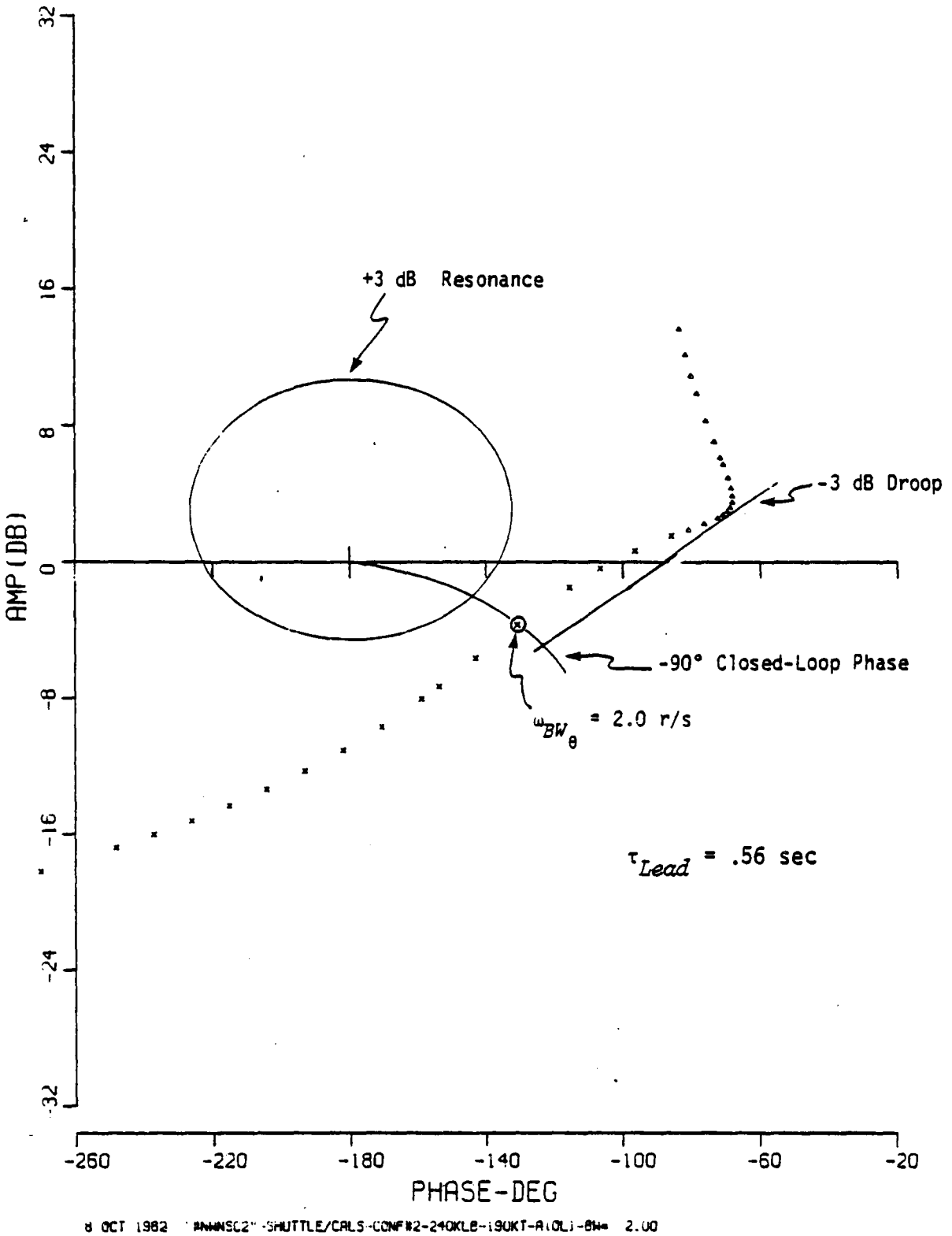

Figure 57. PILOT COMPENSATED ATTITUDE LOOP $\left(\omega_{BW_\theta} = 2 \text{ r/s}\right)$ CALSPAN CONFIGURATION 2

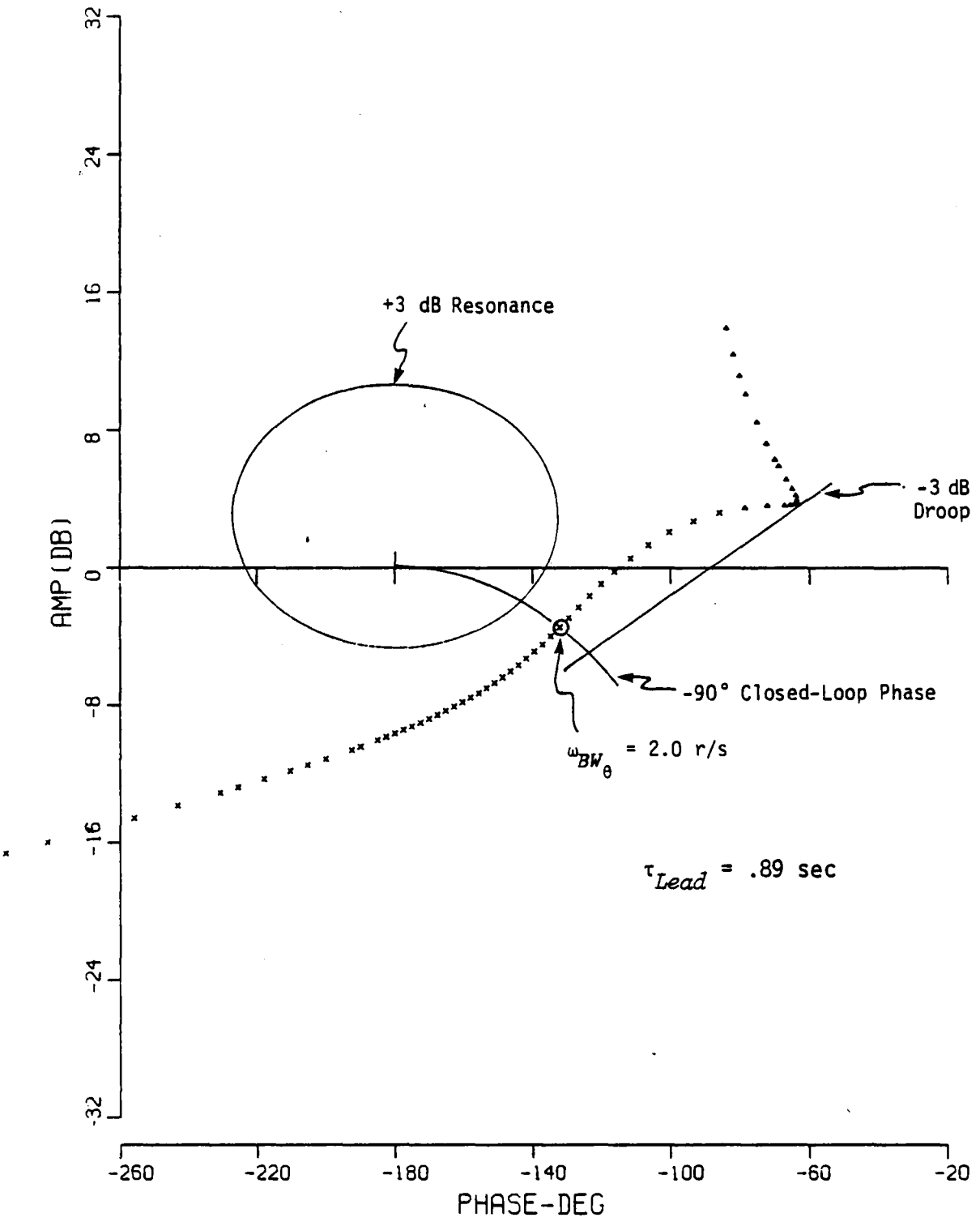

Figure 58. PILOT COMPENSATED ATTITUDE LOOP $\left(\omega_{BW_\theta} = 2 \text{ r/s}\right)$
NASA CONFIGURATION 2

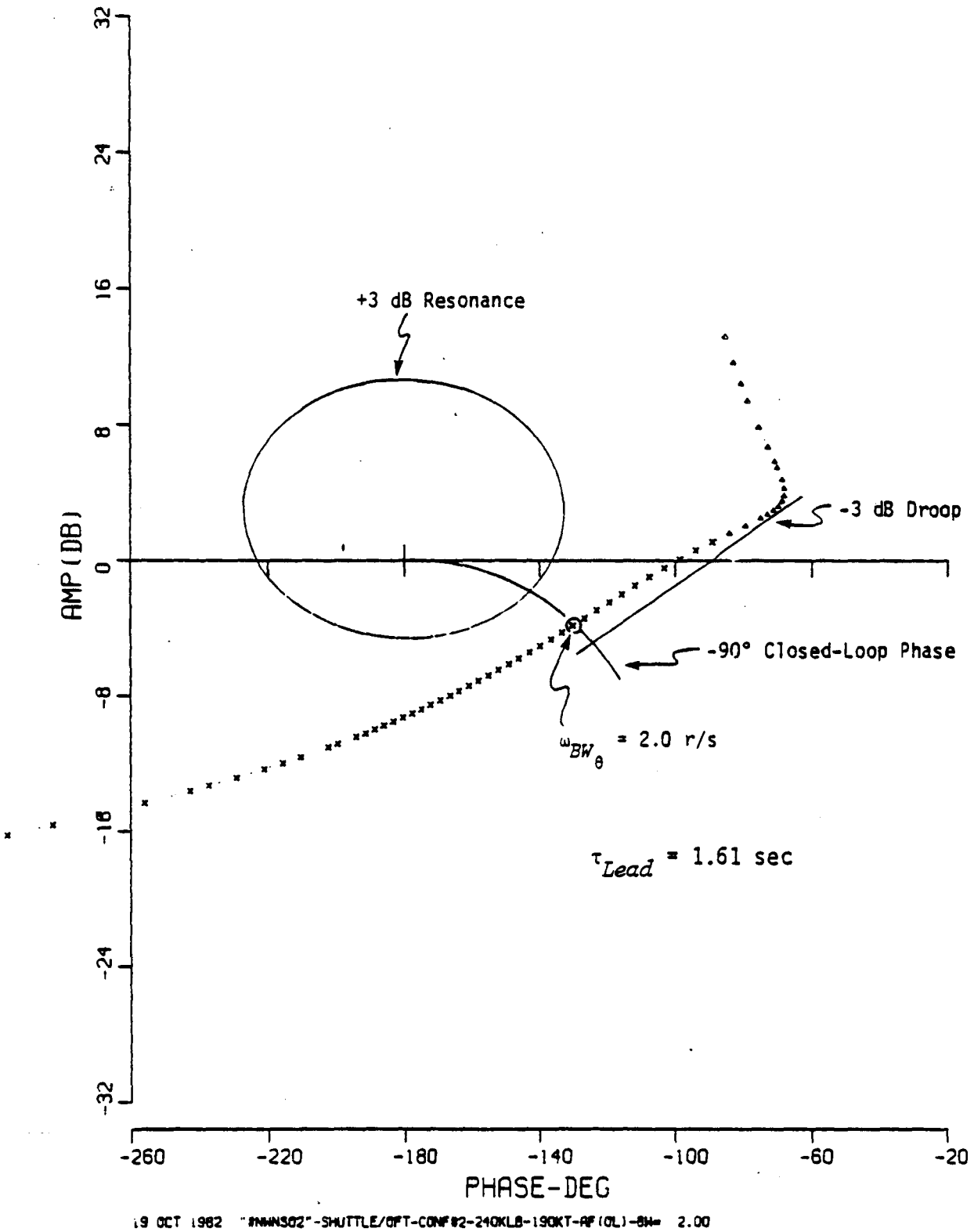

Figure 59 PILOT COMPENSATED ATTITUDE LOOP $\left(\omega_{BW_\theta} = 2 \text{ r/s}\right)$ OFT CONFIGURATION 2

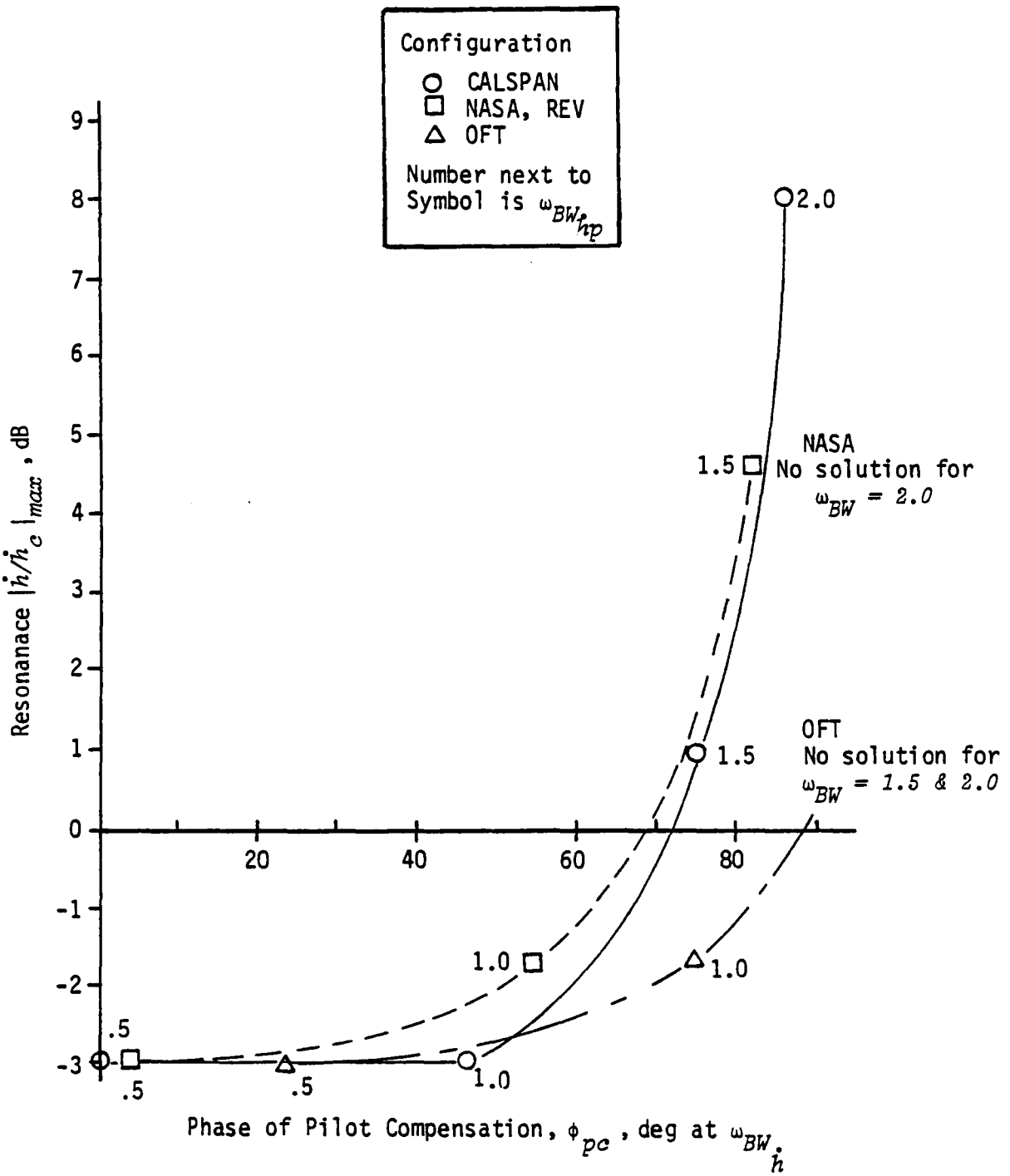

Figure 60. NEAL-SMITH ALTITUDE RATE LOOP RESULTS CONFIGURATION 2

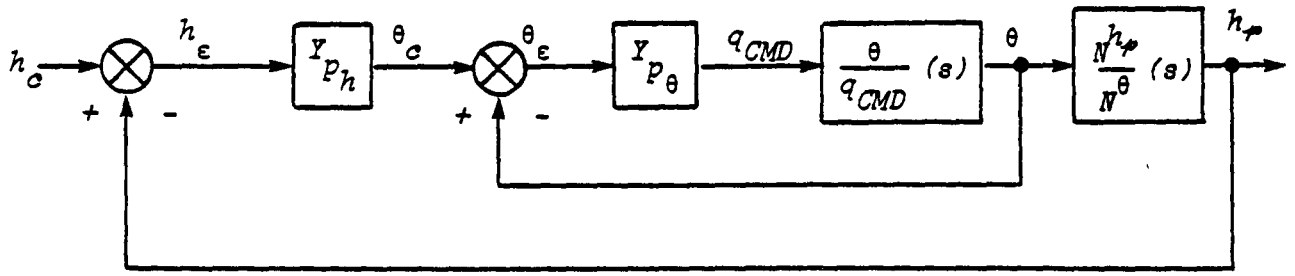

$$Y_{p_h} = K_{p_h}$$

$$Y_{p_\theta} = K_{p_\theta} e^{-.25s} (\tau_{Lead} s + 1)$$

N^{h_p}, N^θ = Numerators of pilot altitude and pitch attitude transfer functions

Figure 61. MULTI-LOOP CONTROL STRUCTURE

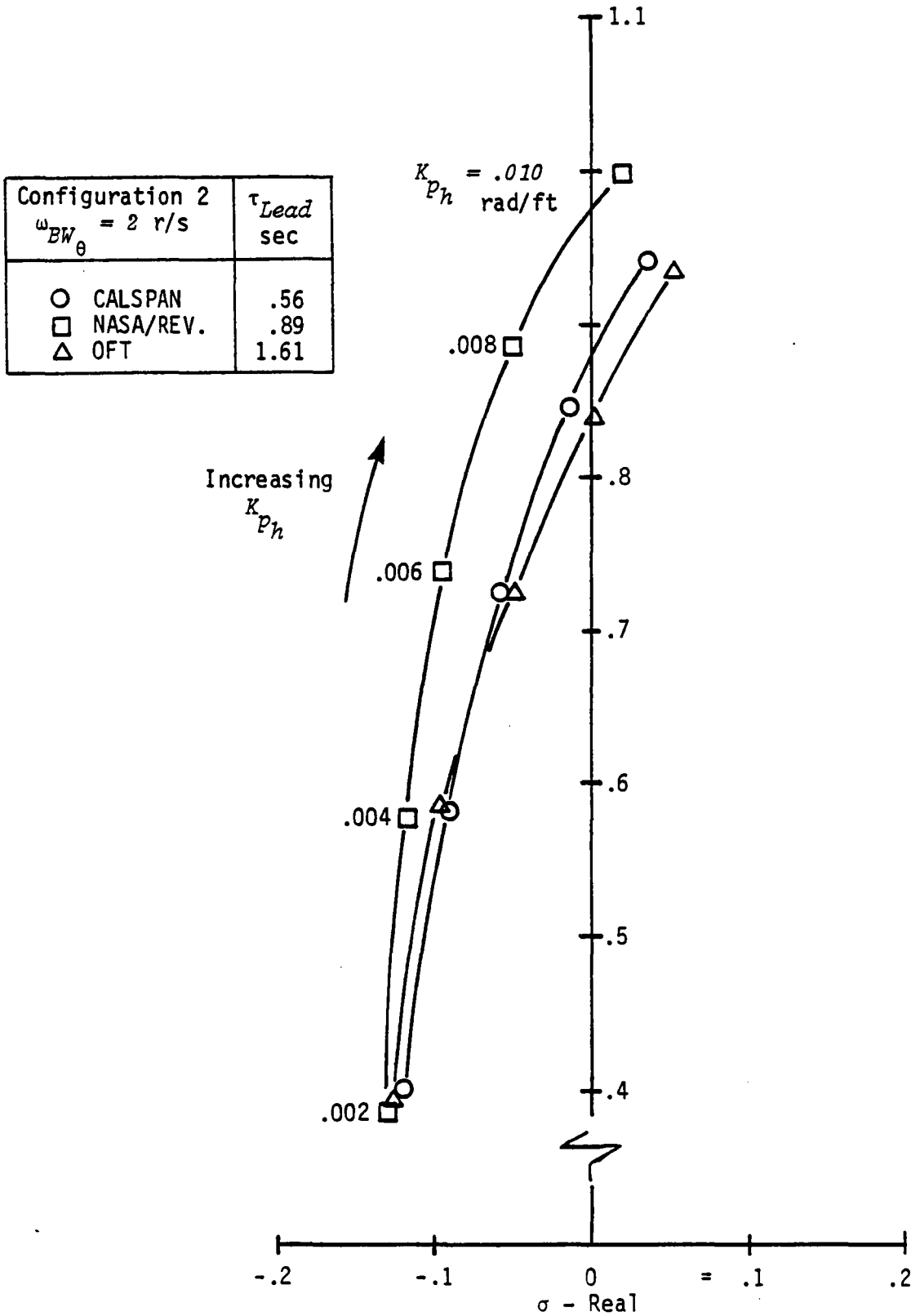

Figure 62. ALTITUDE MODE ROOT LOCUS WITH ω_{BW_θ} = 2.0 RAD/SEC

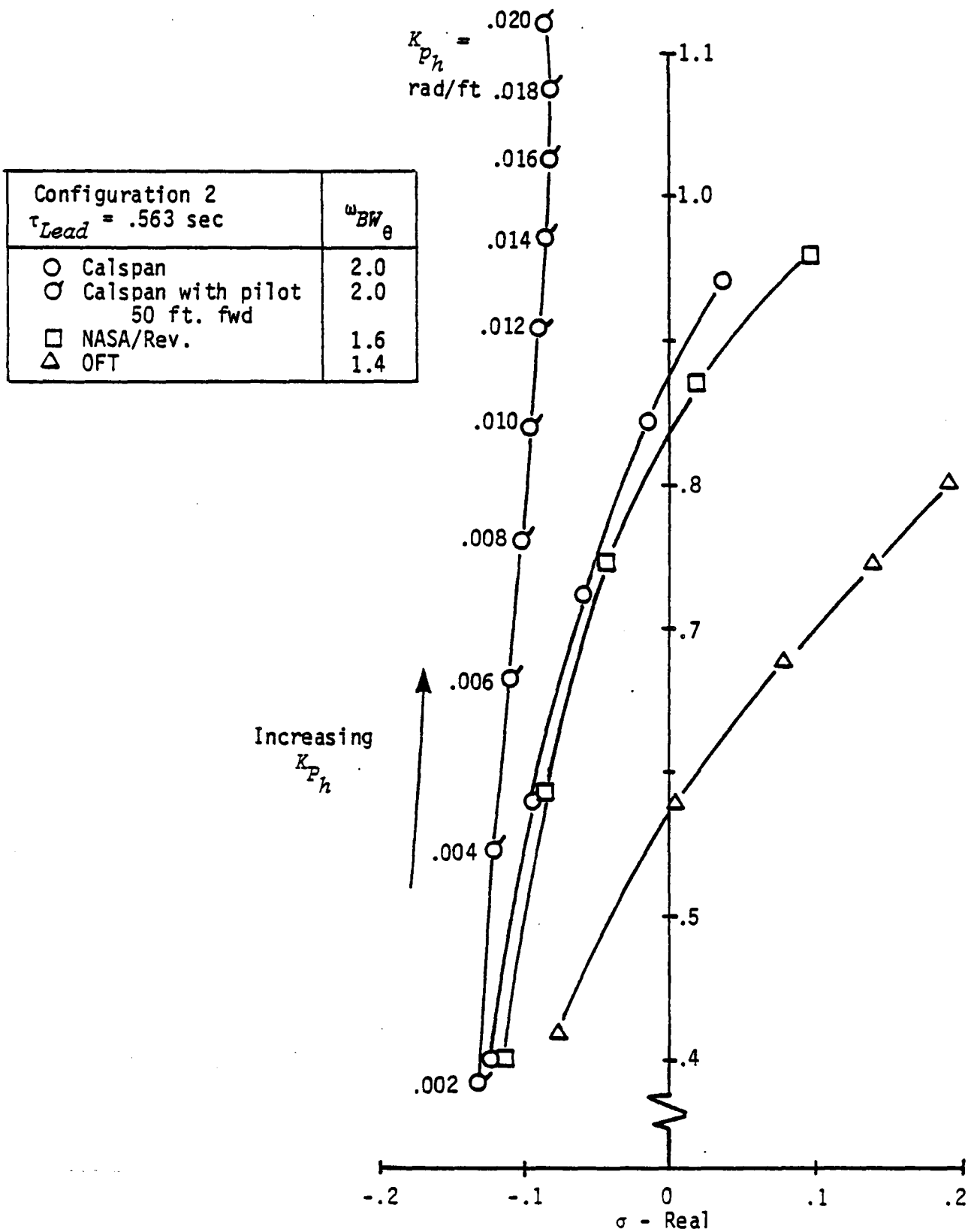

Figure 63. ALTITUDE MODE ROOT LOCUS WITH CONSTANT INNER-LOOP PILOT LEAD ($.563s + 1$)

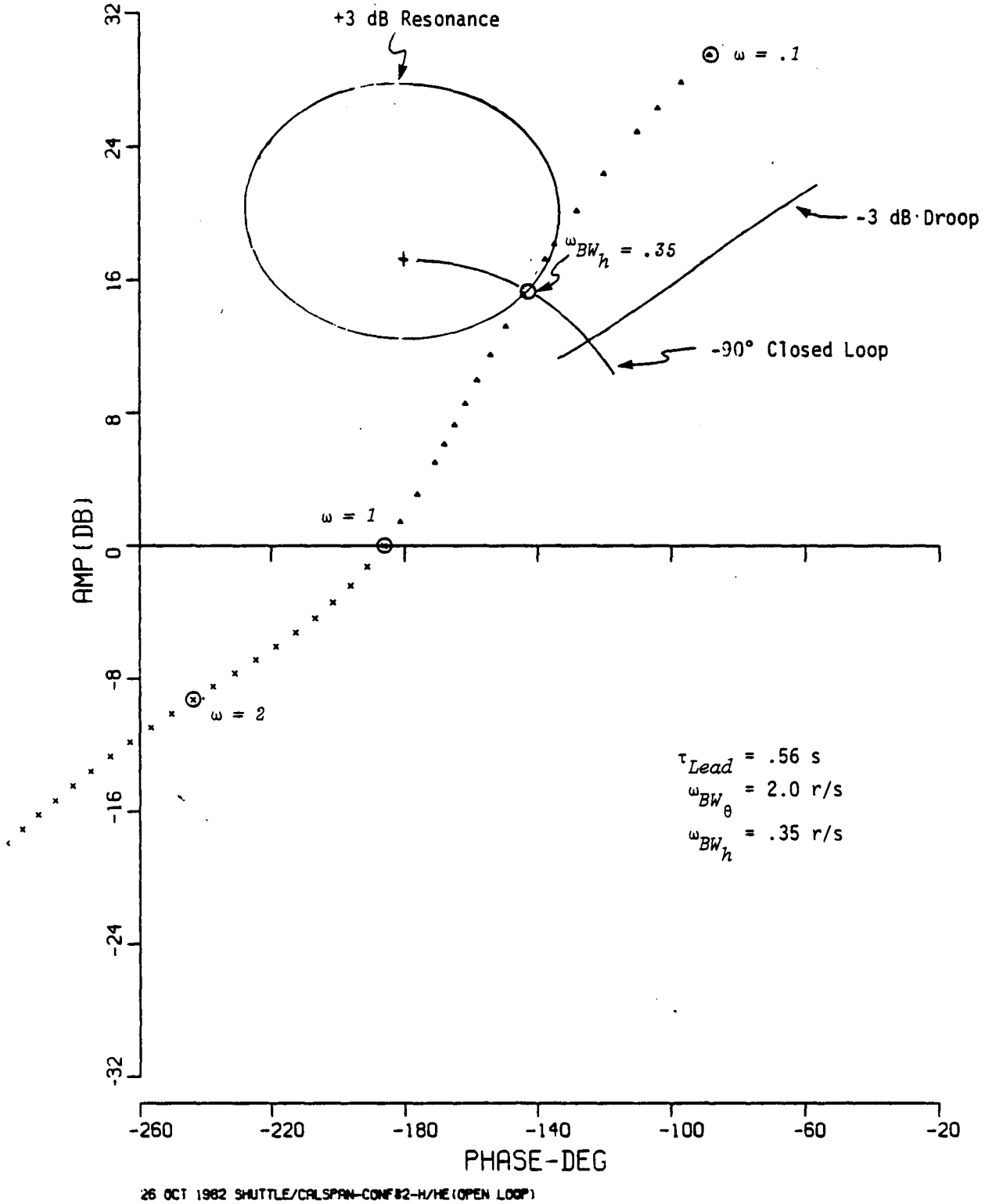

Figure 64. MULTI-LOOP (h_p and θ) NICHOLS PLOT, h/h_ε, CALSPAN CONFIGURATION 2 WITH INNER LOOP LEAD = .56 SEC

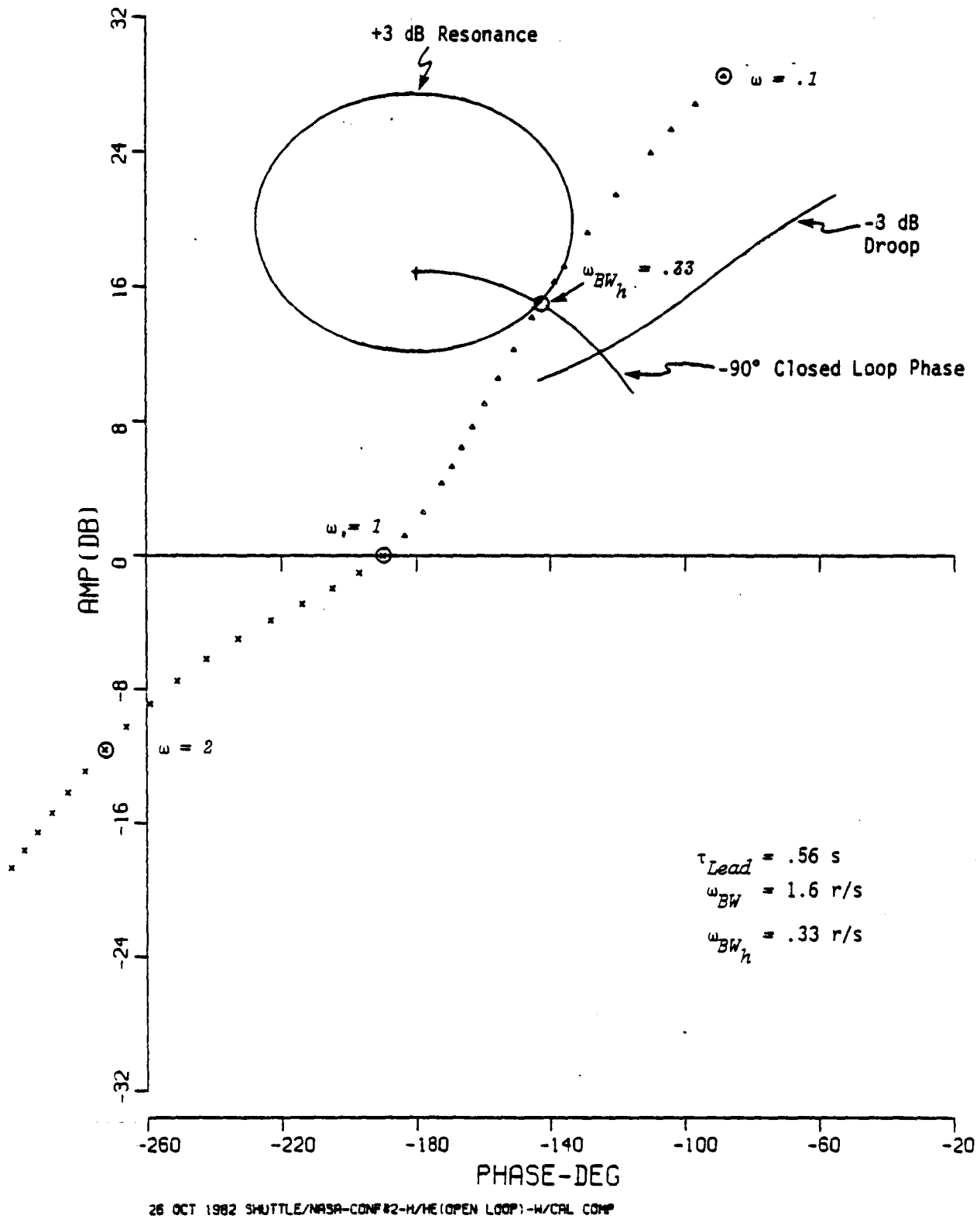

Figure 65. MULTI-LOOP (h_p and θ) NICHOLS PLOT, h/h_ε, NASA/REVISED CONFIGURATION 2 WITH INNER LOOP LEAD = .56 SEC

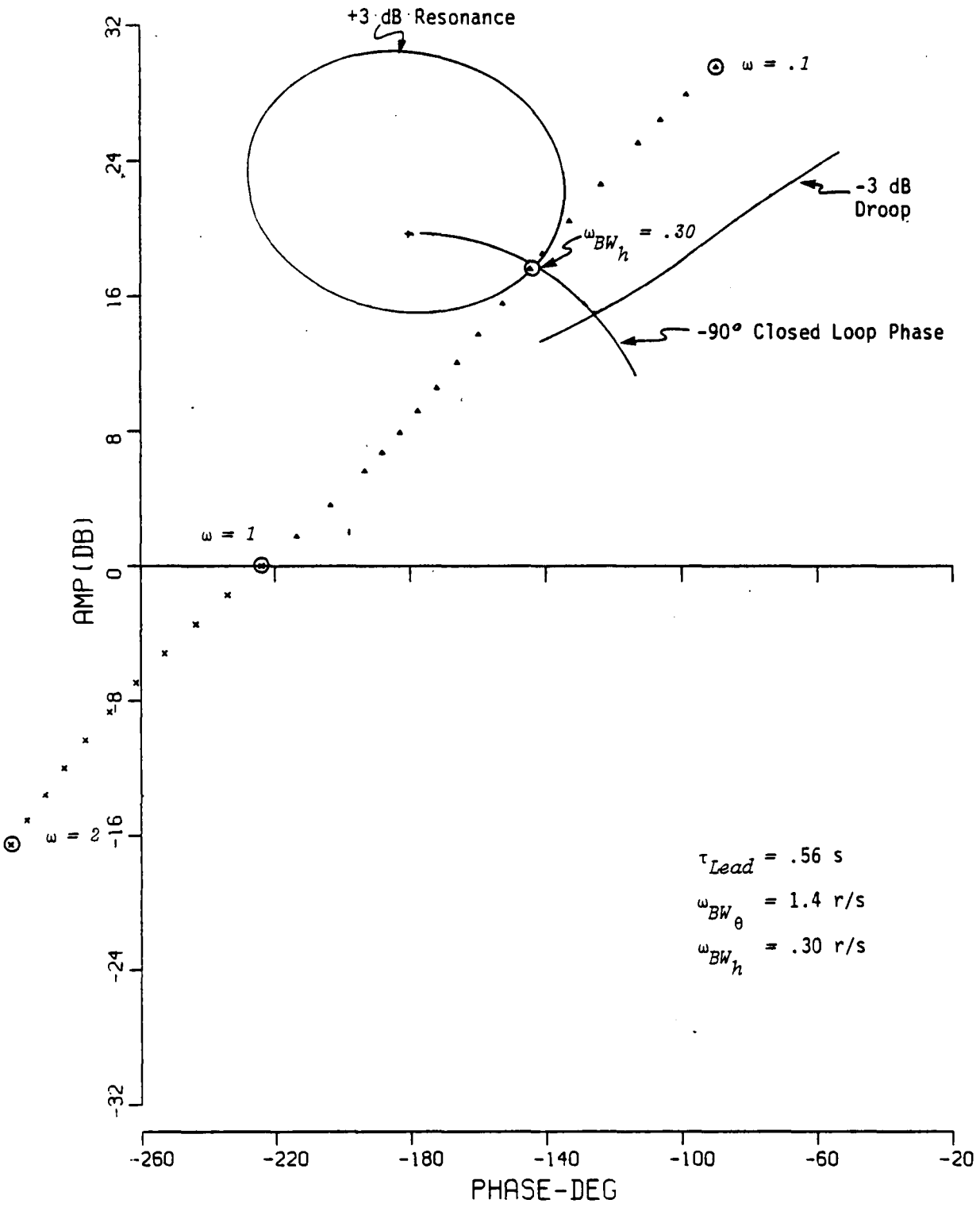

Figure 66. MULTI-LOOP (h_p and θ) NICHOLS PLOT, h/h_ε, OFT CONFIGURATION 2 WITH INNER LOOP LEAD = .56 SEC

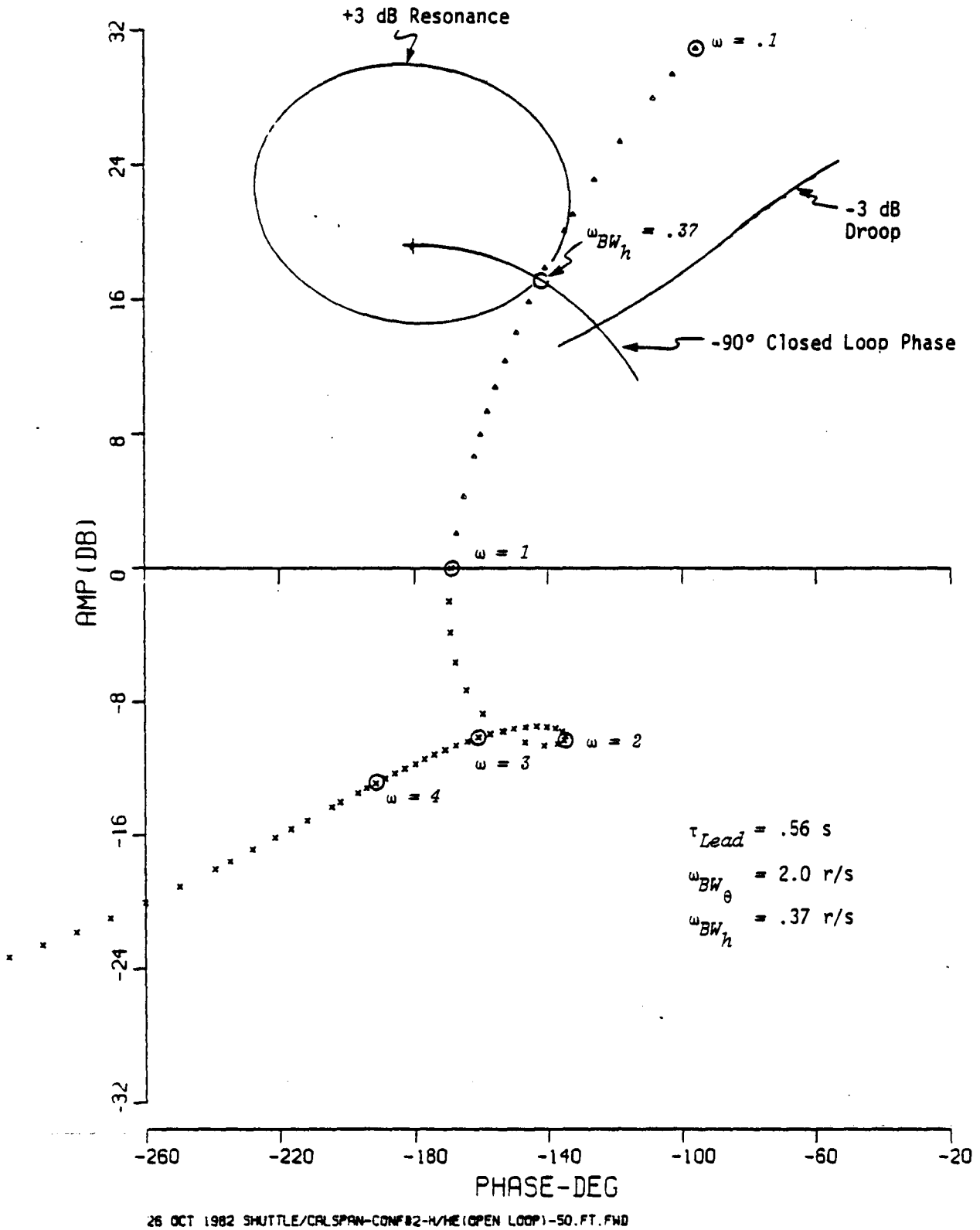

Figure 67. MULTI-LOOP ($\dot{h}_p$ and θ) NICHOLS PLOT, h/h_ε, CALSPAN CONFIGURATION 2 (PILOT SHIFTED 50 FT. FORWARD) WITH INNER LOOP LEAD = .56 SEC

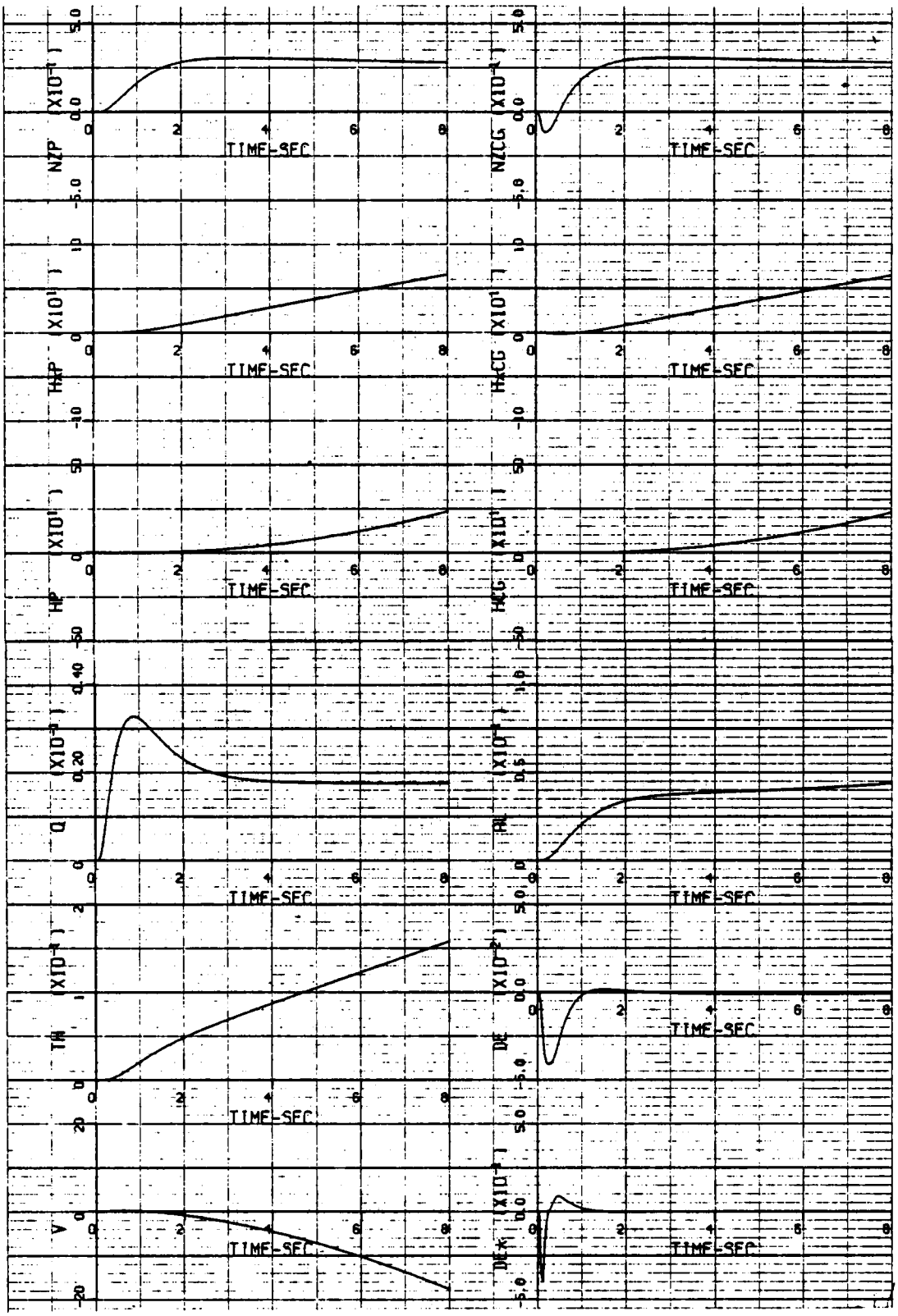

Figure 68. CALSPAN CONFIGURATION 1, WITH CONSTANT q FEEDBACK FILTER, q_{CMD} STEP RESPONSE

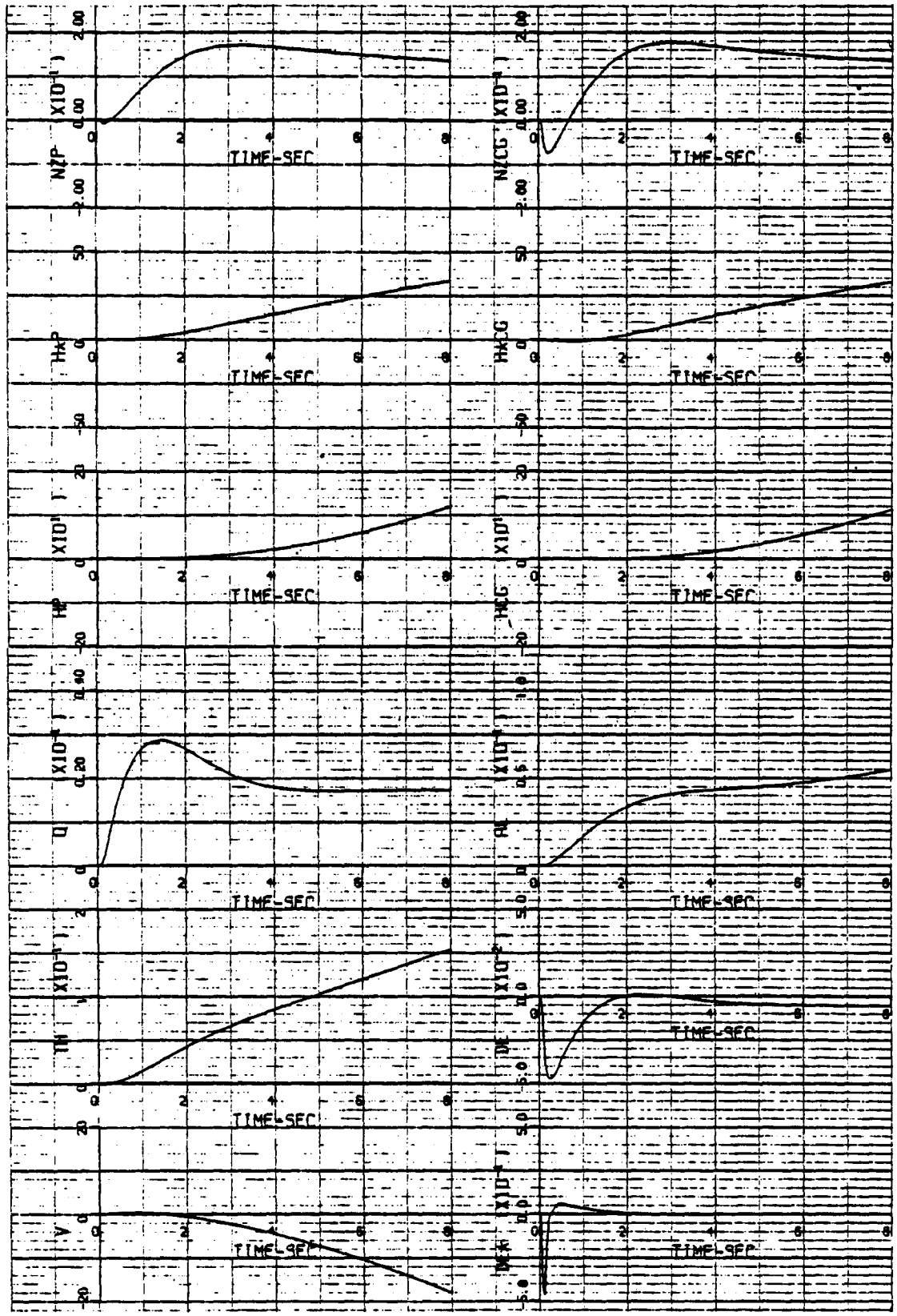

Figure 69. CALSPAN CONFIGURATION 3, WITH CONSTANT q FEEDBACK FILTER, q_{CMD} STEP RESPONSE

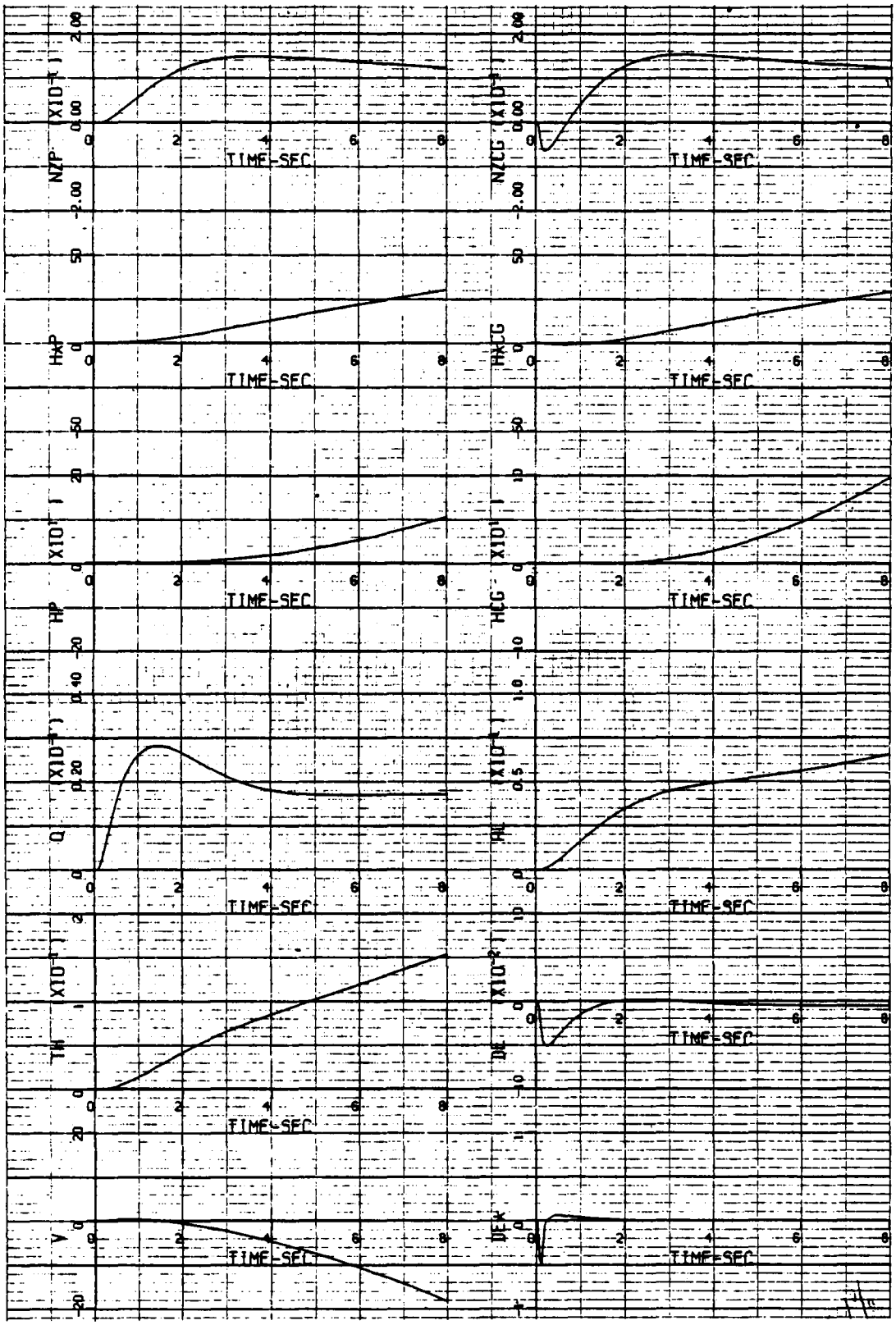

Figure 70. CALSPAN CONFIGURATION 4, WITH CONSTANT q FEEDBACK FILTER, q_{CMD} STEP RESPONSE

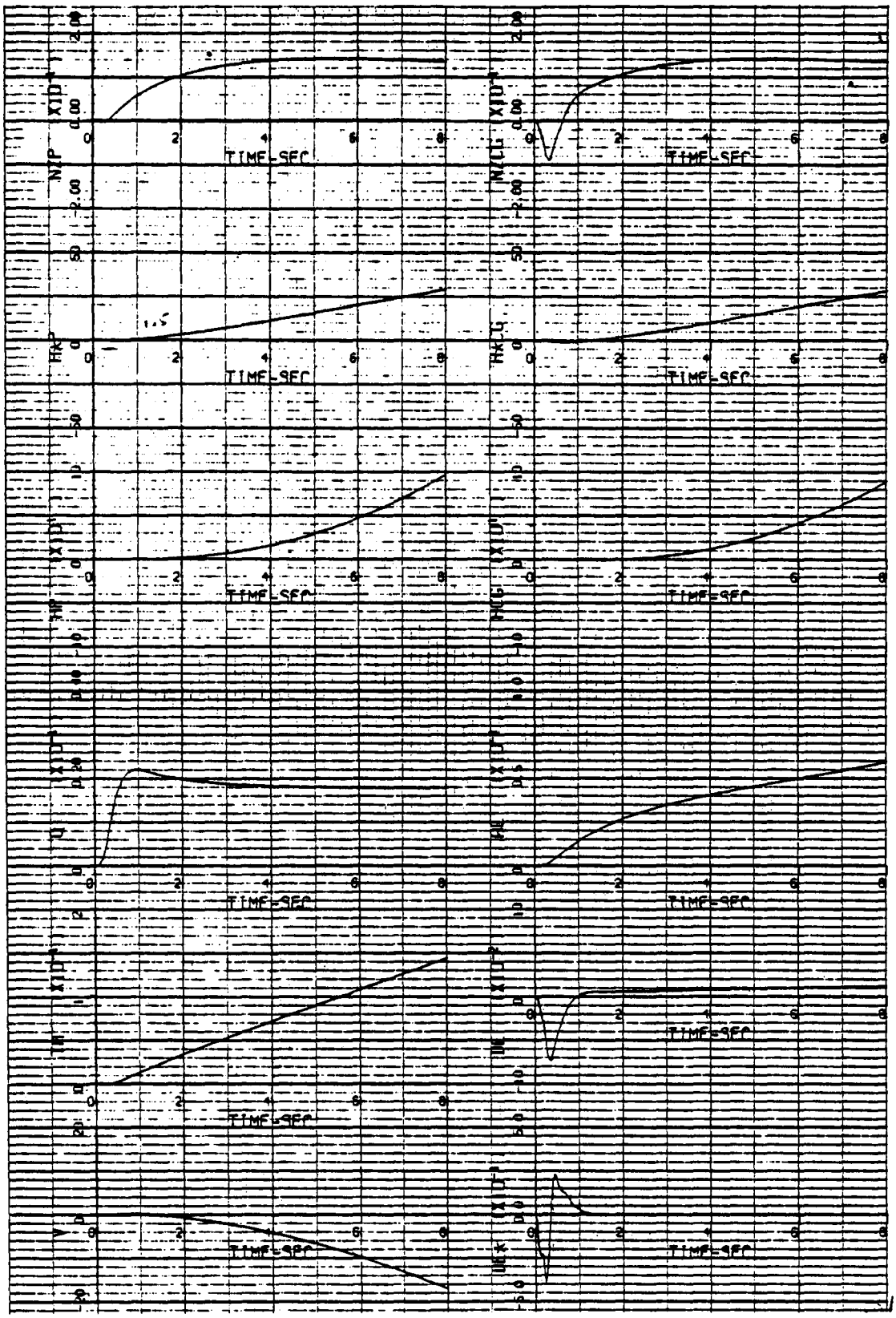

Figure 71. OFT CONFIGURATION 2 WITH 2 X GDQ GAIN, q_{CMD} STEP RESPONSE

APPENDIX 1

TRANSFER FUNCTIONS

The following is a tabulation of important transfer functions of the shuttle configurations under investigation. It is written in the shorthand notation where:

$K\,(a)[\zeta\ ,\ \omega]$ is equivalent to $K\,(s + a)[s^2 + 2\zeta\omega\, s + \omega^2]$

All angular units are radians, accelerations are g's.

Unaugmented Configurations

Configuration 1 - 290 KEAS, 240,000 lb, aft C.G., γ = -20 degrees

Denominator	[.803, .127](.793)(-.066)
$N^{\theta}_{\delta_e}$	-1.96 (.041)(.521)
$N^{\alpha}_{\delta_e}$	-.177 [.341, .083](11.41)
$N^{N_{z_{CG}}}_{\delta_e}$	-3.17 [.975, .025](2.57)(-2.21)

Configuration 2 - 190 KEAS, 240,000 lb, aft C.G., γ = -3 degrees

Denominator	[.319, .139](.700)(-.268)
$N^{\theta}_{\delta_e}$	-.787 (.040)(.406)
$N^{\alpha}_{\delta_e}$	-.130 [.179, .137](6.10)
$N^{N_{z_{CG}}}_{\delta_e}$	-1.44 (.025)(-.028)(1.57)(-1.45)

Configuration 3 - 190 KEAS, 191,000 lb, forward C.G., γ = -3 degrees

Denominator [.871, .364][.023, .089]

$N^{\theta}_{\delta_e}$ -.964 (.046)(.451)

$N^{\alpha}_{\delta_e}$ -.163 [.175, .137](5.99)

$N^{N_{z_{CG}}}_{\delta_e}$ -1.77 (.030)(-.023)(1.67)(-1.52)

Configuration 4- 190 KEAS, 240,000 lb, Forward C.G., γ = -3 degrees

Denominator [.816, .314][-.049, .099]

$N^{\theta}_{\delta_e}$ -.874 (.044)(.363)

$N^{\alpha}_{\delta_e}$ -.130 [.178, .137](6.76)

$N^{N_{z_{CG}}}_{\delta_e}$ -1.45 (.027)(-.033)(1.56)(-1.45)

Augmented Configurations

Configuration 1 - 290 KEAS, 240,000 lb, aft C.G., γ = -20 degrees

Calspan Control System

Denominator [.710, 1.74][.476, 19.7][.731, 35.3][.50, 157.]·
(0)(.040)(.521)(.792)(21.7)

$N^{\theta}_{q_{CMD}}$ 1.54×10^{5} [.4, 20.][0., 157.](.041)(.52)(.521)(.791)

$N^{\alpha}_{q_{CMD}}$ 1.39×10^{4} [.4, 20][0., 157.][.341, .083](.52)(.791)(11.4)

$N^{N_{z_p}}_{q_{CMD}}$ 3.51×10^{3} [.4, 20.][0, 157](0)(.028)(.52)(.79)(15.2)(-25.9)

NASA/Revised Control System

Denominator [.791, 1.27][.706, 6.83][.391, 23.5][.60, 39.2][.874, 41.1]·
(0)(.040)(.516)(.769)(100.)

$N^{\theta}_{q_{CMD}}$ 2.06×10^{8} [.4, 20](.041)(.5)(.521)(1.)(2.)(100.)

$N^{\alpha}_{q_{CMD}}$ 1.87×10^{7} [.4, 20][.341, .083](.5)(1.)(2.)(11.4)(100.)

$N^{N_{z_p}}_{q_{CMD}}$ 4.70×10^{6} [.4, 20](0)(.028)(.5)(1.)(2.)(15.2)(100.)(-25.9)

OFT Control System

Denominator [.972, .586][.466, 21.2][.822, 32.9][.657, 38.7]·
(0)(.040)(1.13)(2.98)(17.6)

$N^{\theta}_{q_{CMD}}$ 4.56×10^{7} [.04, 32.7](.041)(.521)(.587)(1.)

$N^{\alpha}_{q_{CMD}}$ 4.12×10^{6} [.04, 32.7][.341, .083](.587)(1.)(11.4)

$N^{N_{z_p}}_{q_{CMD}}$ 1.04×10^{6} [.04, 32.7](0)(.028)(.587)(1.)(15.2)(-25.9)

Configuration 2 - 190 KEAS, 240,000 lb, aft C.G., γ = -3 degrees

Calspan Control System

Denominator [.709, 1.28][.464, 19.7][.728, 35.4][.5, 157]·
(0)(.035)(.407)(.7)(22.7)

$N^{\theta}_{q_{CMD}}$ 1.10×10^{5} [.4, 20][0,157.](.040)(.406)(.41)(.7)

$N^{\alpha}_{q_{CMD}}$ 1.82×10^{4} [.4, 20][0,157.][.179, .137](.41)(.7)(6.1)

$N^{N_{z_p}}_{q_{CMD}}$ 1.42×10^{4} [.4, 20][0, 157.](0)(-.007)(.41)(.7)(3.9)(-8.13)

NASA/Revised Control System

Denominator [.497, 1.08][.416, 22.5][.622, 38.3][.855, 38.3]·
(0)(.034)(.434)(.714)(4.79)(11.1)(100.)

$N^{\theta}_{q_{CMD}}$ 1.27×10^{8} [.4, 20](.040)(.406)(.5)(1.)(2.)(100.)

$N^{\alpha}_{q_{CMD}}$ 2.09×10^{7} [.4, 20][.179, .137](.5)(1.)(2.)(6.1)(100)

$N^{N_{z_p}}_{q_{CMD}}$ 1.64×10^{7} [.4, 20](0)(-.007)(.5)(1.)(2.)(3.9)(100)(-8.13)

OFT Control System

Denominator [.95, .626][.816, 1.05][.424, 20.3][.757, 33.8][.672, 37.8]·
(0)(.030)(25.2)

$N^{\theta}_{q_{CMD}}$ 2.80×10^{7} [.04, 32.7](.04)(.406)(.587)(1.)

$N^{\alpha}_{q_{CMD}}$ 4.62×10^{6} [.04, 32.7][.179, .137](.587)(1.)(6.1)

$N^{N_{z_p}}_{q_{CMD}}$ 3.62×10^{6} [.04, 32.7](0)(-.007)(.587)(1.)(3.9)(-8.13)

Configuration 3 - 190 KEAS, 191,000 lb, Forward C.G., γ = -3 degrees

Calspan Control System

Denominator [.715, 1.22][.448, 19.8][.723, 35.5][.5, 157]·
(0)(.048)(.416)(.45)(24.0)

$N^{\theta}_{q_{CMD}}$ 8.98×10^{4} [.4, 20][0, 157.](.046)(.45)(.45)(.451)

$N^{\alpha}_{q_{CMD}}$ 1.52×10^{4} [.4, 20][0, 157.][.175, .137](.45)(.45)(5.99)

$N^{N_{z_p}}_{q_{CMD}}$ 2.32×10^{4} [.4, 20][0, 157.](0)(.004)(.45)(.45)(3.36)(-5.34)

NASA/Revised Control System

Denominator [.607, 1.32][.949, 6.9][.407, 22.9][.613, 38.7][.864, 39.4]·
(0)(.047)(.445)(.619)(100)

$N^{\theta}_{q_{CMD}}$ 1.55×10^{8} [.4, 20](.046)(.451)(.5)(1.)(2.)(100)

$N^{\alpha}_{q_{CMD}}$ 2.63×10^{7} [.4, 20][.175, .137](.5)(1.)(2.)(5.99)(100)

$N^{N_{z_p}}_{q_{CMD}}$ 4.01×10^{7} [.4, 20](0)(.004)(.5)(1.)(2.)(3.36)(100)(-5.34)

OFT Control System

Denominator [.826, 1.46][.44, 20.5][.78, 33.2][.666, 38.2]·
(0)(.048)(.408)(.71)(23.1)

$N^{\theta}_{q_{CMD}}$ 3.43×10^{7} [.04, 32.7](.046)(.451)(.587)(1.)

$N^{\alpha}_{q_{CMD}}$ 5.80×10^{6} [.04, 32.7][.175, .137](.587)(1.)(5.99)

$N^{N_{z_p}}_{q_{CMD}}$ 8.84×10^{6} [.04, 32.7](0)(.004)(.587)(1.)(3.36)(-5.34)

Configuration 4 - 190 KEAS, 240,000 lb, Forward C.G., γ = -3 degrees

Calspan Control System

Denominator [.704, 1.07][.442, 19.8][.721, 35.6][.5, 157]·
(0)(.047)(.330)(.36)(24.4)

$N^{\theta}_{q_{CMD}}$ 8.77×10^{4} [.4, 20][0, 157](.044)(.36)(.361)(.363)

$N^{\alpha}_{q_{CMD}}$ 1.30×10^{4} [.4, 20][0, 157][.178, .137](.36)(.361)(6.76)

$N^{N_{z_p}}_{q_{CMD}}$ 3.72×10^{3} [.4, 20][0, 157.](0)(-.008)(.36)(.361)(5.23)(-16.7)

NASA/Revised Control System

Denominator [.552, 1.27][.411, 22.7][.617, 38.5][.86, 38.8]·
(0)(.045)(.354)(.619)(5.73)(8.66)(100.)

$N^{\theta}_{q_{CMD}}$ 1.41×10^{8} [.4, 20](.044)(.363)(.5)(1.)(2.)(100)

$N^{\alpha}_{q_{CMD}}$ 2.09×10^{7} [.4, 20][.178, .137](.5)(1.)(2.)(6.76)(100.)

$N^{N_{z_p}}_{q_{CMD}}$ 5.98×10^{6} [.4, 20](0)(-.008)((.5)(1.)(2.)(5.23)(100)(-16.7)

OFT Control System

Denominator [.768, 1.34][.432, 20.4][.769, 33.5][.669, 38.0]·
(0)(.047)(.333)(.717)(24.2)

$N^{\theta}_{q_{CMD}}$ 3.11×10^{7} [.04, 32.7](.044)(.363)(.587)(1.)

$N^{\alpha}_{q_{CMD}}$ 4.62×10^{6} [.04, 32.7][.178, .137](.587)(1.)(6.76)

$N^{N_{z_p}}_{q_{CMD}}$ 1.32×10^{6} [.04, 32.7](0)(-.008)(.587)(1.)(5.23)(-16.7)

Appendix 2
ALTERNATE PITCH RATE CONTROL SYSTEM

In Section 2 of the report, a pitch rate control system concept was defined which used pitch rate feedback through a first order lag-lead filter and proportional plus integral gains in the forward path.

An alternate design concept has recently been formulated which uses a lead-lag prefilter and eliminates the filter in the feedback. The attached block diagram (Figure A2-1), root locus sketches (Figure A2-2) and design guidelines outlined below adequately define the alternate concept.

This Appendix serves to document the Calspan development of this concept.

Control System Parameters

K_c ∿ Command gain control

$Z_c = \lambda_2' \simeq 1/T_{\theta_2}$

K_q = Loop gain
Z_I = Integrator gain

} Combination used to control short period ζ_{SP}, $\omega_{n_{SP}}$

Design Guidelines for an Alternate Pitch Rate Control System Design

The following design rules and observations are applicable to the prefilter design:

1) The system order can be kept low because exact cancellation of the prefilter pole with the proportional plus integral zero can be guaranteed.

2) Also, if λ_2' is accurately known, then, exact cancellation by the prefilter zero can be achieved which further lowers the order of the system. If λ_2' is not known exactly, then scheduling $Z_c \simeq 1/T_{\theta_2}$ will probably be adequate.

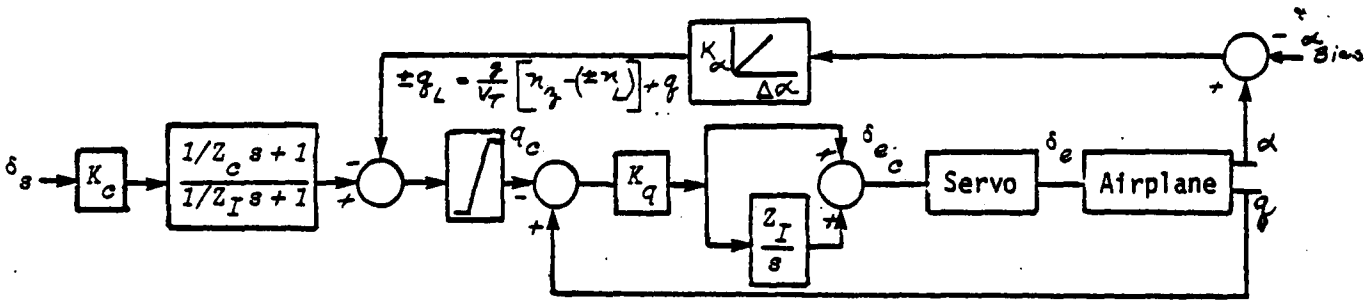

Figure A2-1. ALTERNATE PITCH RATE CONTROL SYSTEM - BLOCK DIAGRAM

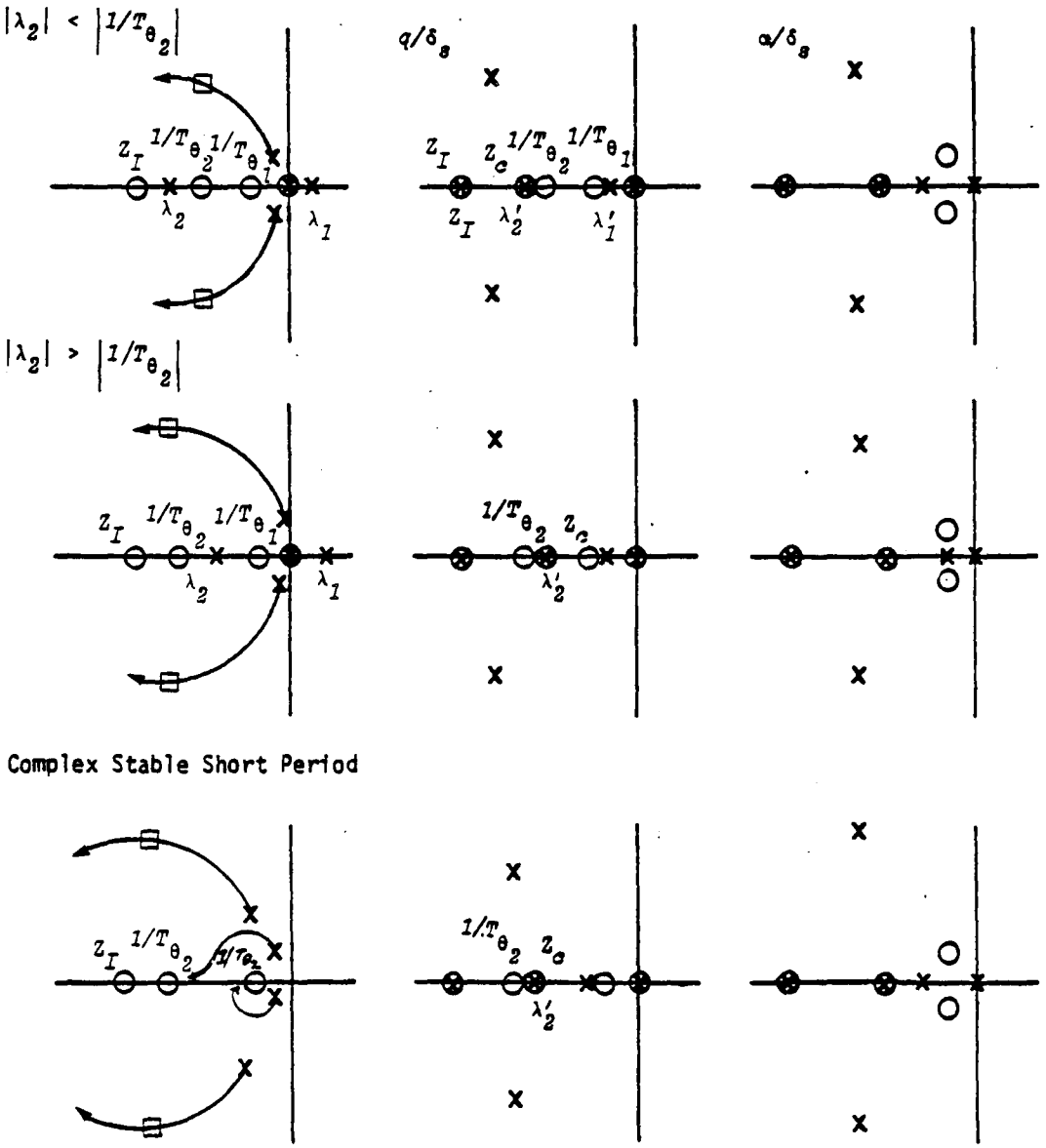

Figure A2-2. ALTERNATE PITCH RATE CONTROL SYSTEM - ROOT LOCUS

3) The augmented short period roots are controlled by the proportional and integral gains, K_q and Z_I. The transfer function for the feedback path to the elevator is always $\delta e/_q = K_q\ (s+Z_I)/s$.

4) The design is conceptually simpler and easier to understand than the previous design which had a lag-lead in the feedback.

Stick to Elevator Transfer Function

The transfer function for elevator in response to stick inputs is derived below. This transfer function is identical to the δ_{e_c}/δ_s transfer function for the control system with the filter in the feedback.

Transfer Function of Elevator Response to Stick Deflection:

$$\delta_{e_c} = \left[q - q_c\right] K_q \frac{(s + Z_I)}{s}$$

$$1 = \left[\frac{q}{\delta_{e_c}} - \frac{K_c(1/Z_c\, s + 1)}{(1/Z_I\, s + 1)} \frac{\delta_s}{\delta_{e_c}}\right] K_q \frac{(s + Z_I)}{s}$$

$$\frac{\delta_{e_c}}{\delta_s} = \frac{-K_c \dfrac{(1/Z_c\, s + 1)}{(1/Z_I\, s + 1)}}{\dfrac{s}{K_q(s + Z_I)} - \dfrac{q}{\delta_{e_c}}}$$

Ignore Servo Dynamics:

$$\frac{\delta_{e_c}}{\delta_s} = \frac{-K_q K_c Z_I}{Z_c} \frac{\cancel{(s + Z_c)}(s - \lambda_1)(s + \lambda_2)\left[\zeta_p, \omega_{n_p}\right]}{s(s + \lambda_1')\cancel{(s + \lambda_2')}\left[\zeta'_{SP}, \omega'_{n_{SP}}\right]}$$

Comparison of Design Concept

The two pitch rate control system designs i.e., filter-in-feedback and prefilter, are compared below through block diagram manipulations and choice of design rules.

Prefilter

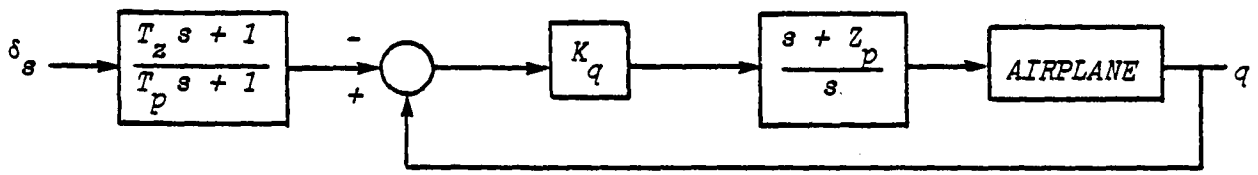

Move prefilter past summing junction

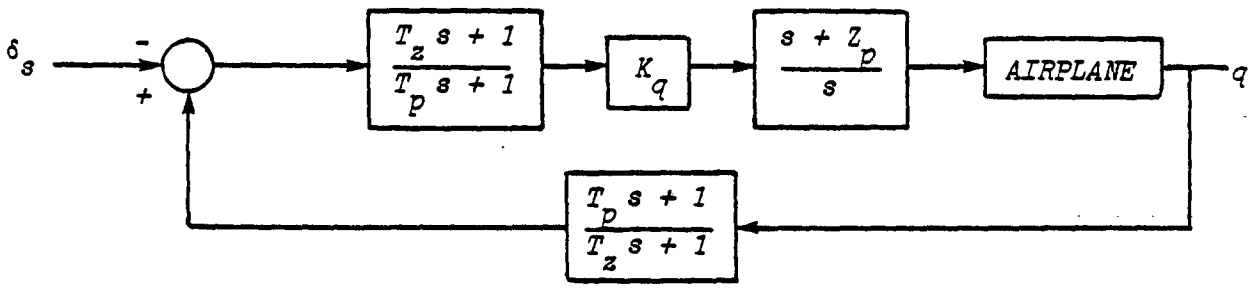

Design Rules: $\frac{1}{T_p} = Z_p \quad \frac{1}{T_z} = \lambda_2'$

Simplify

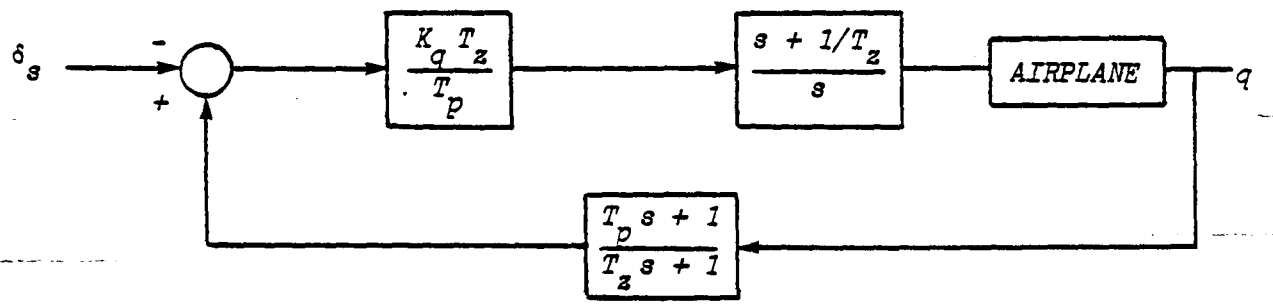

This is equivalent form of the pitch rate system defined in Section 2 and analyzed for NASA/DFRF. To be equivalent dynamically to the prefilter design, the parameters must be chosen as follows:

$1/T_p$ and $K_q T_z/T_p$ Control Short Period

$1/T_z = \lambda_2'$

Root Locus

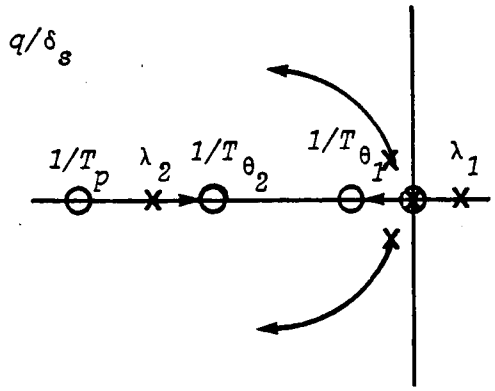

Closed Loop

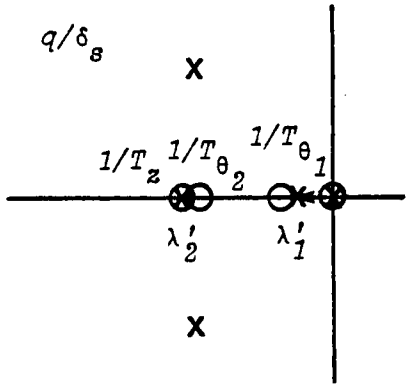

where $1/T_z = \lambda_2'$

The alternate design rules require the feedback pole be equal to the proportional plus integral zero and that this zero and feedback pole be scheduled such that $1/T_z = \lambda_2'$, the augmented real root.

Since $1/T_{\theta_2}$ is the limiting value of the augmented real root, λ_2' , then $1/T_z$ must be scheduled essentially to track $1/T_{\theta_2}$. For exact cancellation of λ_2' , however, $1/T_z$ should track λ_2' .

1. Report No.	2. Government Accession No.	3. Recipient's Catalog No.
NASA CR-170402		

4. Title and Subtitle	5. Report Date
APPLICATION OF CALSPAN PITCH RATE CONTROL SYSTEM TO THE SPACE SHUTTLE FOR APPROACH AND LANDING	May 1983
	6. Performing Organization Code

7. Author(s)	8. Performing Organization Report No.
Norman C. Weingarten and Charles R. Chalk	7102-F-1
	10. Work Unit No.

9. Performing Organization Name and Address	11. Contract or Grant No.
Calspan Advanced Technology Center P.O. Box 400 Buffalo, New York 14225	NAG4-2995
	13. Type of Report and Period Covered
12. Sponsoring Agency Name and Address	Contractor Report — Final Oct.-Dec. 1982
National Aeronautics and Space Administration Washington, D.C. 20546	14. Sponsoring Agency Code

15. Supplementary Notes

NASA Technical Monitor: Bruce G. Powers, NASA Ames Research Center, Dryden Flight Research Facility, Edwards, CA 93523.

16. Abstract

An analytical study was performed on a new pitch rate control system designed by the Calspan Corporation for use in the shuttle during approach and landing. Comparisons were made with a revised control system developed by NASA and the existing OFT control system. The Calspan design concept is discussed. The control system uses filtered pitch rate feedback with proportional plus integral paths in the forward loop. Control system parameters were designed as a function of flight configuration. Analysis included time and frequency domain techniques. Results indicate that both the Calspan and NASA systems significantly improve the flying qualities of the shuttle over the OFT. Better attitude and flight path control and less time delay are the primary reasons. The Calspan system is preferred by the authors over the revised NASA system because of reduced time delay and simpler mechanization. Further testing of the improved flight control systems in an in-flight simulator is recommended before a decision is made on which control system should be used in the actual shuttle.

17. Key Words (Suggested by Author(s))	18. Distribution Statement
Shuttle Flight control system Flying qualities	Unclassified-Unlimited STAR category 08

19. Security Classif. (of this report)	20. Security Classif. (of this page)	21. No. of Pages	22. Price*
Unclassified	Unclassified	144	A07

*For sale by the National Technical Information Service, Springfield, Virginia 22161.

End of Document